Vortex Interactions and Barotropic Aspects of Concentric Eyewall Formation

Hung-Chi Kuo

Department of Atmospheric Sciences
National Taiwan University
Taipei, Taiwan

郭鴻基 教授
國立臺灣大學 大氣科學系

HyARC
Nagoya University

July 29 2008

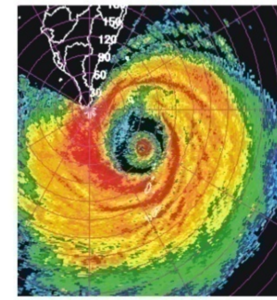

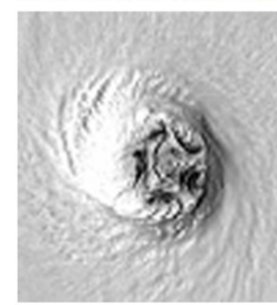

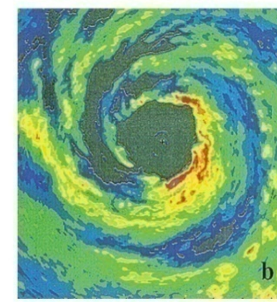

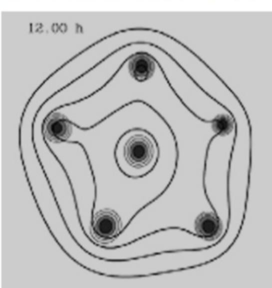

1. Two-dimensional turbulence

2. Double eyewall dynamics

3. Discussion

The Downstream Influences of the Extratropical Transition of Tropical Cyclones

Patrick Harr
Naval Postgraduate School

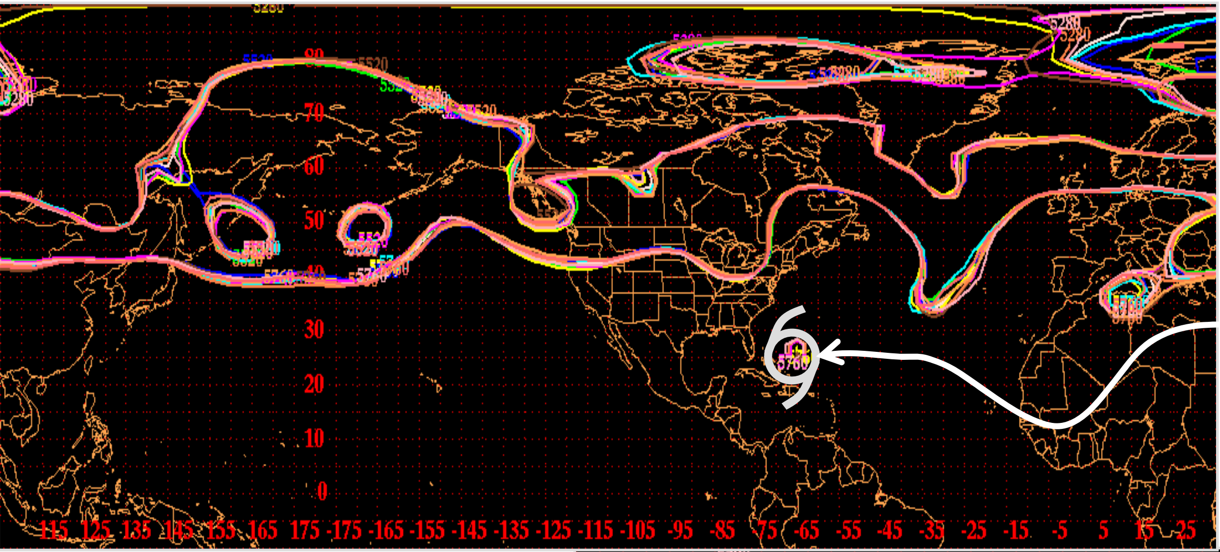

0000 UTC 16 Sep 2003
GFS Ensembles +00

Hurricane Isabel

GFS 500 hPa Ensembles
+108 h
VT 1200 UTC 20 Sep 03

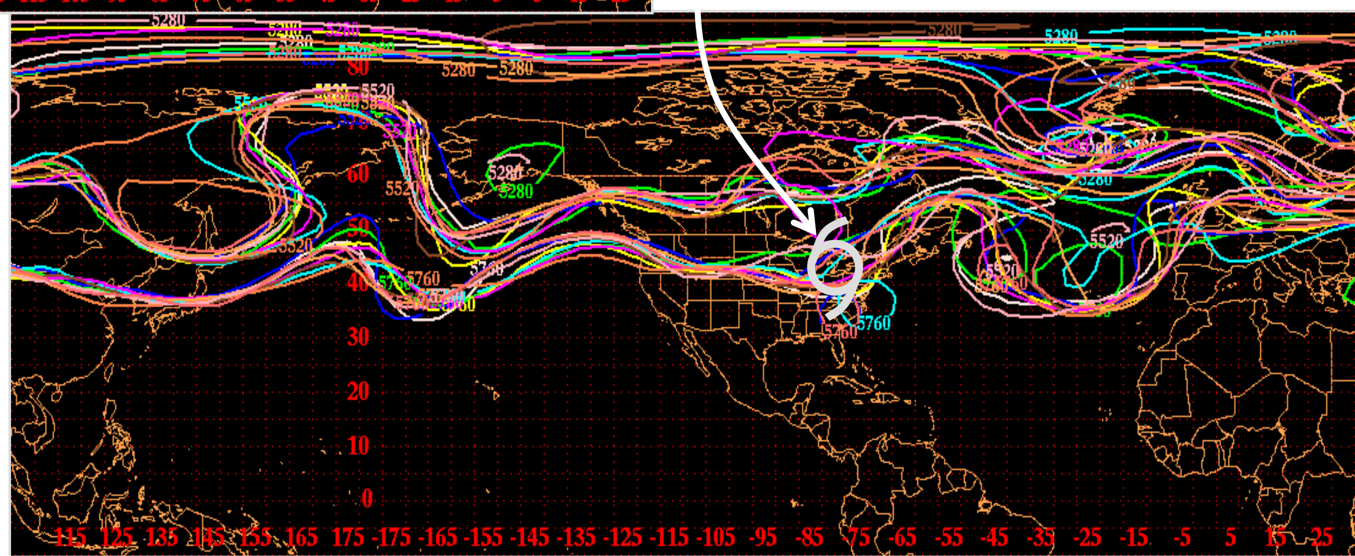

Acknowledgment: Office of Naval Research, Marine Meteorology Program

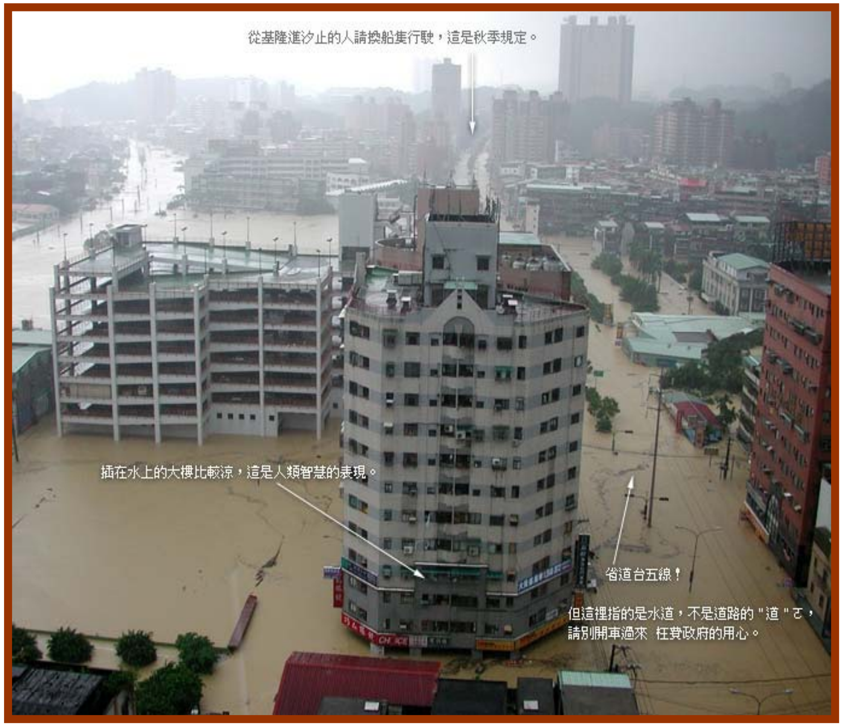
從基隆進汐止的人請換船隻行駛，這是秋季規定。
插在水上的大樓比較涼，這是人類智慧的表現。
省道台五線！
但這裡指的是水道，不是道路的 "道 "ㄛ，
請別開車過來 枉費政府的用心。

CWB is capable of 24 hr and 100km scale ppn (phase locked with topography)

0 to 12 hr and 10 km ppn remain biggest challenges

355mm in 5 hr in the city of KaoShung (5 pm to 10 pm at the beginning of the rush hour)

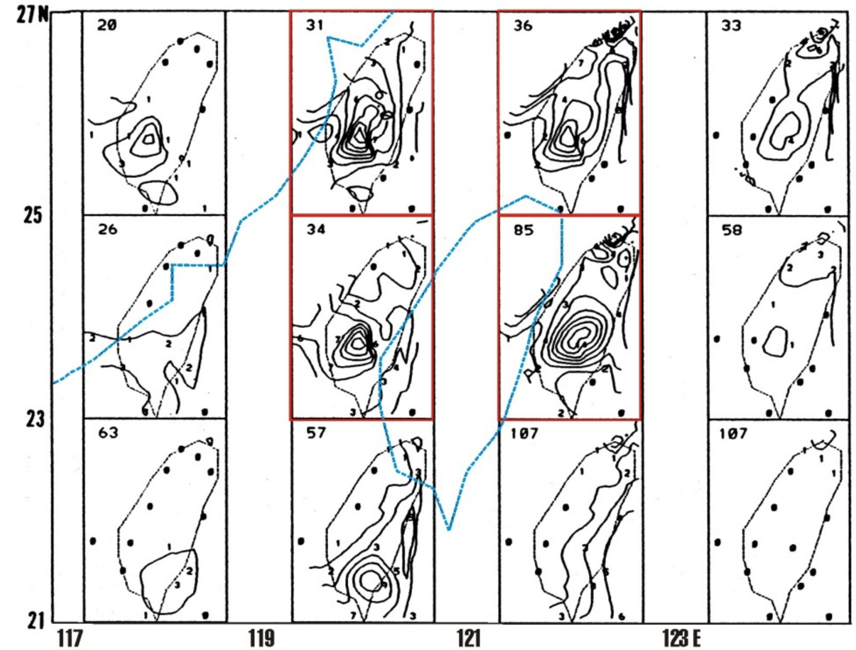

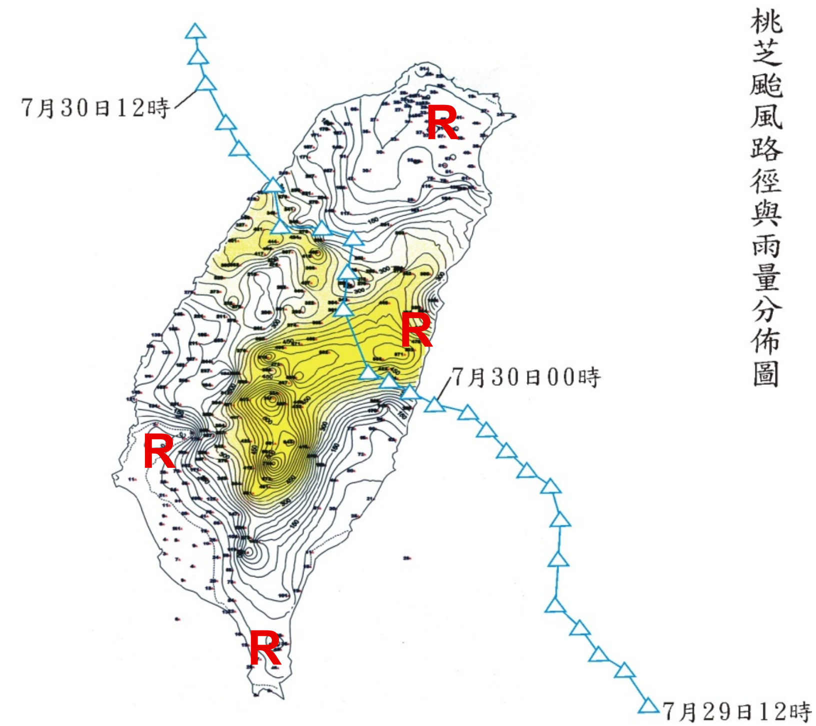

Concentric eyewalls near Taiwan

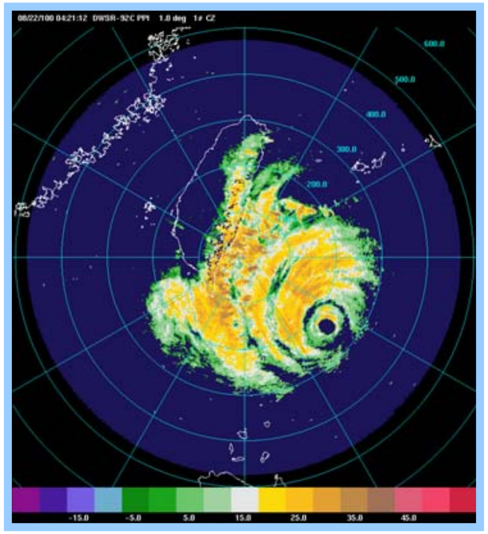

Bilis(2000)

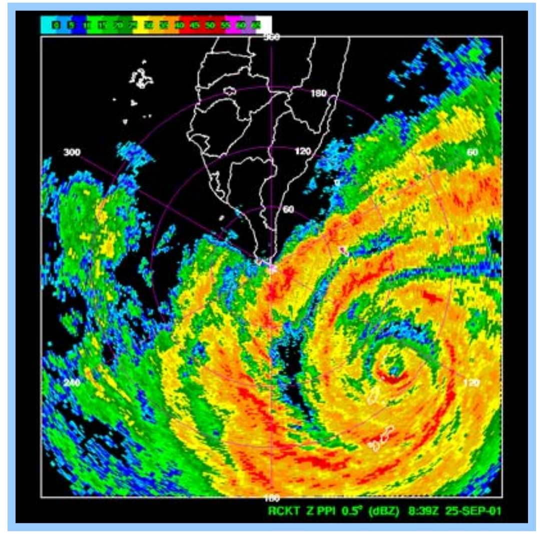

Lekima(2001)

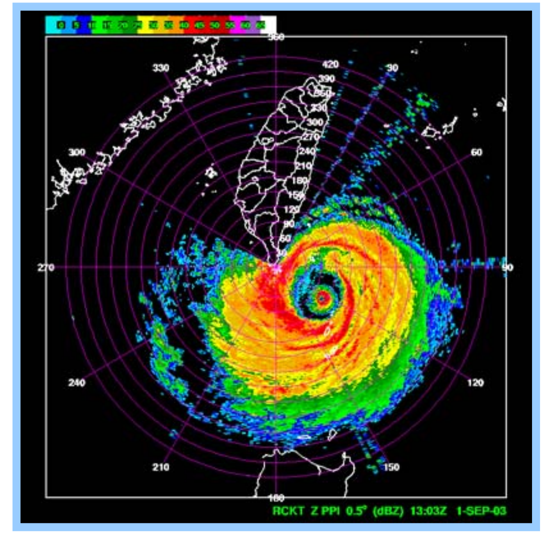

Dujuan(2003)

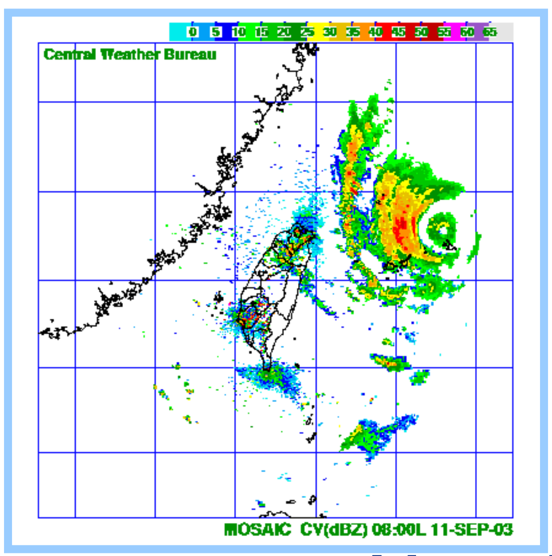

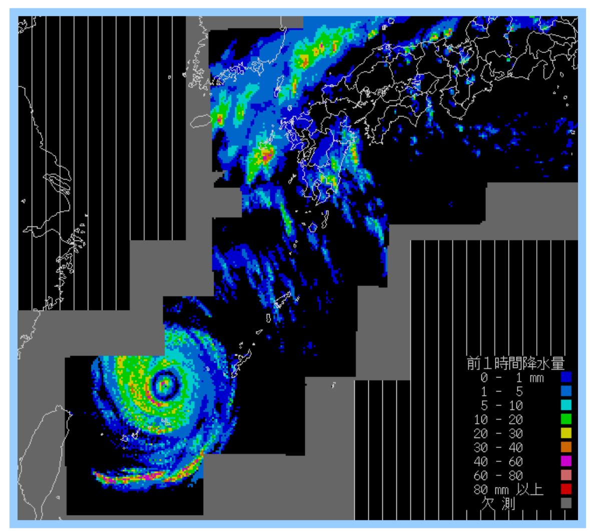

Maemi(2003)

Kuo et al. (2008)

- 1997~2005
- 221 tropical cyclones
- 205 tropical cyclones examined
- 48 concentric tropical cyclones (23%)
- higher intensity, higher percentage of concentric eyewall

Intensity at the concentric eyewalls formation time

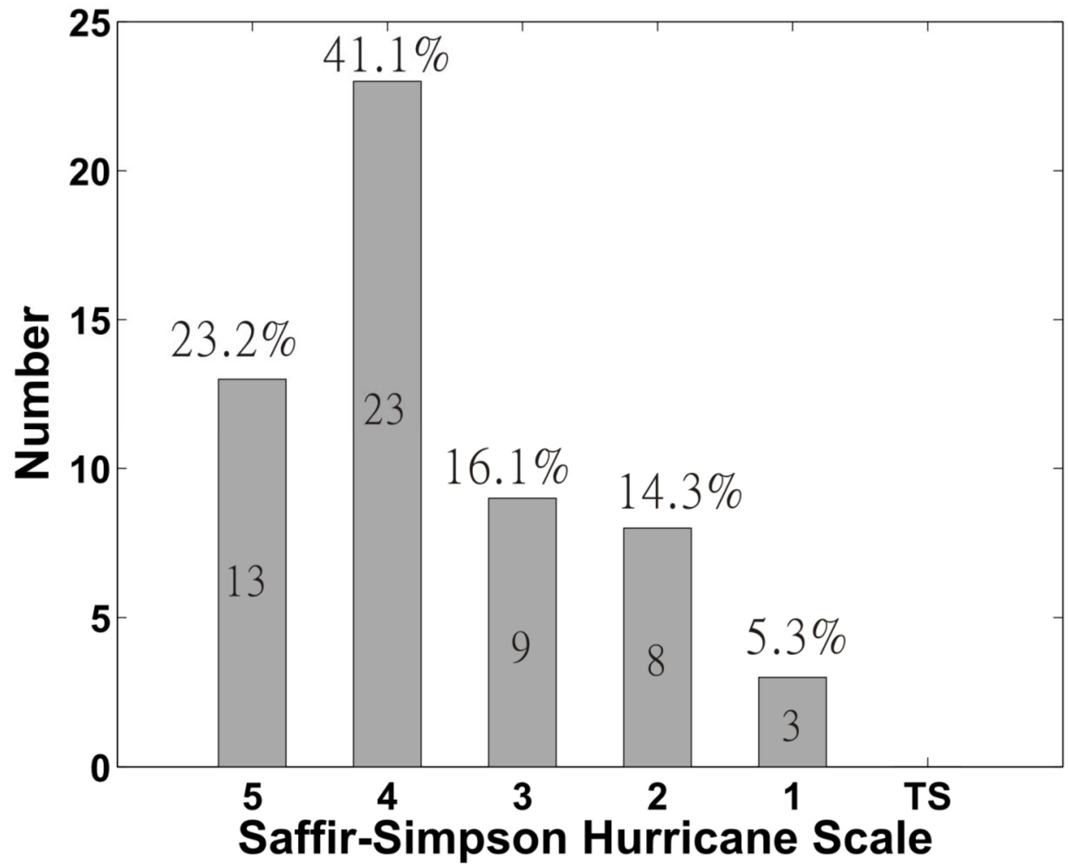

- **64.3% in categories 4 and 5 in the western North Pacific.**

Knaff and Kossin (2003)

- color-enhanced IR image of Hurricane Luis (1995) at 2015 UTC 3 Sep

dimensionless	24-h weakening
ATL(56)	0.14
Annular hurricanes(6)	0.05

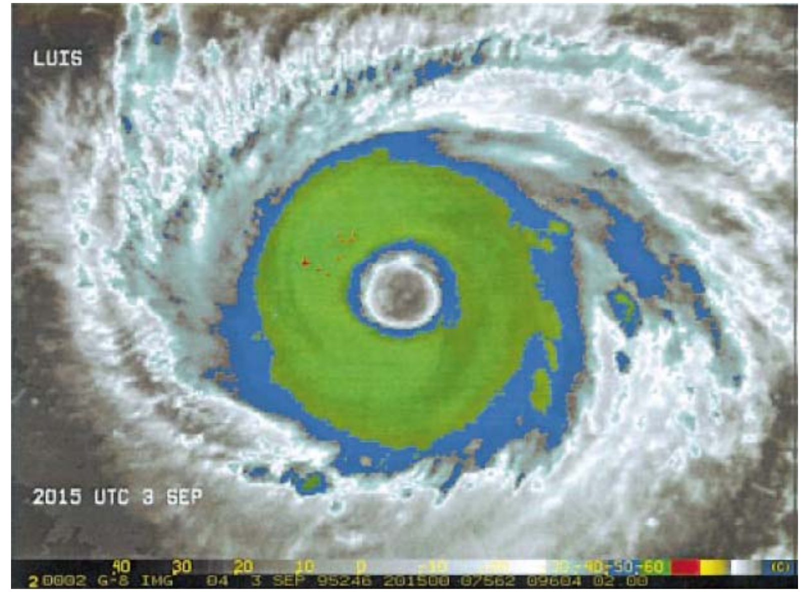

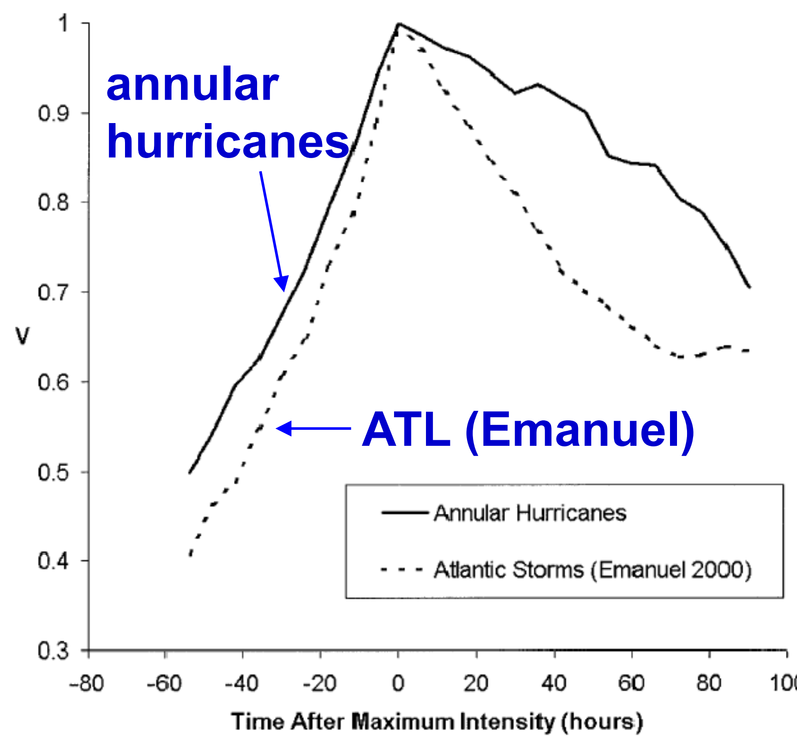

Composite Time Series of the Normalized Intensity

Kuo et al. (2008)

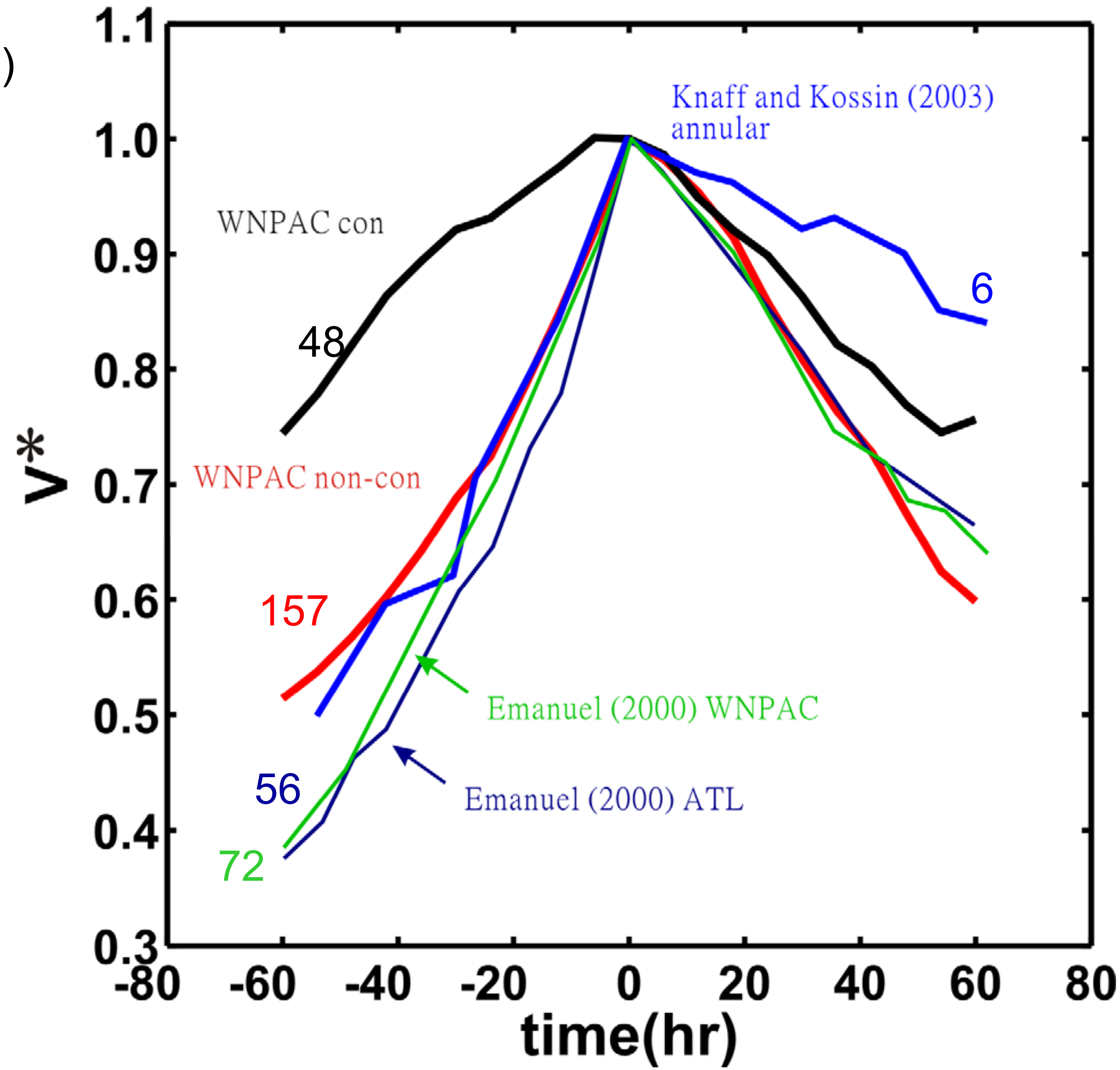

Coriolis Force

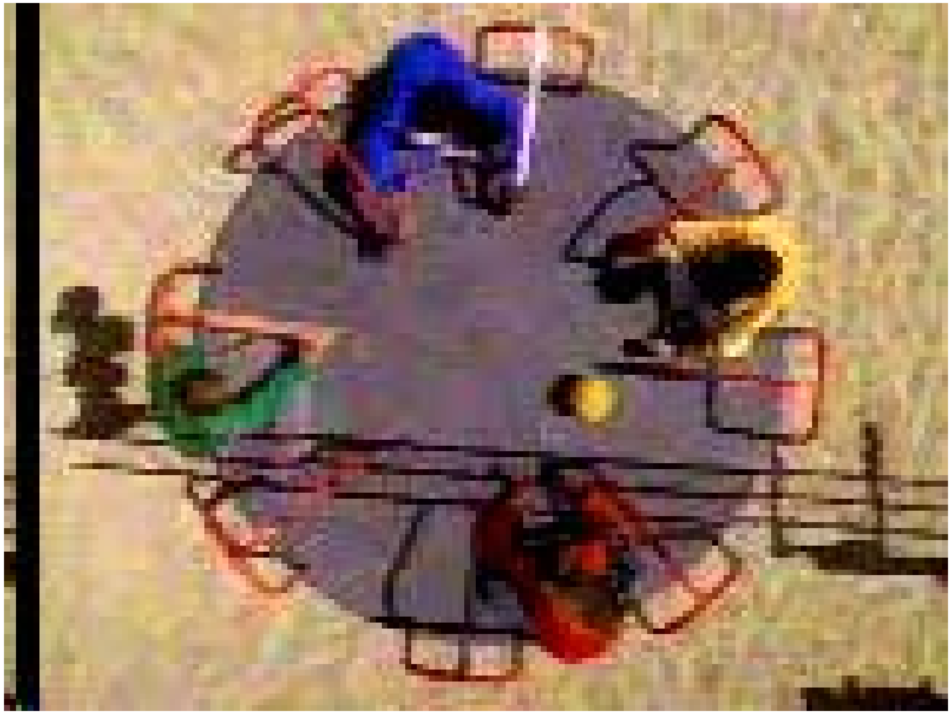

Non-inertial Frame

3D

2D (strong rotation)

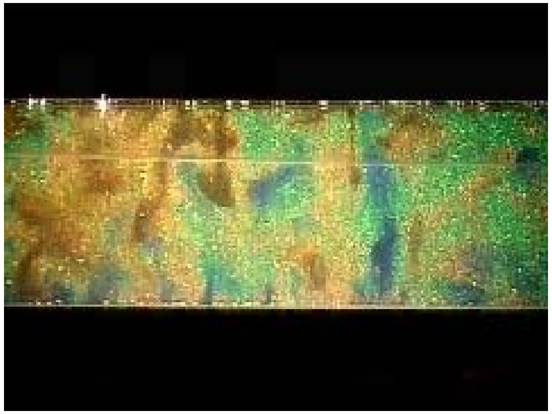

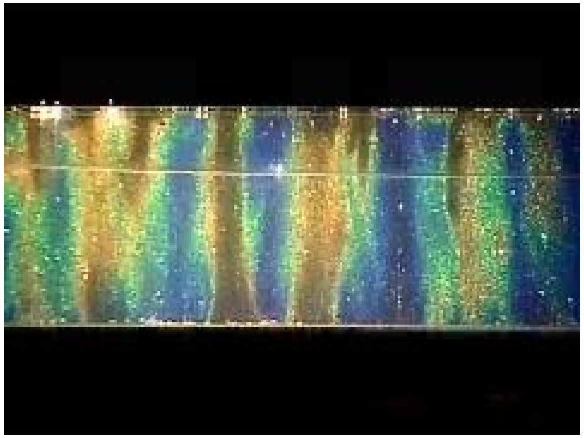

Taylor columns

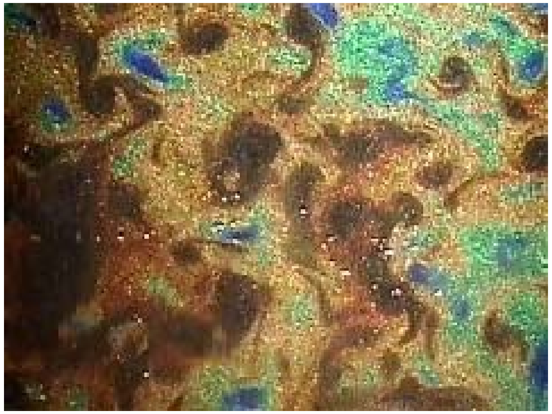

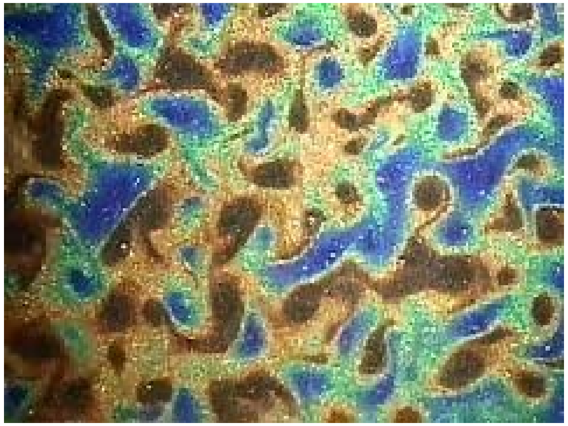

Vortices with sharp edge

Kyoto Univ. GFD group

$$\vec{f} = 2\Omega\cos\phi\,\hat{j} + 2\Omega\sin\phi\,\hat{k}$$

$$\vec{f} \cong 2\Omega\sin\varphi\,\hat{k}$$

deep atmosphere
(Jupiter??)

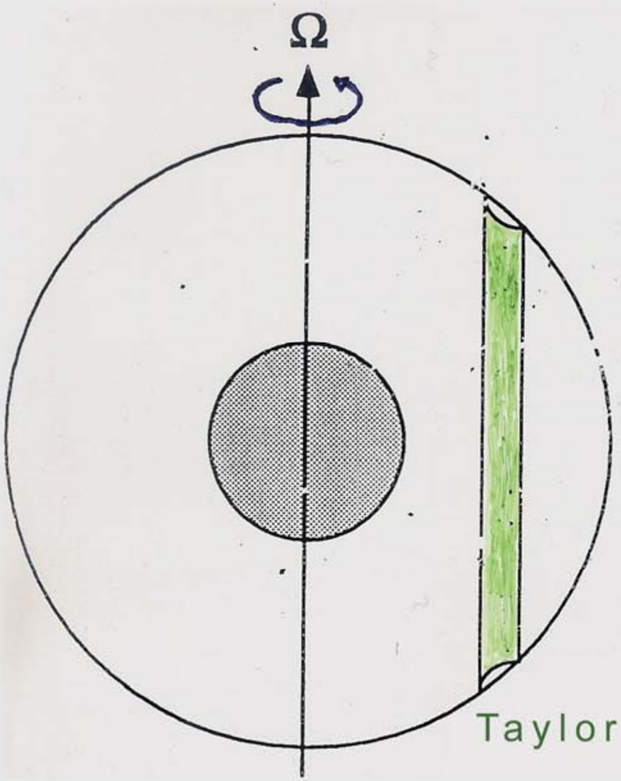

shallow atmosphere
(Earth)

z<<a

traditional
approximation

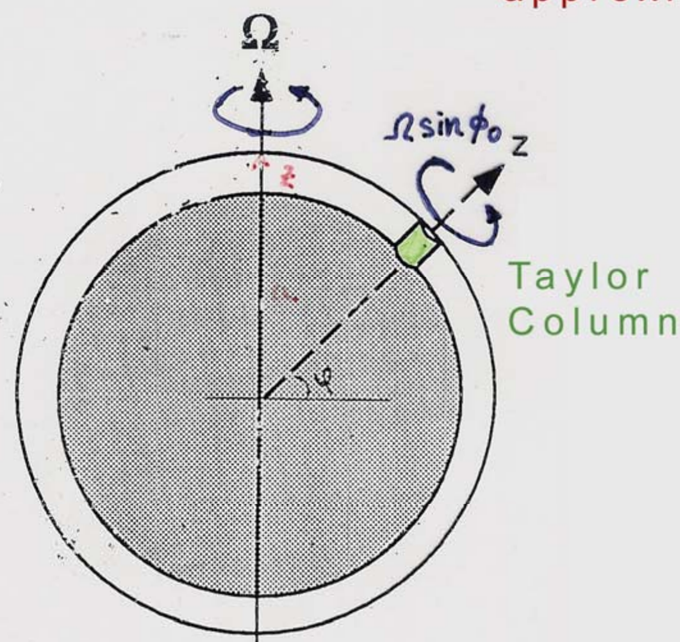

$$\frac{DP}{Dt} = \frac{\partial P}{\partial t} + u\frac{\partial P}{\partial x} + v\frac{\partial P}{\partial y} + w\frac{\partial P}{\partial z} \qquad P = \frac{\vec{\zeta} \cdot \nabla \theta}{\rho}$$

$$\frac{D\zeta}{Dt} = \frac{\partial \zeta}{\partial t} + u\frac{\partial \zeta}{\partial x} + v\frac{\partial \zeta}{\partial y}$$

$$\frac{D\zeta_g}{Dt} = \frac{\partial \zeta_g}{\partial t} + u_g\frac{\partial \zeta_g}{\partial x} + v_g\frac{\partial \zeta_g}{\partial y}$$

$$\zeta_g = \nabla^2\psi \qquad u_g = -\frac{\partial \psi}{\partial y} \qquad v_g = \frac{\partial \psi}{\partial x}$$

$$\boxed{\frac{\partial \zeta}{\partial t} + \frac{\partial(\psi, \zeta)}{\partial(x, y)} = \nu\nabla^2\zeta}$$

Potential Vorticity

$$\cancel{\frac{\partial}{\partial z}} \qquad P \rightarrow \zeta$$

Barotropic Vorticity

Quasi-Geostrophic Vorticity

(Strong Rotation)

$$\nabla \cdot \vec{V} = 0$$

Nondivergent Barotropic Equation

2D Turbulence

Stratification and/or Rotation

Vortex Waves Turbulence

$$\frac{\partial \zeta}{\partial t} + u\frac{\partial \zeta}{\partial x} + v\frac{\partial \zeta}{\partial y} = \nu \nabla^2 \zeta$$

$$u = -\frac{\partial \psi}{\partial y}, \qquad v = \frac{\partial \psi}{\partial x}.$$

$$\boxed{\frac{\partial \zeta}{\partial t} + \frac{\partial(\psi, \zeta)}{\partial(x, y)} = \nu \nabla^2 \zeta}$$

Weiss(1981,1991), Rozoff et al. (2006)

$$\frac{D}{Dt}(\nabla\zeta) = -J(\nabla\psi,\zeta)$$

$$\rightarrow \nabla\zeta(t) \propto \exp(\lambda t) \quad \lambda = \pm\frac{1}{2}\sqrt{Q} = \pm\frac{1}{2}\sqrt{S_1{}^2 + S_2{}^2 - \zeta^2}$$

$$S_1 = \frac{\partial u}{\partial x} - \frac{\partial v}{\partial y} \quad \text{(stretch deformation)}$$

$$S_2 = \frac{\partial v}{\partial x} + \frac{\partial u}{\partial y} \quad \text{(shear deformation)}$$

Q > 0 (strain dominates)

→vorticity gradient will be stretched

Q < 0 (vorticity dominates)

→vortex is stable (survival of eyewall meso-vortices)

RAINEX (2005)

Shear/strech deformation outside the radius of maximum wind

ELDORA composite
~120 x 120 km^2

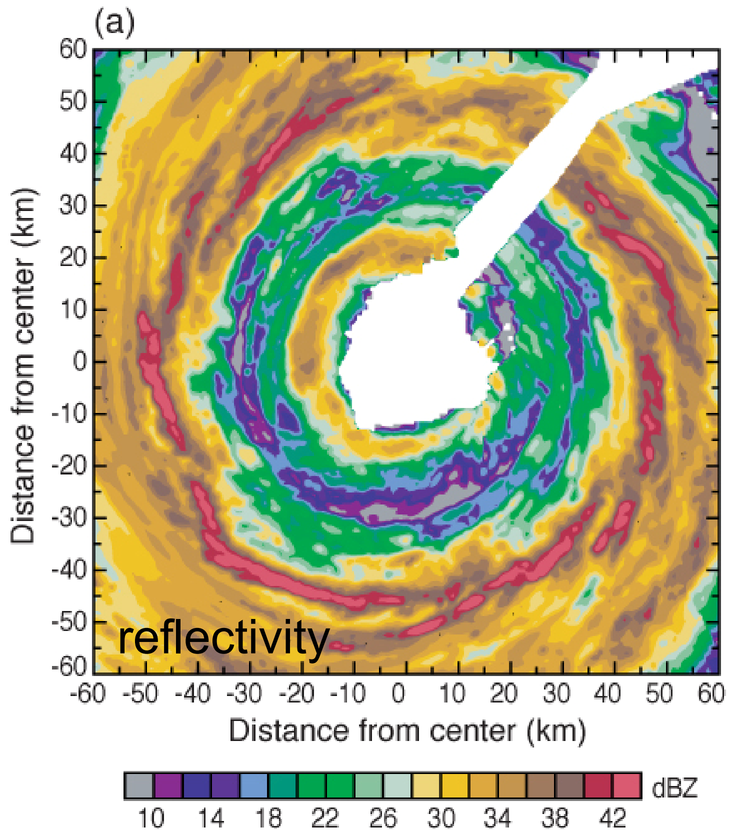

Kossin et al. (2000)
Instability Experiment

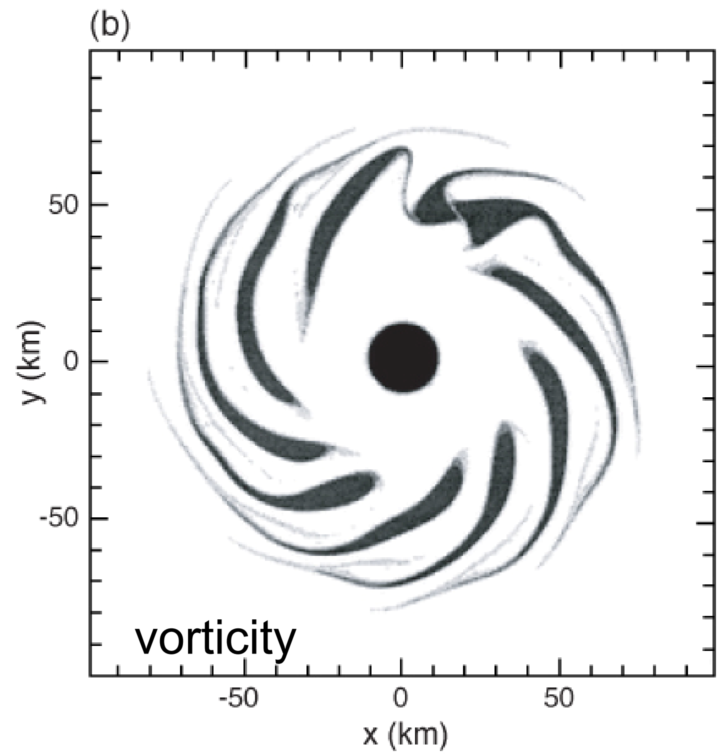

Bowmen and Mangus (1993)

Observations of deformation and mixing of the total ozone field in the Antarctic polar vortex

Surf Zone Dynamics

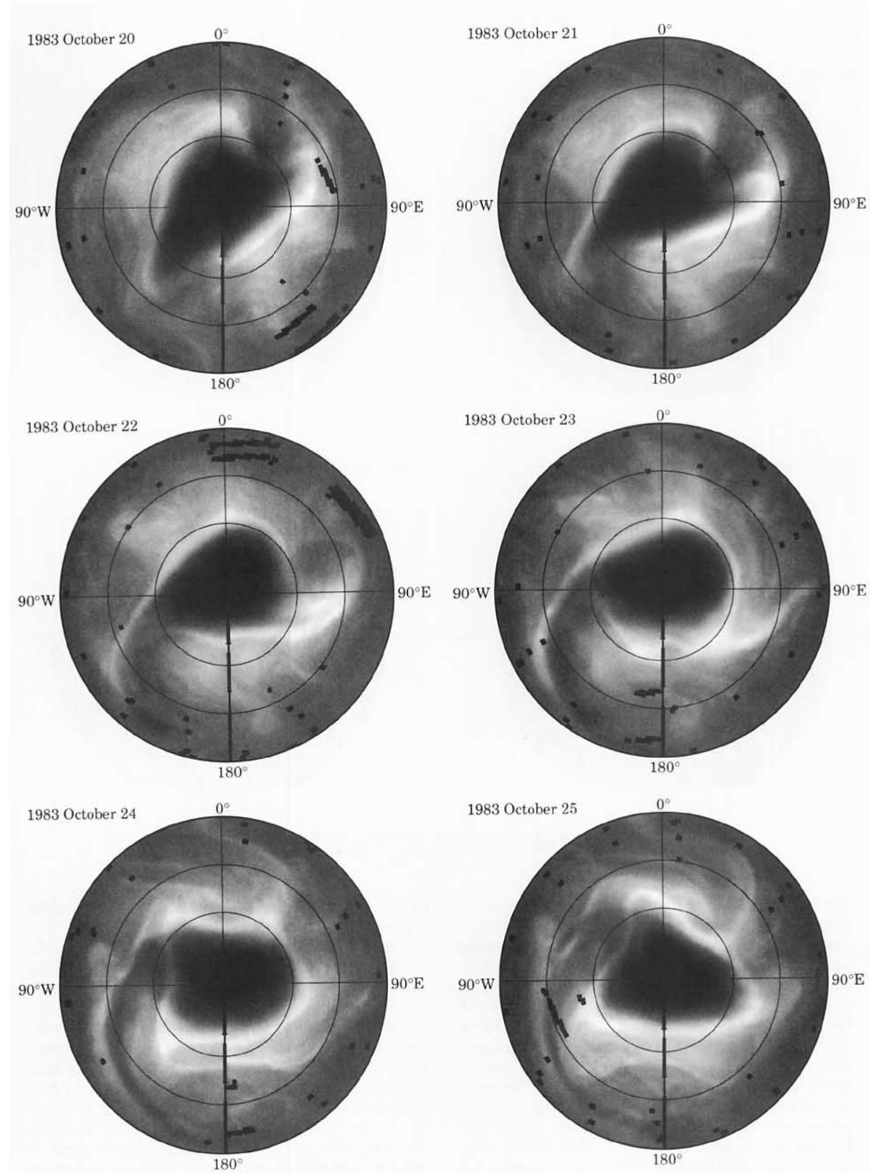

Fig.1: Daily TOMS images of total ozone in the Southern Hemisphere for six consecutive days in October 1983. Latitude circles are drawn at 40°,60°, and 80 °S. The outermost latitude is 20 °S.

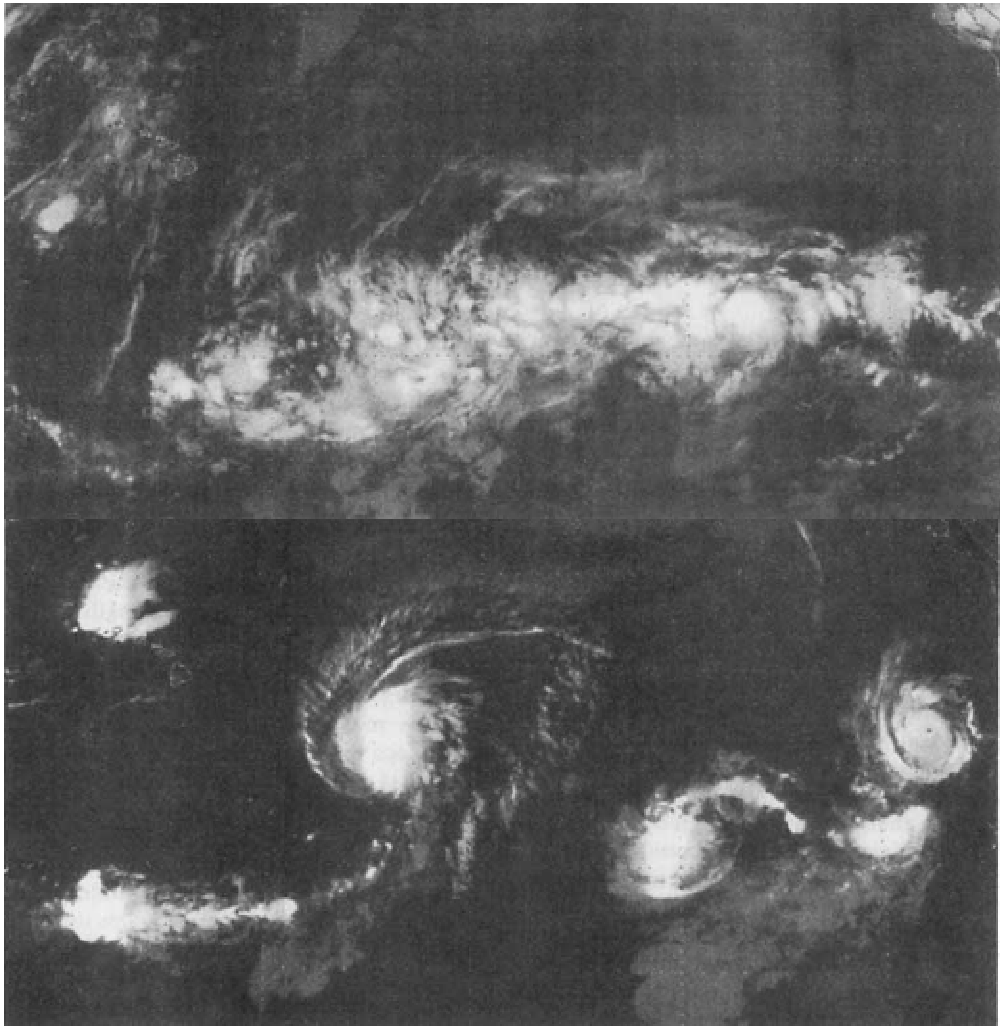

(a)

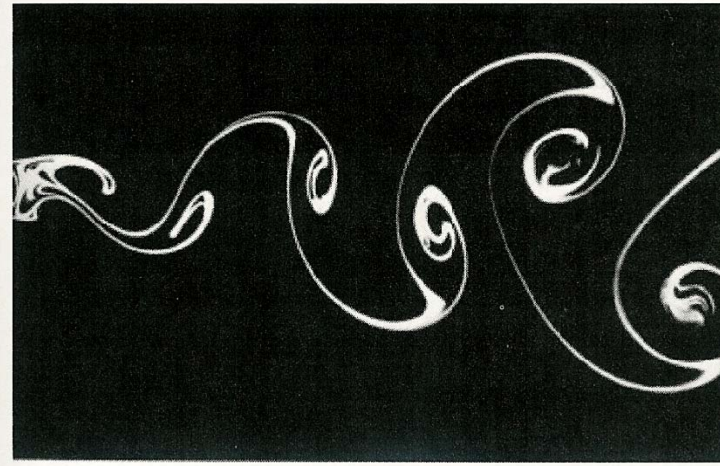

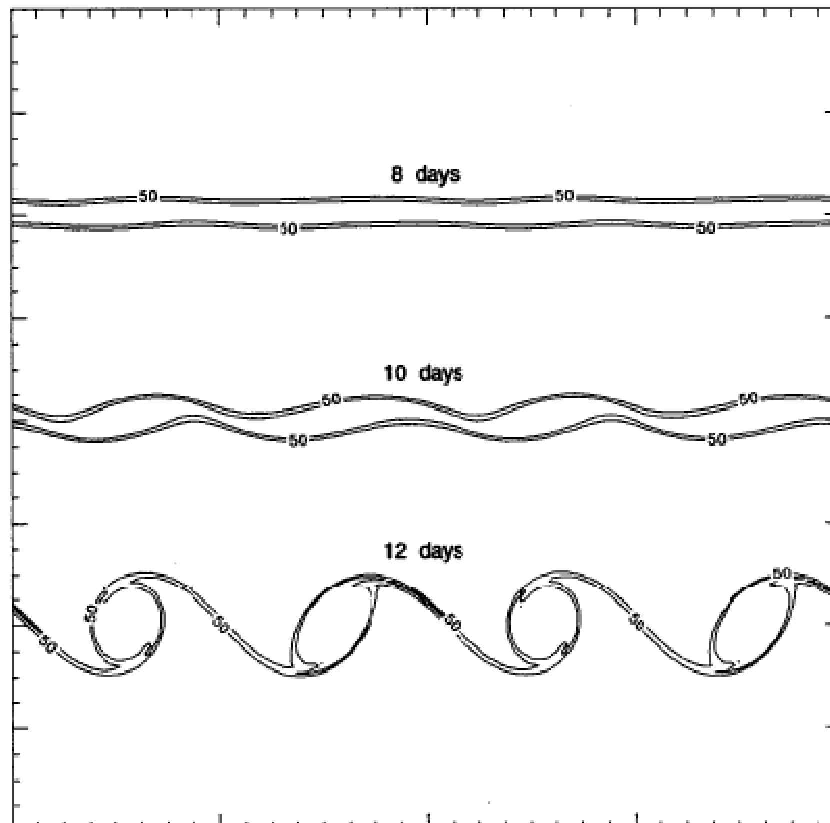

Non-divergent barotropic model (Nearly Inviscid Fluid)

$$\frac{\partial}{\partial t}\zeta + \mathrm{J}(\psi, \zeta) = \upsilon \nabla^2 \zeta \qquad \boxed{\nabla^2 \psi = \zeta}$$

The energy and enstrophy relations

$$\frac{d\mathcal{E}}{dt} = -2\,\upsilon\,\mathcal{Z}$$

$$\mathcal{E} = \iint \frac{1}{2}\left(u^2 + v^2\right) dx\,dy$$ kinetic energy

$$\frac{d\mathcal{Z}}{dt} = -2\,\upsilon\,\mathcal{P}$$

$$\mathcal{Z} = \iint \frac{1}{2}\zeta^2\,dx\,dy$$ enstrophy

$$\mathcal{P} = \iint \frac{1}{2}\nabla\zeta \cdot \nabla\zeta\,dx\,dy$$ palinstrophy

Batchelor 1969

Small viscosity led to large palinstrophy and the large enstrophy cascade

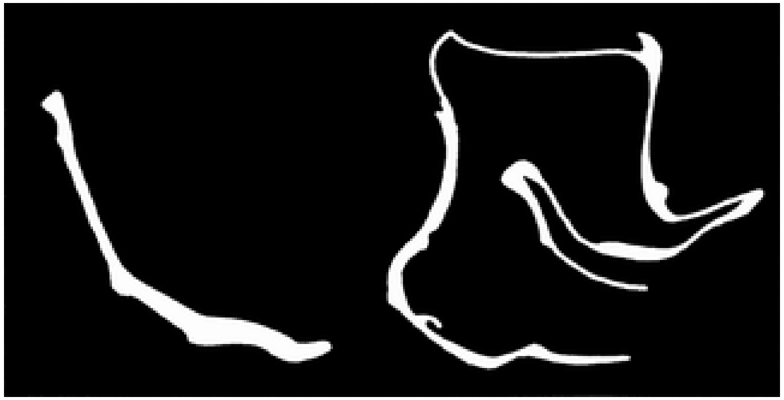

Stirring

$$\frac{D\theta}{Dt} = \frac{\partial\theta}{\partial t} + \vec{V}\cdot\nabla\theta = \nu\nabla^2\theta$$

$$C = \frac{1}{2}\int \nabla\theta\cdot\nabla\theta\, dV$$

$$\frac{dC}{dt} = \int(\vec{V}\cdot\nabla\theta)\nabla^2\theta\, dV - \nu\int(\nabla^2\theta)\, dV$$

Stirring **Mixing**

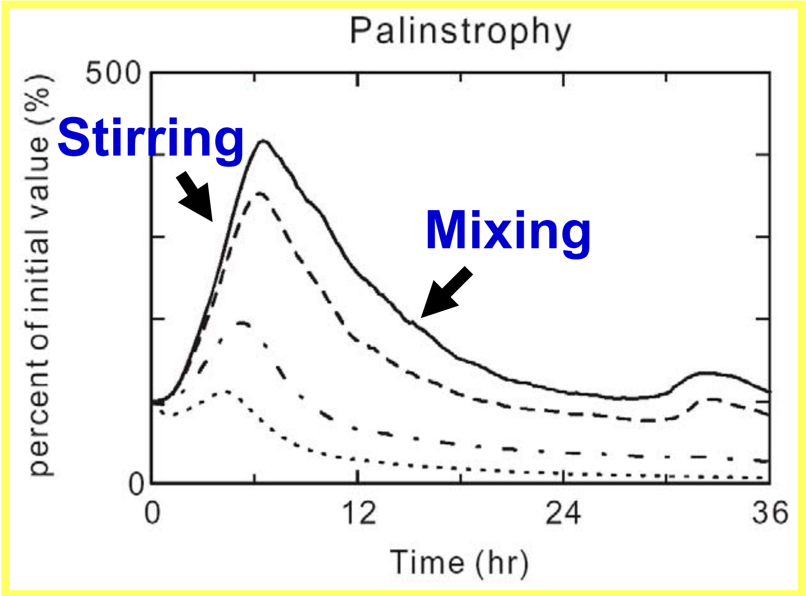

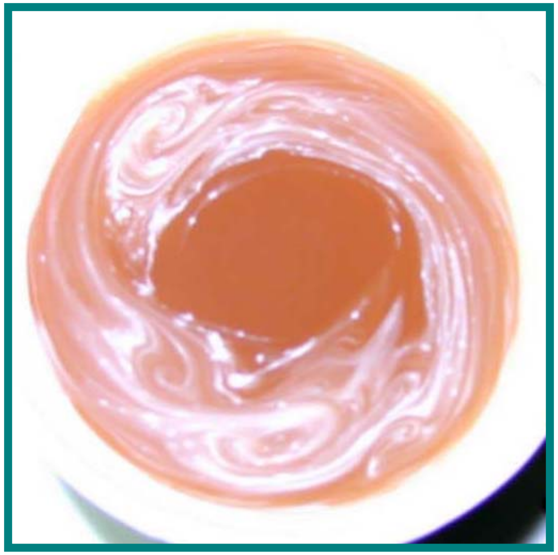

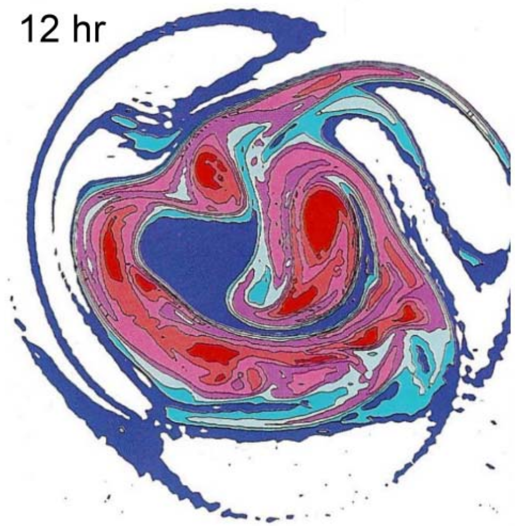

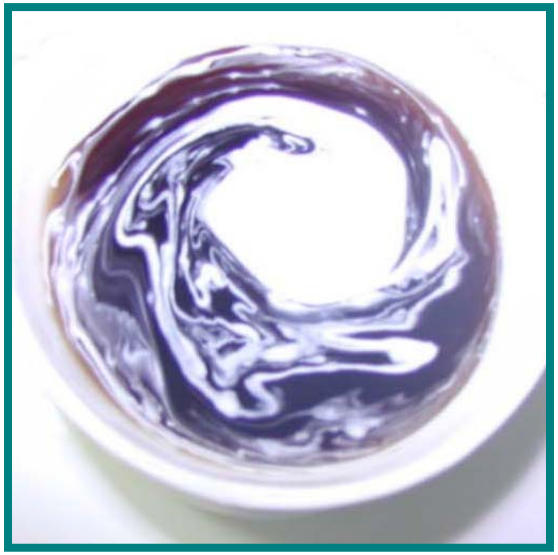

Selective Decay of 2D turbulence

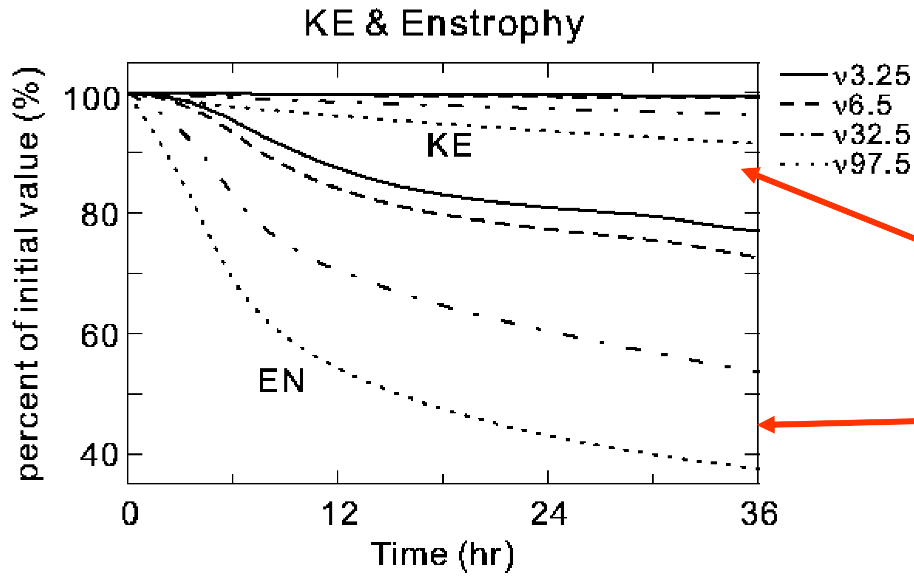

KE nearly conserved

Enstrophy cascade

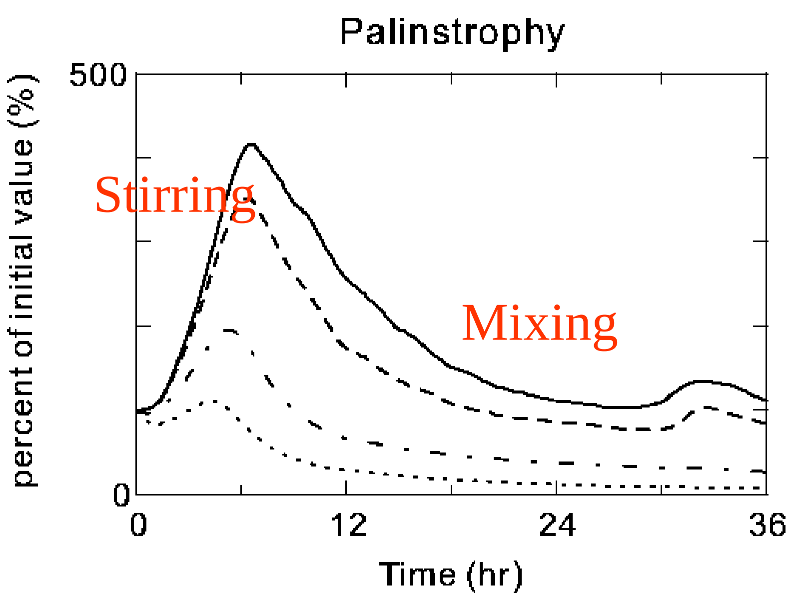

$$\frac{d}{dt}\int E(k)dk = 0. \qquad \frac{d}{dt}\left(\int k^2 E(k)dk\right) = \frac{d}{dt}\int Z(k)dk = 0;$$

$$\frac{d}{dt}\left(\int (k-k_1)^2 E(k)dk\right) > 0$$

$$\frac{d}{dt}\left(\int k^2 \cancel{E}(k)dk + k_1^2 \int \cancel{E}(k)dk - 2k_1 \int kE(k)dk\right) > 0$$

$$\frac{d}{dt}\left(\frac{\int kE(k)dk}{\int E(k)dk}\right) < 0,$$

Kinetic energy moves toward large scales

$$\frac{d}{dt}\left(\int (k^2-k_1^2)^2 E(k)dk\right) > 0$$

$$\frac{d}{dt}\left(\int k^2 Z(k)dk + k_1^4 \int \cancel{E(k)}dk - 2k_1^2 \int k^2 \cancel{E(k)}dk\right) > 0$$

$$\frac{d}{dt}\left(\frac{\int k^2 Z(k)dk}{\int Z(k)dk}\right) > 0,$$

Enstrophy moves toward small scales

$E \sim p'^2 / L^2$ (KE) geostrophy

$Z \sim p'^2 / L^4$ (Enstrophy)

KE nearly conserved $L \sim p'$

Enstrophy cascade $L \uparrow$ (L increase Z decrease)

Selective Decay of 2D turbulence

The vortices become, on the average,
larger, stronger, and fewer.

Merger and Axisymmetrization Dynamics

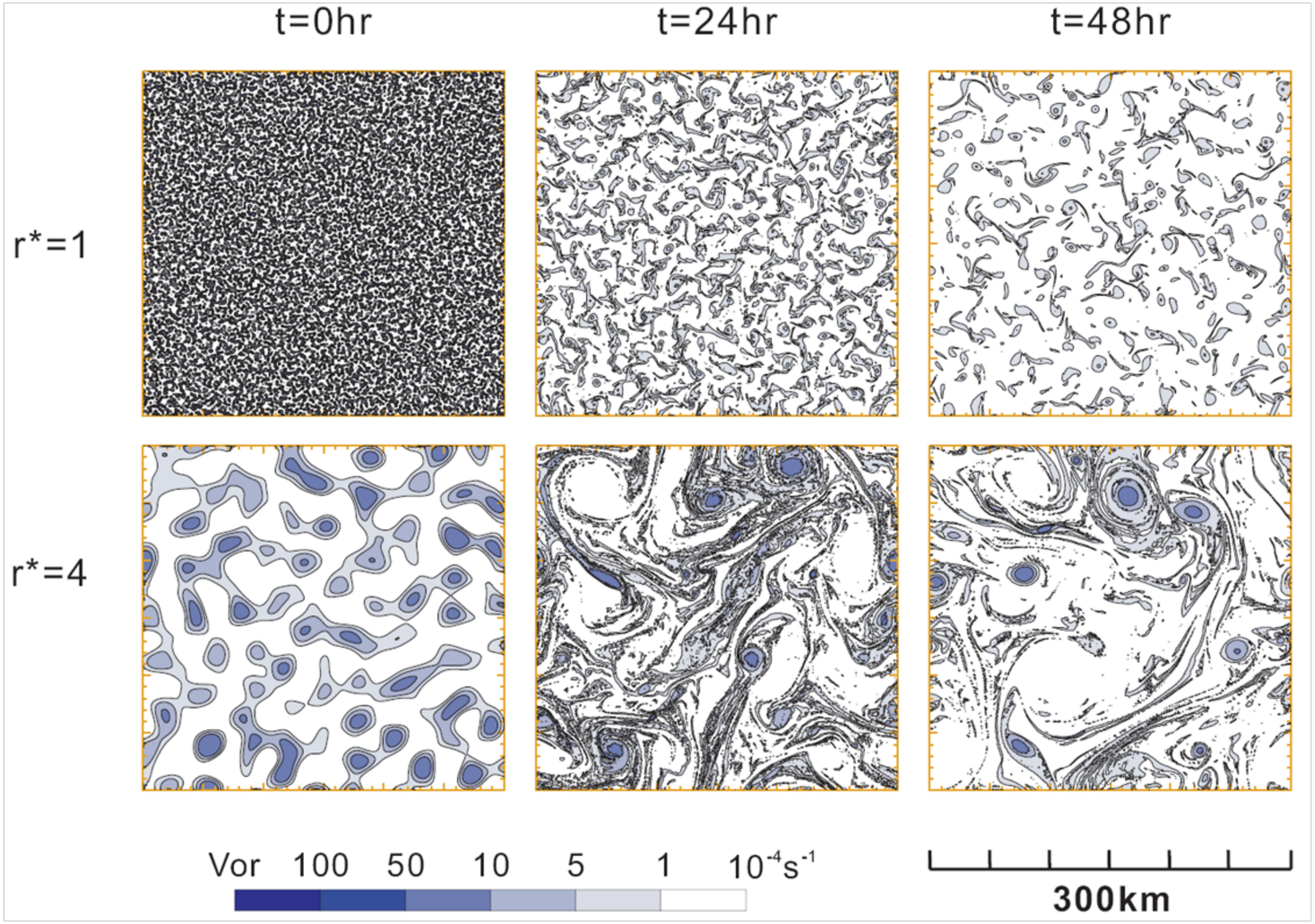

Fewer and stronger vortices !!!

小尺度變大尺度

Coherent structure with filamentations in 2-D turbulence

Spiral Band in Hurricane and Galaxy

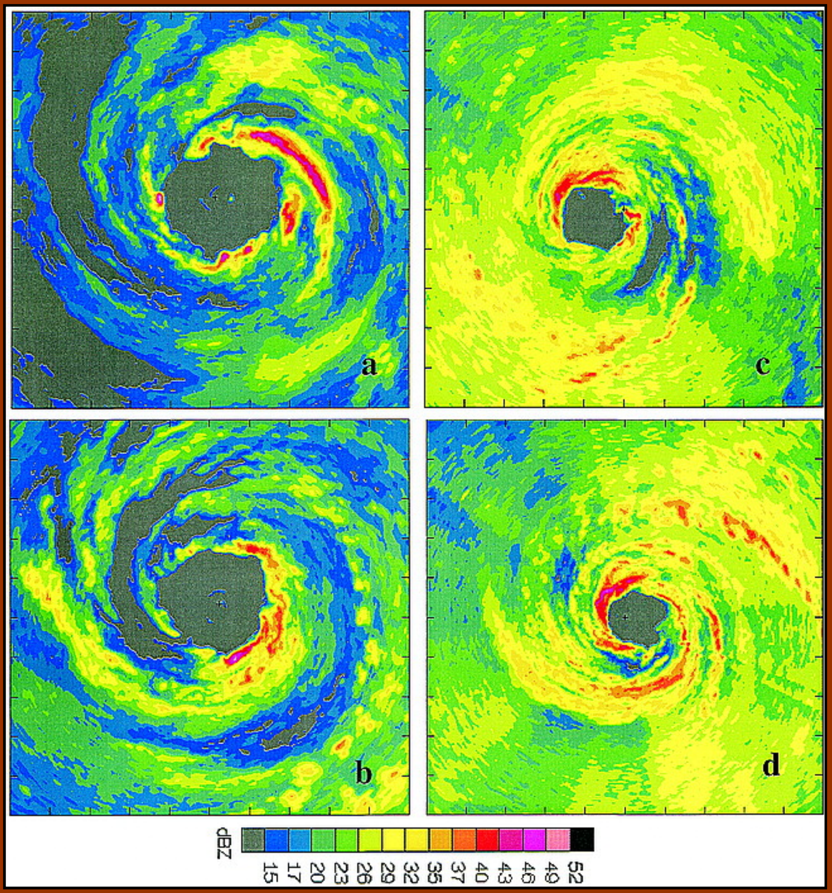

Airborne-radar reflectivity in Hurricanes
Guillermo (1997) (left panels) and Bret (1999) (right panels).

Kossin and Schubert 2001

GALAXY.BMP (894x616x16M bmp)

FIGURE 45–2 Our Galaxy, as it would appear from the outside: (a) "end view," in the plane of the disc; (b) "top view," looking down on the disc. (If only we could see it like this—from the outside!) (c) Infrared photograph of the inner reaches of the Milky Way, showing the central bulge of our Galaxy. This very wide angle photo extends over 180° of sky, and to be viewed properly it should be wrapped in a semicircle with your eyes at the center. The white dots are nearby stars.

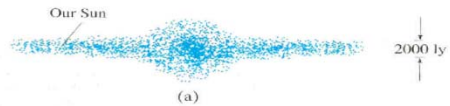

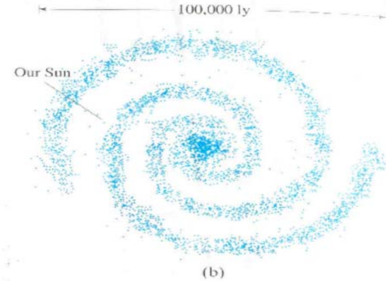

686 Part 8 ASTRONO

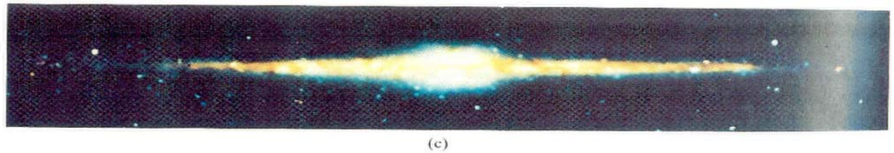

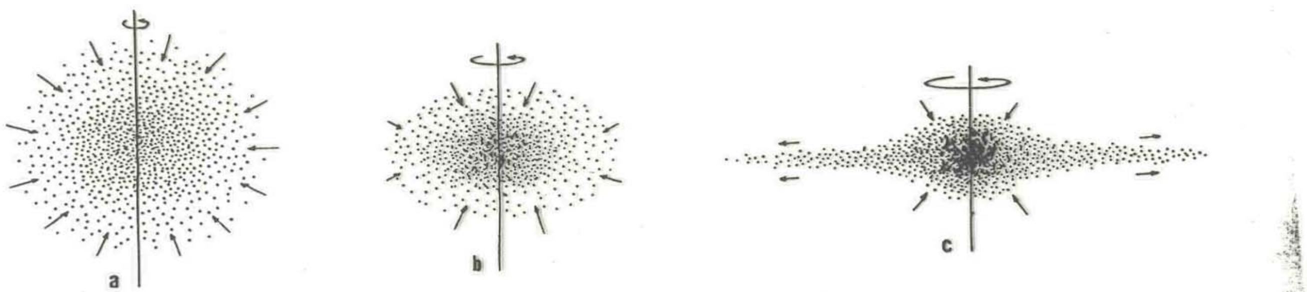

Figure 27.18 A slightly rotating ball of interstellar gas (a) contracts due to mutual gravitation and (b) conserves angular momentum by speeding up. The increased momentum of individual particles and clusters of particles causes them to (c) sweep in wider paths about the rotational axis, producing an overall disk shape.

Conservation of angular momentum

$$\sum r_i^2 P_i = \bar{r}^2 \sum P_i$$

(a symmetrical model)

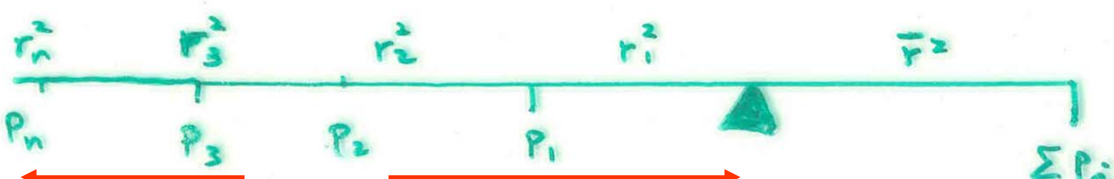

Outward filaments

Contraction

KE conserved

Waves, turbulence, and coherent vortex

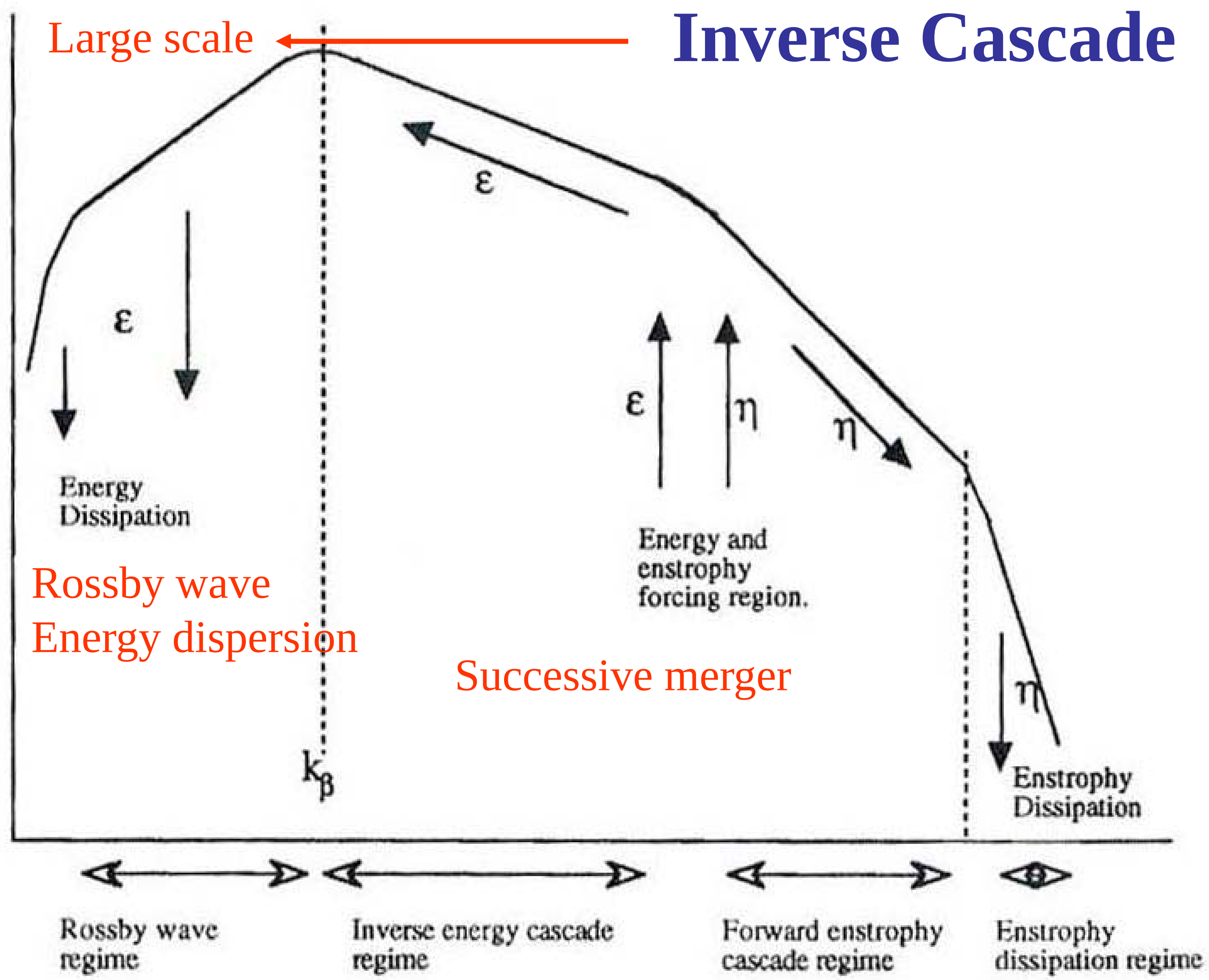

Huang and Robinson
1998

Turbulence

Rhines curve

Waves

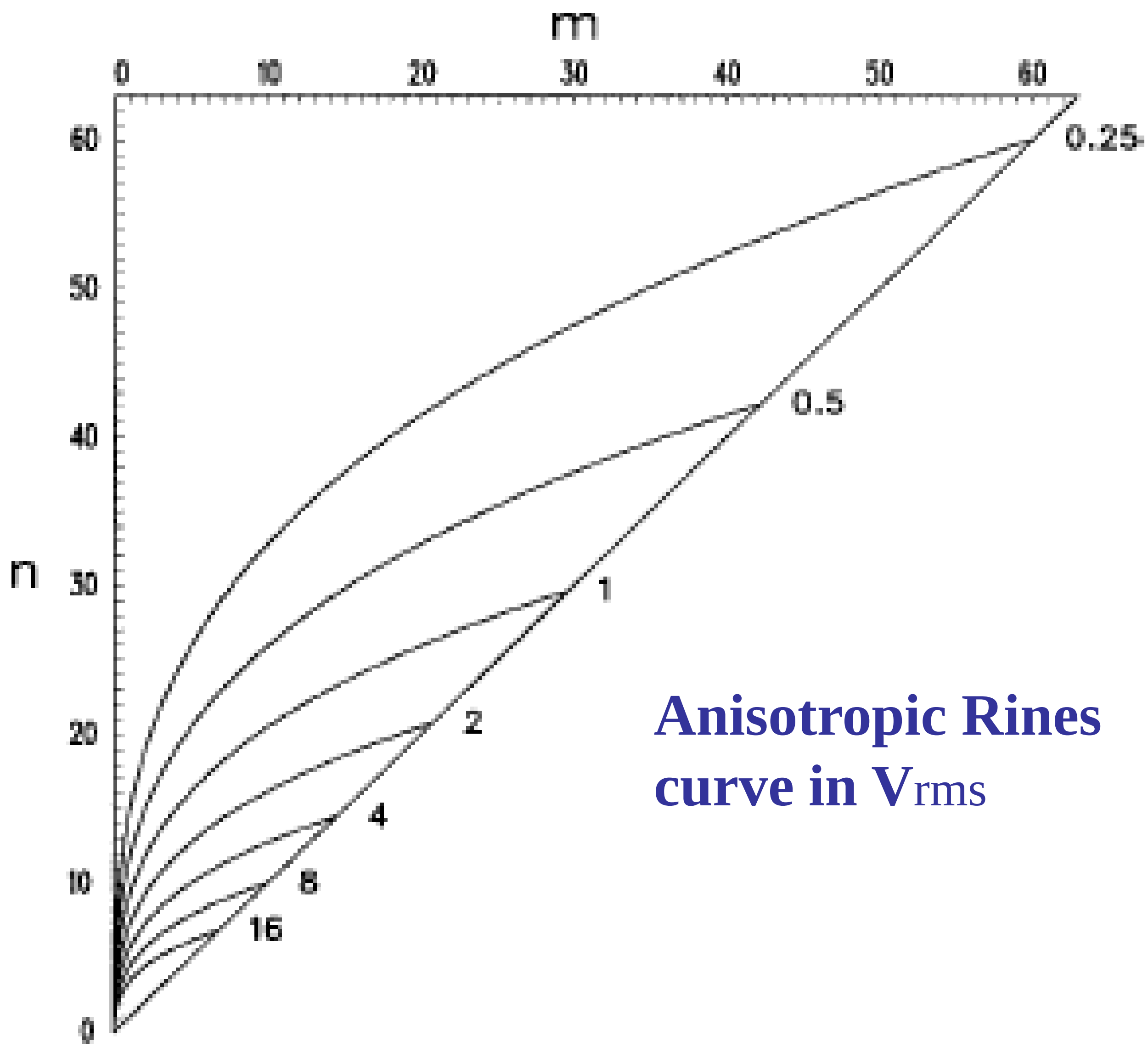

Anisotropic Rines curve in Vrms

FIG. 1. Anisotropic Rhines curve on the wavenumber plane based on Eq. (3). Dimensional values of V_{rms} (in m s^{-1}) are labeled at right.

Huang and Robinson 1998

Forcing added

Inverse energy cascade to zonal Harmonics

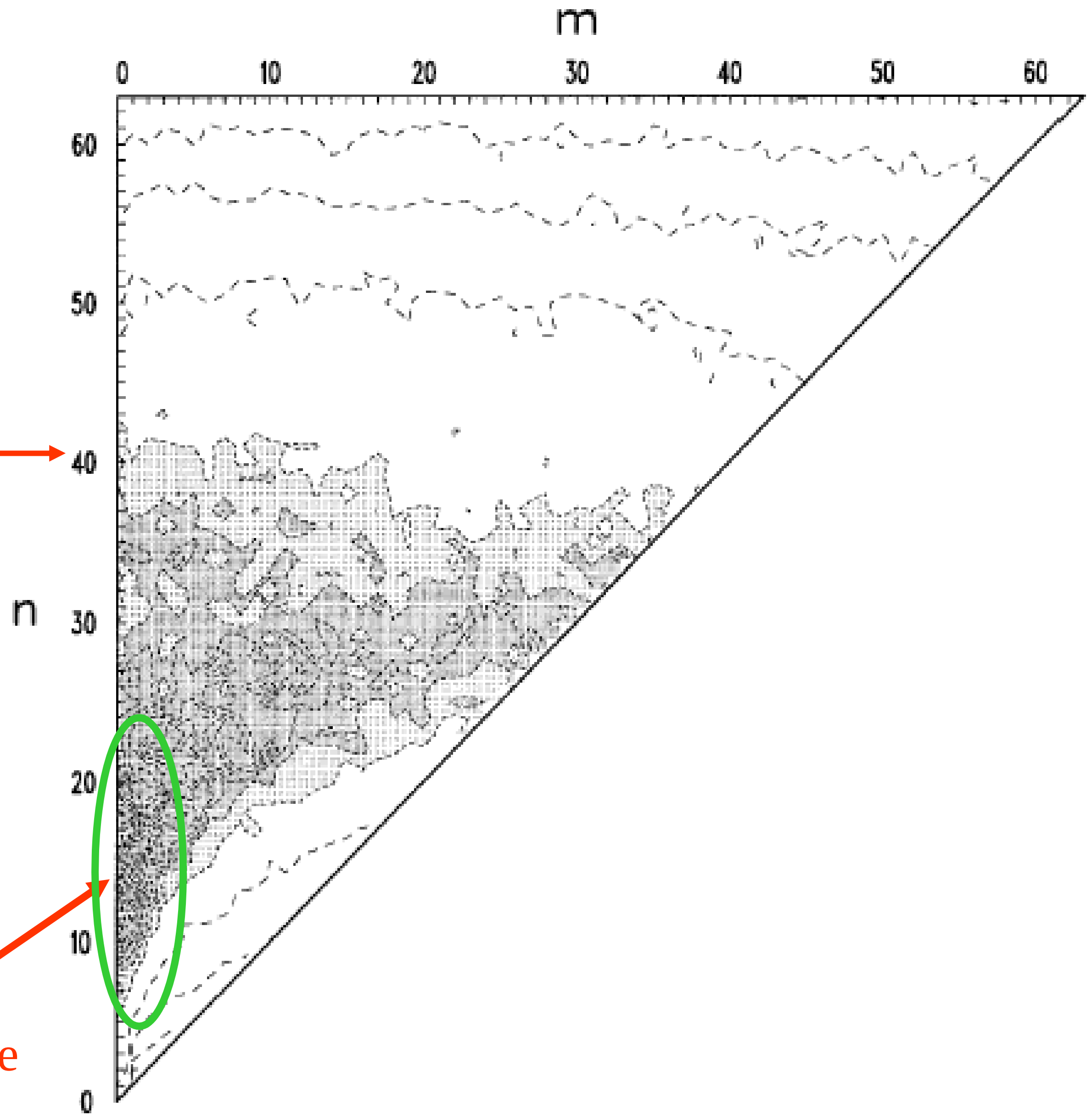

FIG. 2. Energy spectrum $E(m, n)$ of an ensemble mean at day 80 of 10 decaying turbulence experiments. The magnitude of the spectrum is normalized by the maximum value on the map. Contour levels are 0.0001, 0.001, 0.01, 0.1–0.9 with increment 0.1. Area with $E(m, n) > 0.1$ is lightly shaded, $E(m, n) > 0.2$ heavily shaded.

Rotational period 9.84hr

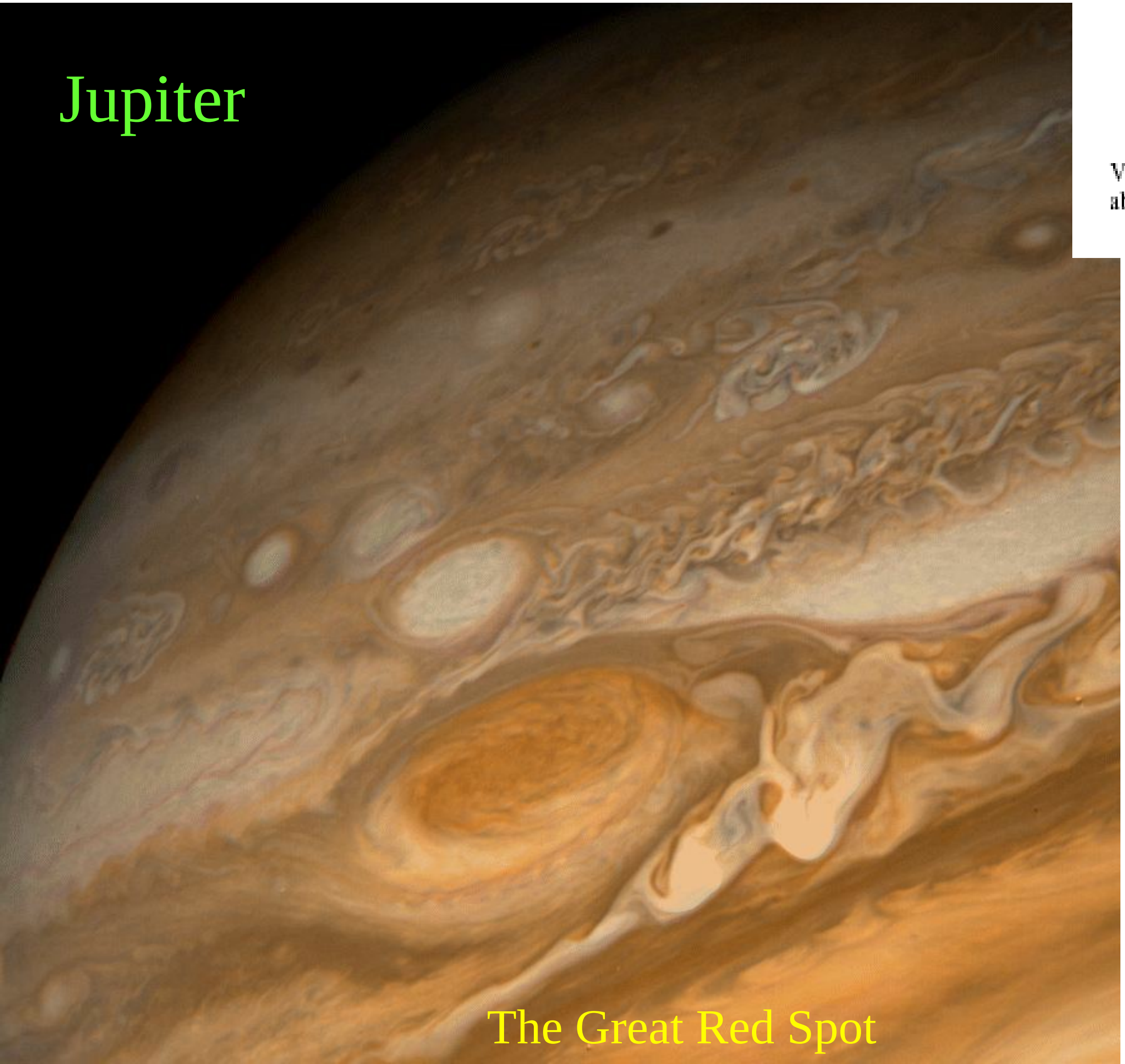

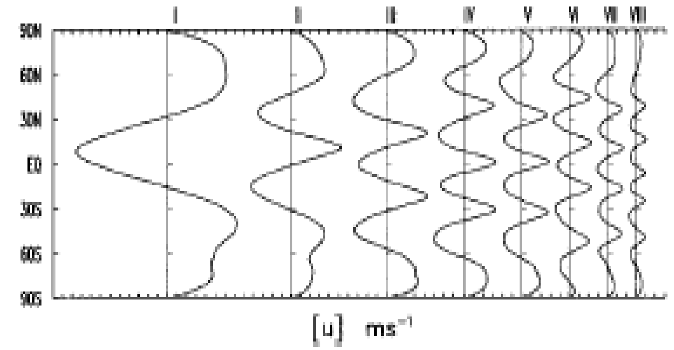

FIG. 4. Time-mean zonal-mean zonal wind profiles for cases I–VIII in Table 1 (the eight open circles in Fig. 3). Each grid on the abscissa represents 1 m s^{-1}.

Huang and Robinson 1998

Alternating Zonal Structures

賀伯颱風的橢圓形眼　Kuo et al. 1999

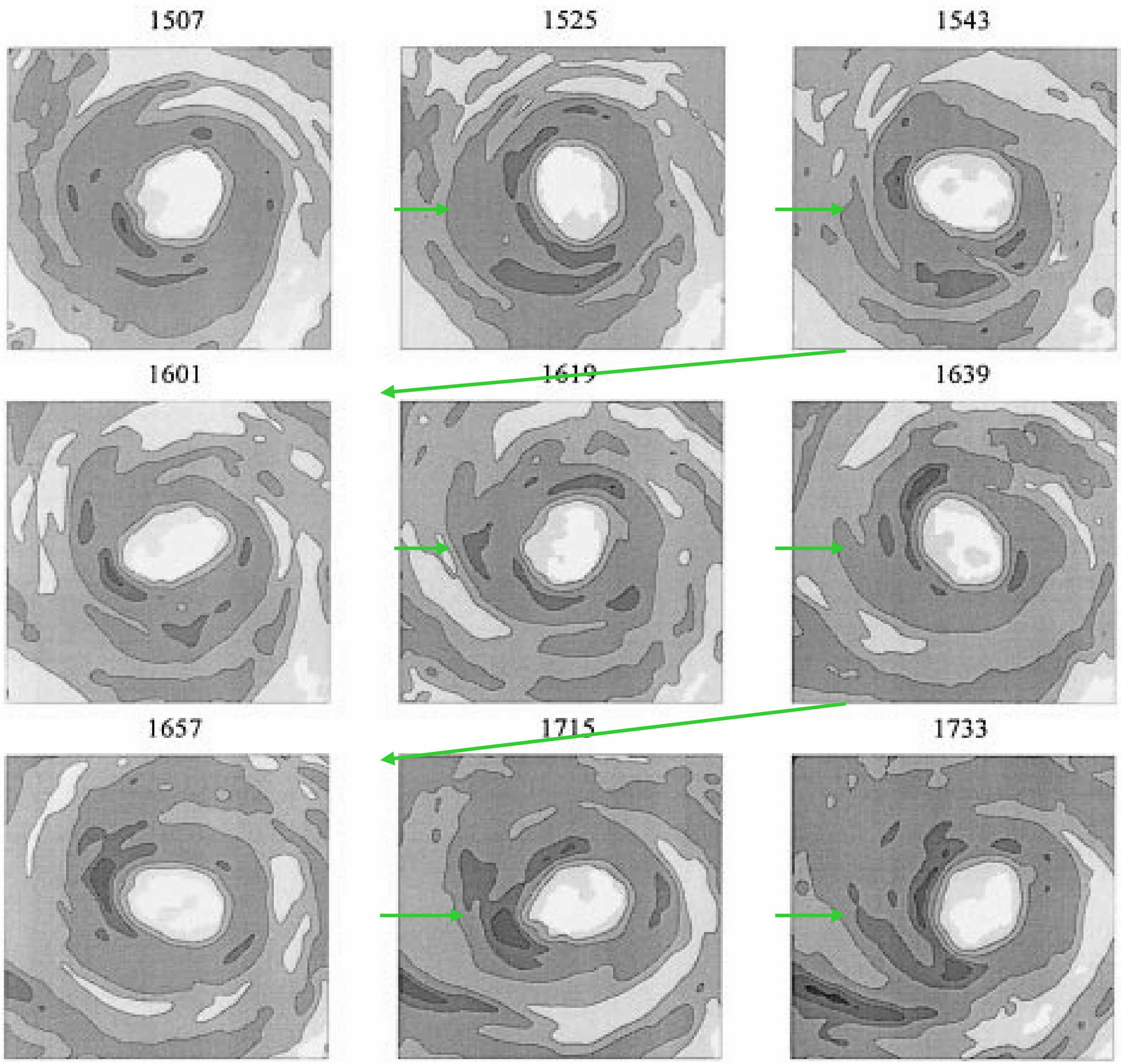

FIG. 1. Horizontal distribution of maximum reflectivity in the vertical column for Typhoon Herb from the Central Weather Bureau WSR-88D (10 cm) radar at Wu-Feng Mountain on 31 Jul 1996. The sequence of images is from left to right and from top to bottom. The time interval between each image is approximately 18 min. The local time of observation is indicated on top of each image. The major axis radius in the eye region is about 30 km and the minor axis radius is about 20 km. The nine images illustrate one eye rotation period of 144 min.

144 min rotation period

Coherent vortex

Dispersion resistant

Vorticity Dynamics

Nonlinear glue

Nonlinear Dynamics

Eye rotation is nonlinear

$J(\psi,\zeta) \quad >> \quad J(\psi,\zeta)$

EXP 1 EXP 2

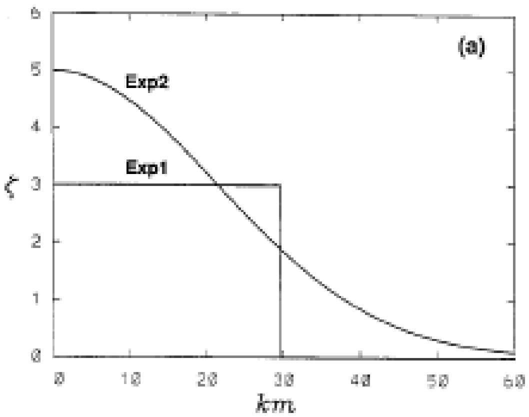

T= 0 min

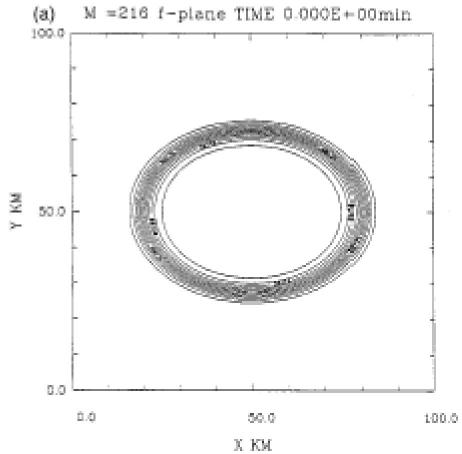

T= 0 min

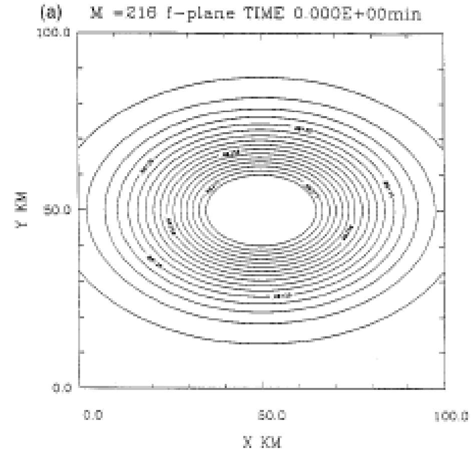

T= 144 min

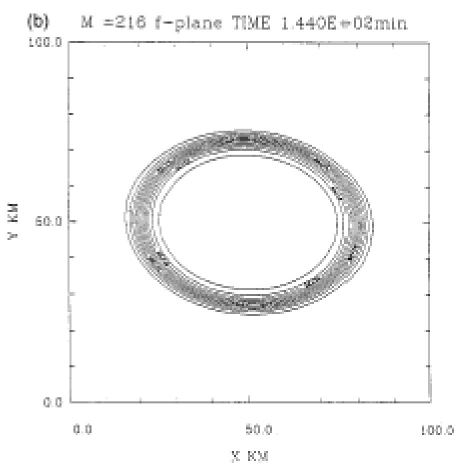

T= 144 min

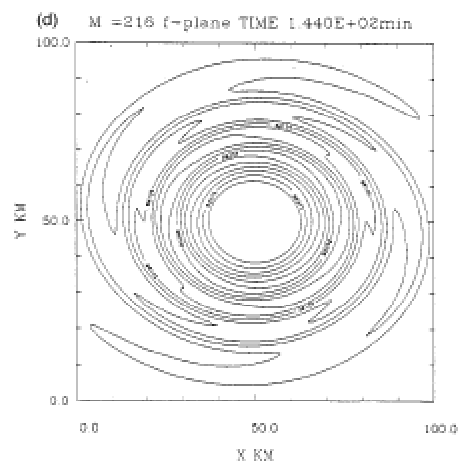

$$\frac{\partial}{\partial t}\zeta + J(\psi,\zeta) = 0$$

Electron density redistribution in experimental plasma physics

single sign charge

+

axial magnetic field

confinement

$$\mathbf{E} = -\nabla\psi$$

$$\nabla\cdot\mathbf{E} = -\nabla^2\psi = \frac{\rho}{\epsilon}$$

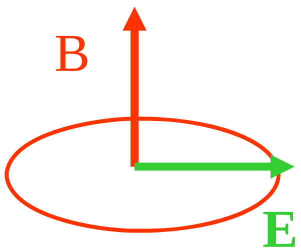

$\vec{E}\times\vec{B}$ drift

Coriolis force

Axisymmetrization 軸對稱化

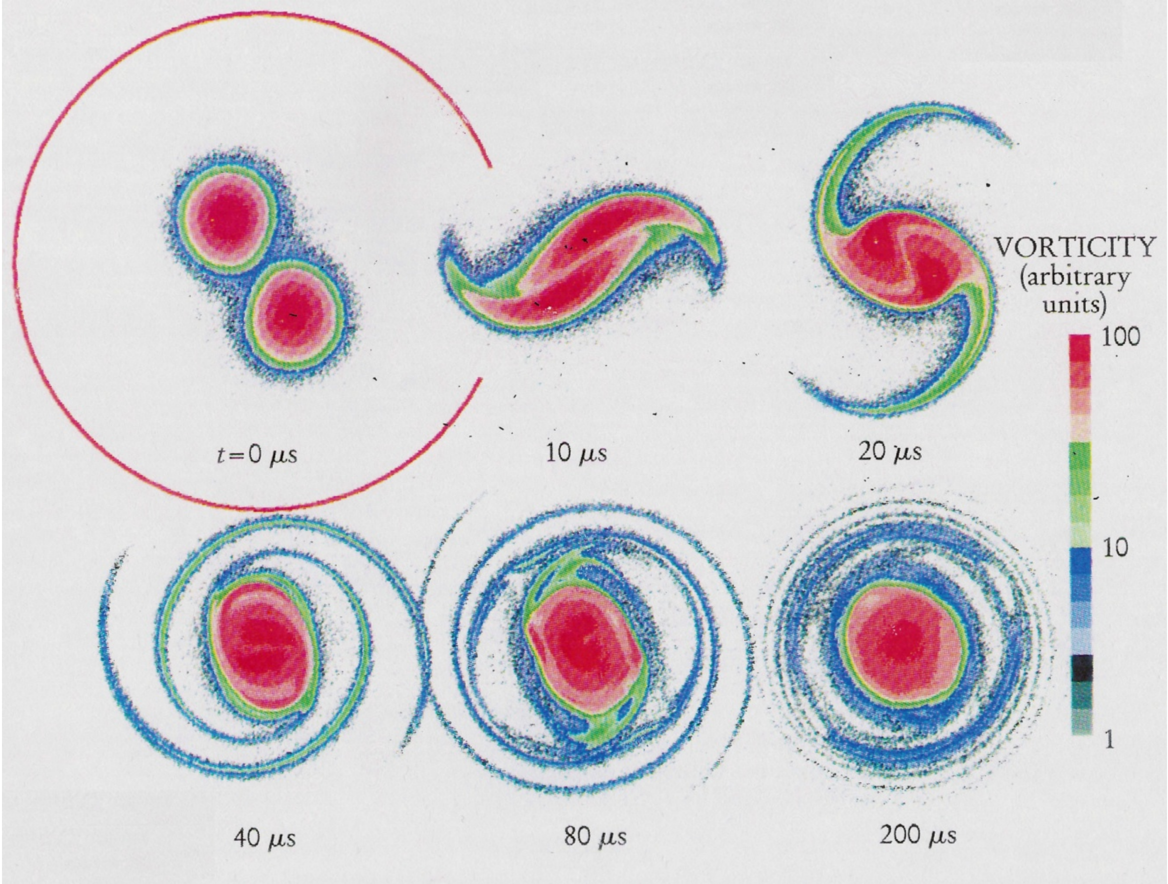

Core is protected, thin filaments from edges

Either Ooyama or WISHE theories,
a finite amplitude disturbance is required
for the cyclongenersis!

Convection

Vorticity dynamics $d\zeta/dt \sim \zeta \nabla \cdot \mathbf{V}$

Turbulence Upscale transfer of convective energy
in rotating environment

A major issue in understanding changes in typhoon intensity

Black and Willoughby (1992)
Hurricane Gilbert (1988)

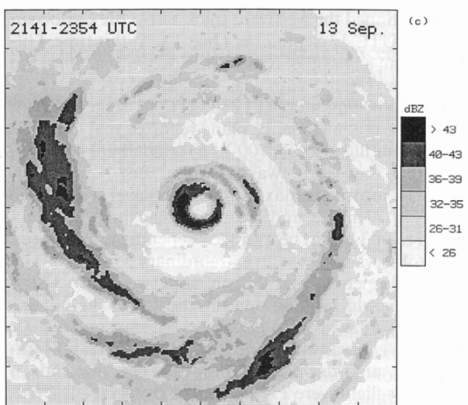

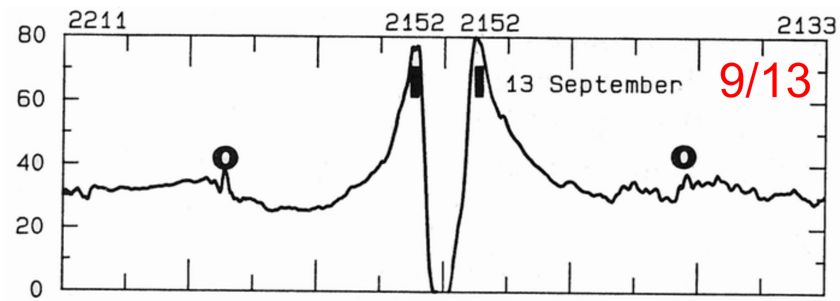

Development of symmetric structure from asymmetric convection in 12 hours

The contraction of the Outer tangential wind maximum

Core vortex intensity remains approximately the same during the contraction period

Inner core dissipate, TC weakens

Thoughts from the 80's and 90's

Shapiro and Willoughby (1982) and Schubert and Hack (1982) proposed that heating-vorticity interaction can lead to convective-ring contraction.

$$d\zeta/dt \sim \zeta \nabla \cdot \mathbf{V}$$

Stronger ζ near the TC core favors the inward response

Symmetrical Model

Moat formation and eyewall replacement are related to the subsidence and the moisture cut-off.

Black and Willoughby (1992)

Vertical cross sections of radar reflectivity of the concentric eyewall

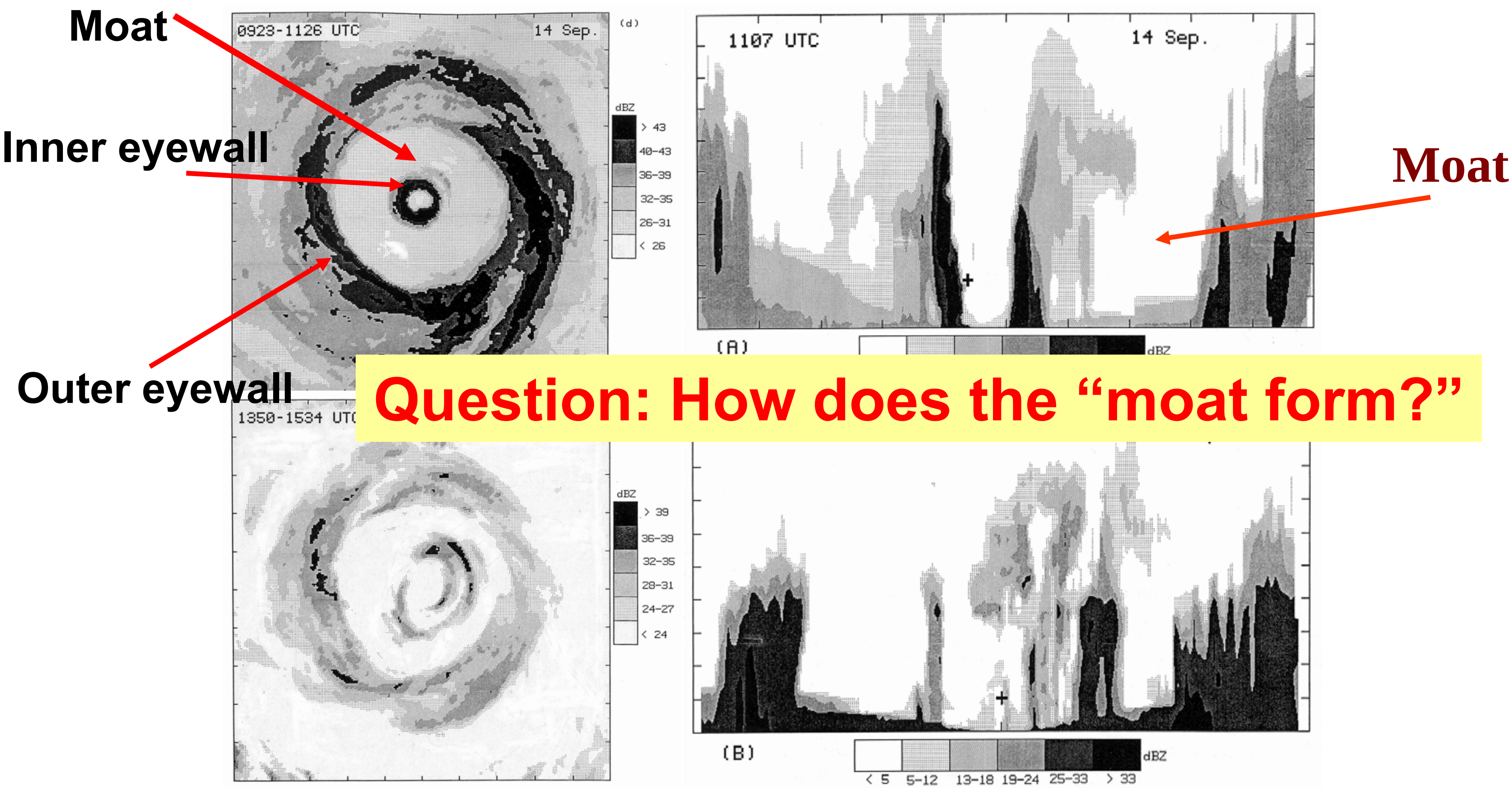

Question: How does the "moat form?"

ELDORA data show downward motion between the two eyewalls

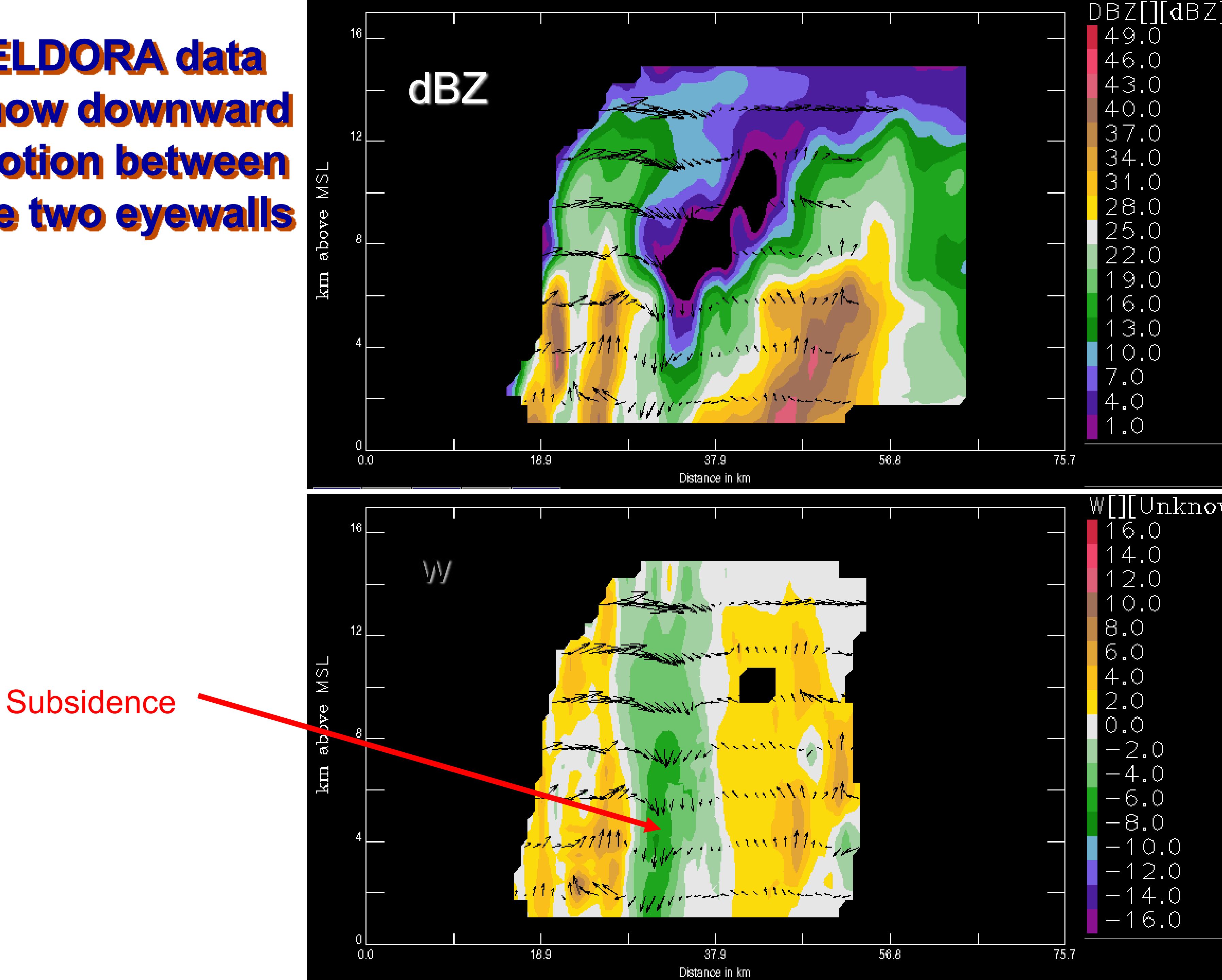

Rozoff et al. (2006)

The strong differential rotation outside the radius of maximum wind of the core vortex may also contribute to the formation and maintenance of the moat.

The Rapid Filamentation Zone: A zone with the filamentation time smaller than the 30 min convective turnover time.

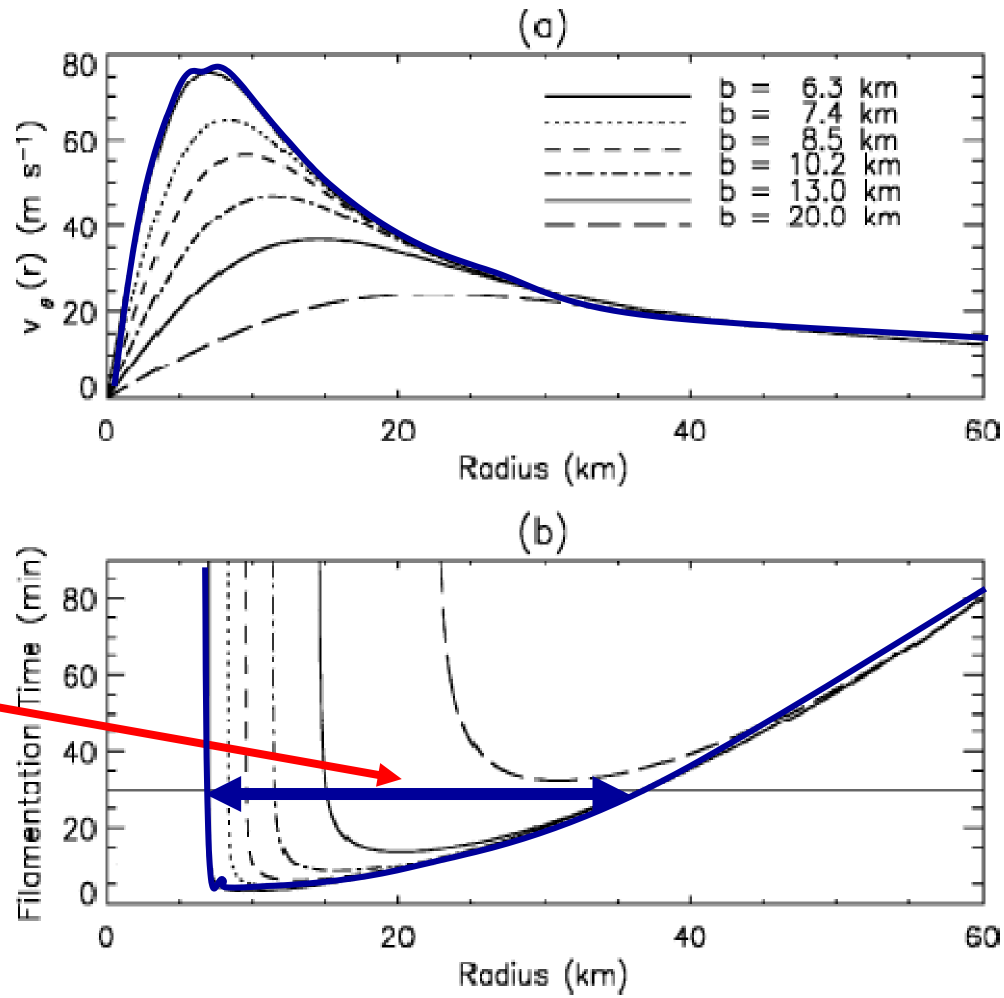

FIG. 2. (a) Radial profiles of $v_\theta(r)$ as given by (15) for six different values of the parameter b. (b) Corresponding radial profiles of $\tau_{fil}(r)$ as given by (16). The filamentation times $\tau_{fil}(r)$ are plotted only in the strain-dominated regions, where $S_1^2 + S_2^2 - \zeta^2 > 0$.

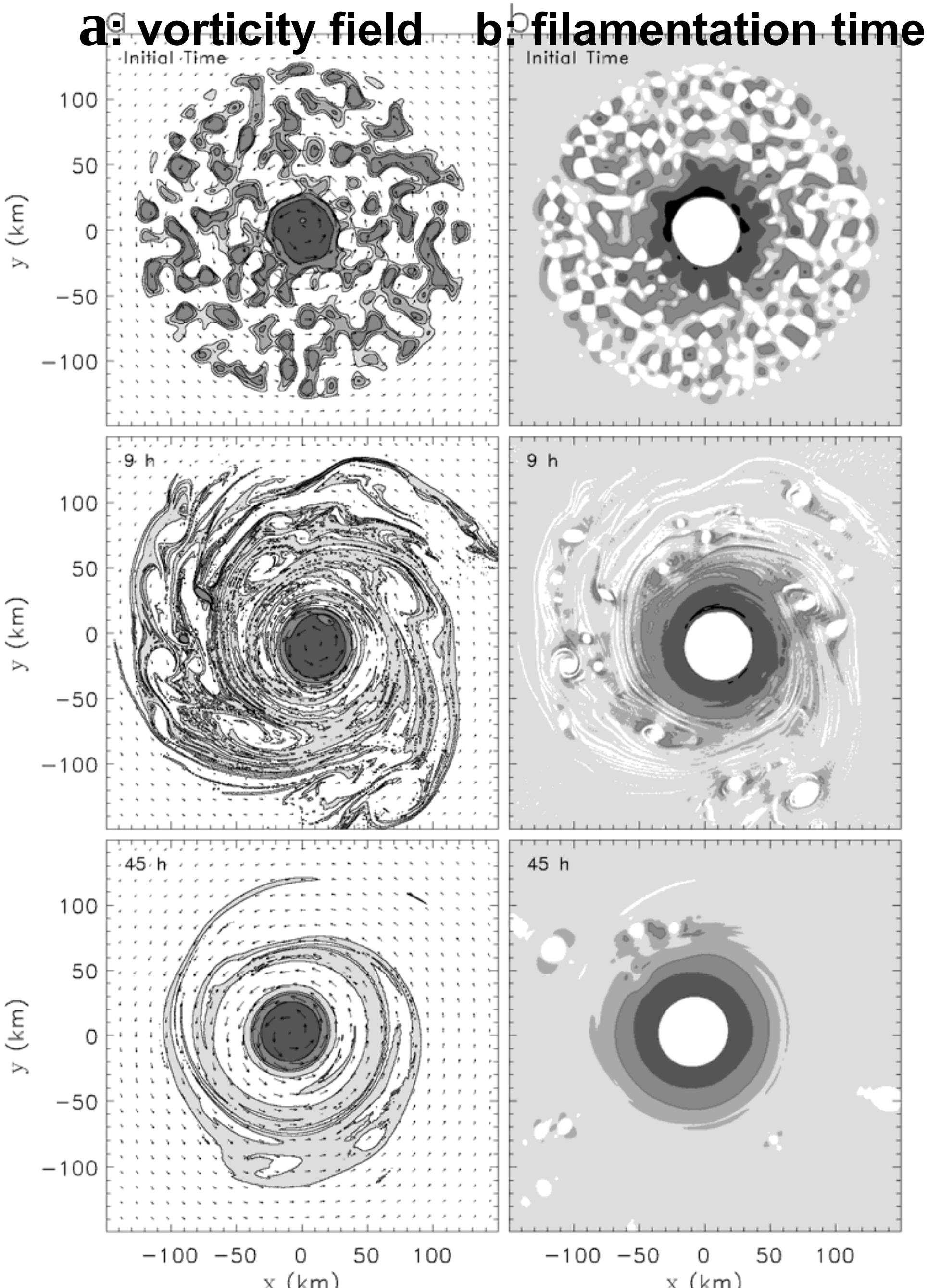

$\zeta \sim 10^{-4} s^{-1}$

Rozoff et al. (2006)

interaction between
a strong core vortex and
a background turbulent vorticity field.

The strong differential rotation outside the radius of maximum wind of the core vortex may also contribute to the formation and maintenance of the moat.

➔ The rapid filamentation zones. (< 30 min?)

Concentric eyewalls formation in Typhoon Lekima (2001) near Taiwan

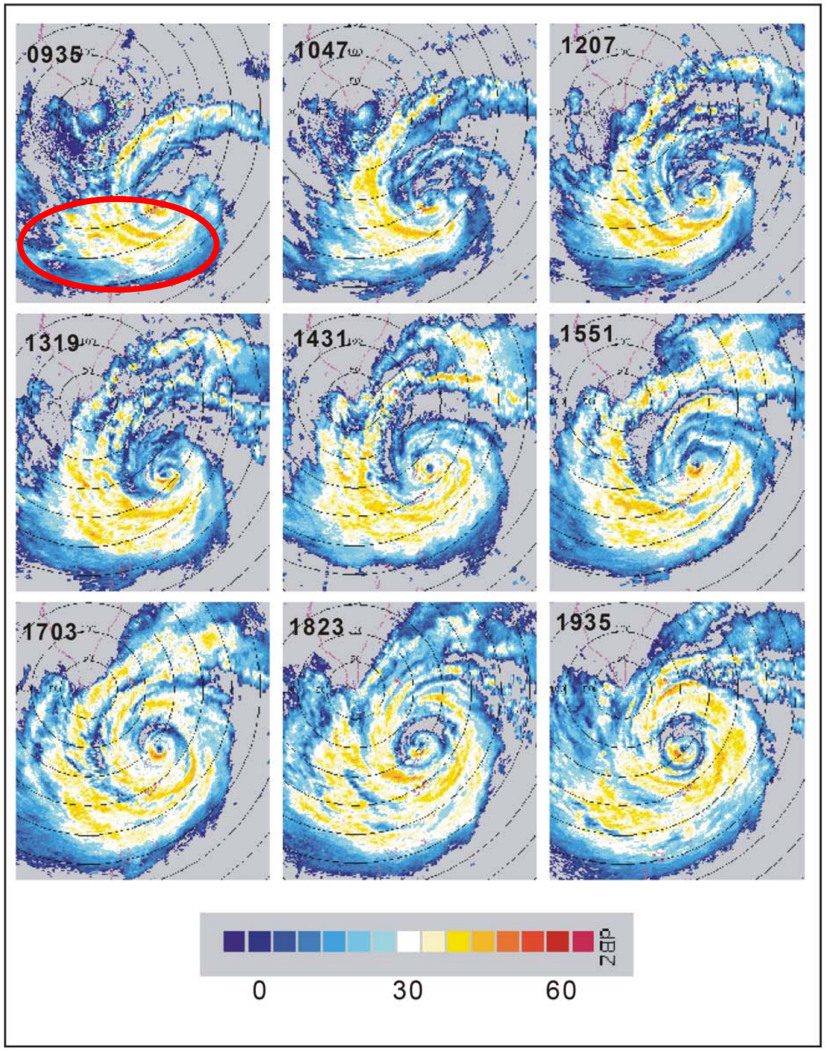

Figure 1a: Reflectivity at 0.5 elevation angle for Typhoon Lekima (2001) from the Central Weather Bureau WSR-88D (10 cm) radar at Kung-Ting for the period 0935 to 1935 September 25. The sequence of the images is from left to right and from top to bottom. The time interval between each image is approximately 75 min. The local time of observation is indicated on top of each image. The radial increment of the circles centered at radar station is 50 km. The nine images illustrate the formation of a concentric eyewalls.

Asymmetric Dynamics

Kuo et al. (2004)

Typhoon Lekima (2001)

0935-1935 LST

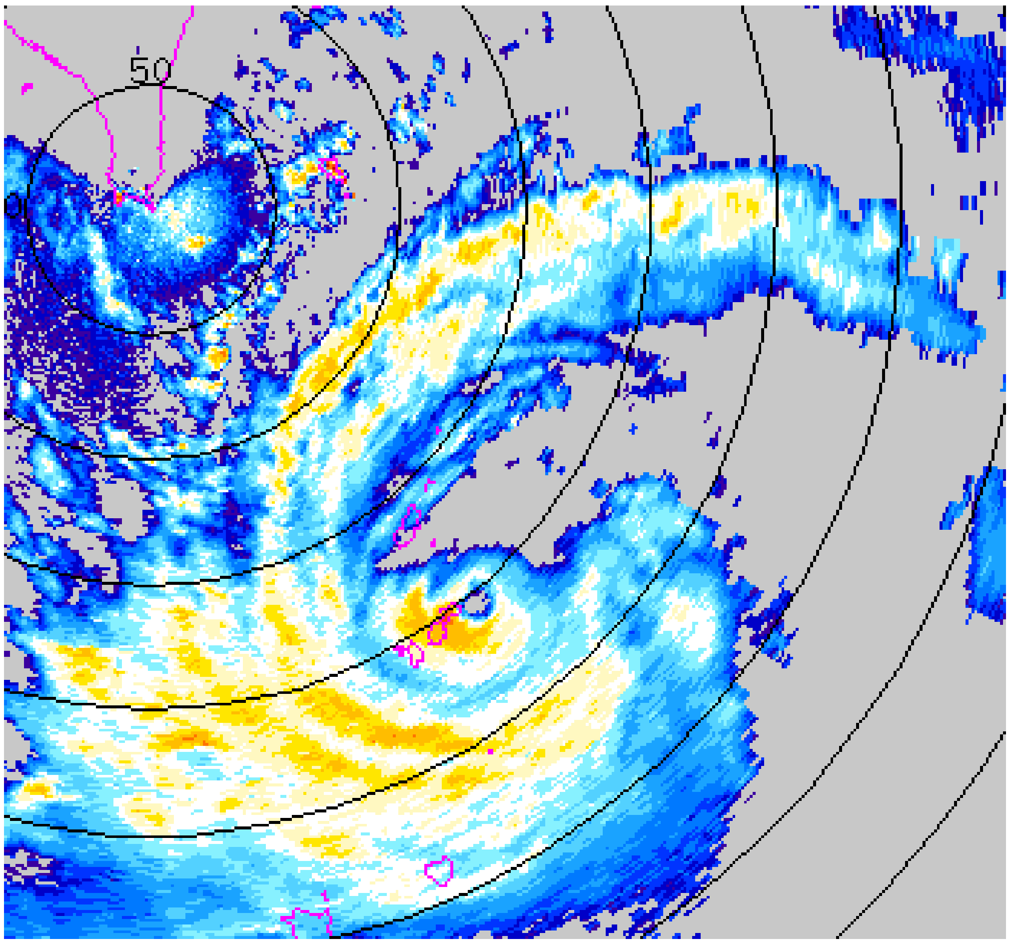

0925 1900LST

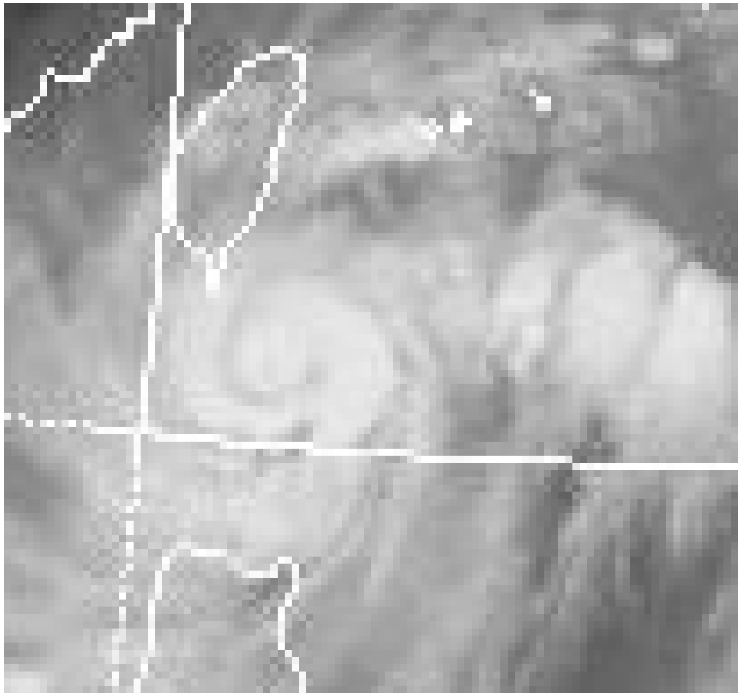

Formation of concentric vorticity structure in Lekima (2001)

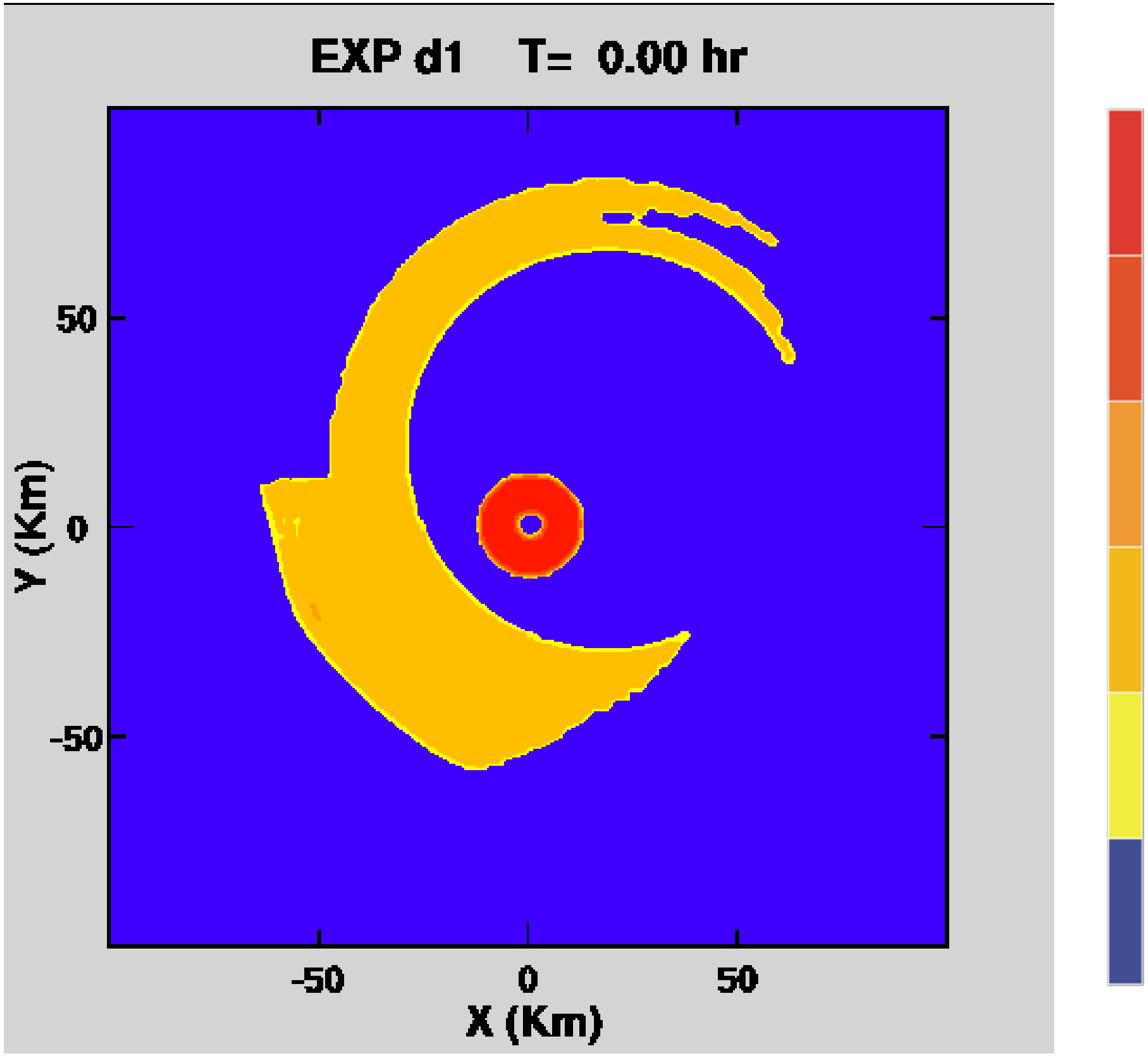

Binary vortex interaction

Dritschel and Waugh (1992)

【Variables】

R_1, R_2

Δ

ζ

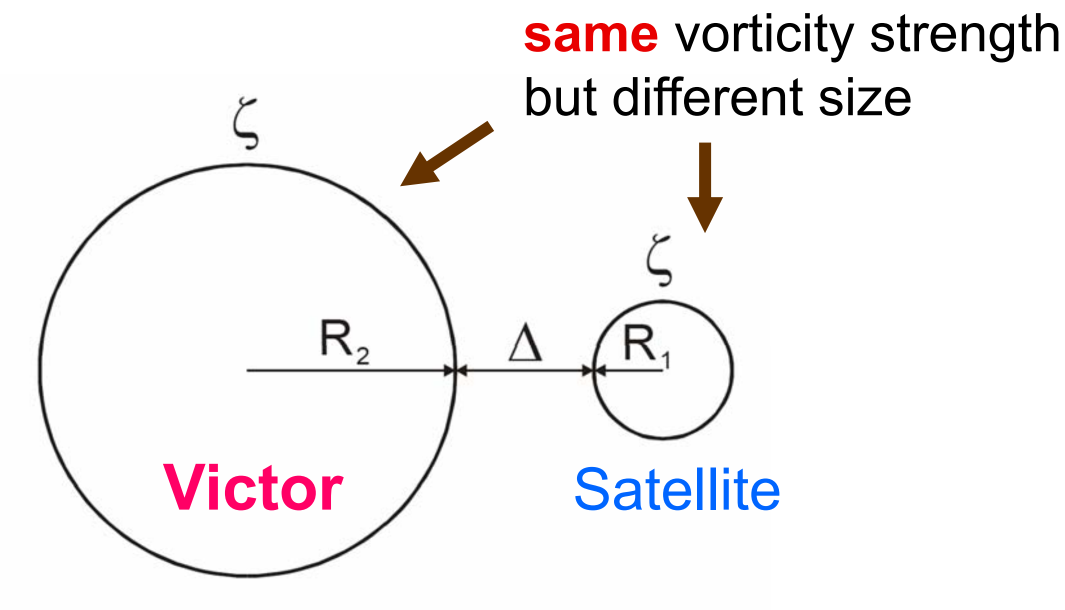

【**Parameters**】

- Vortex radius ratio $(r) = \dfrac{R_1}{R_2}$
- Dimensionl ess gap $(\dfrac{\Delta}{R_1})$

【**Regimes**】

- Elastic Interaction (EI)
- Partial straining-out (PSO)
- Complete straining-out (CSO)
- Partial merger (PM)
- Complete merger (CM)

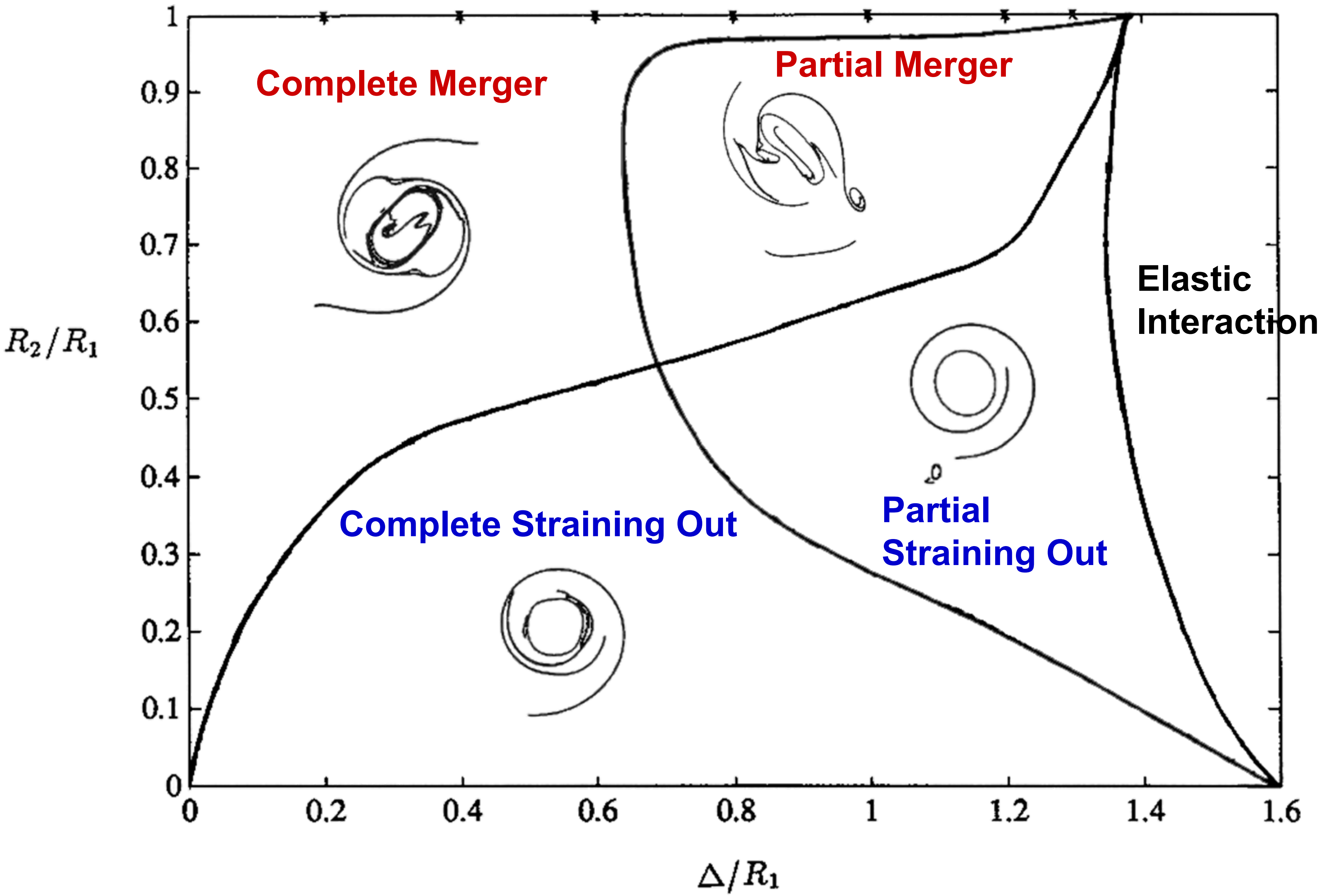

(Adapted from Dritschel and Waugh 1992.)

Elastic interaction regime

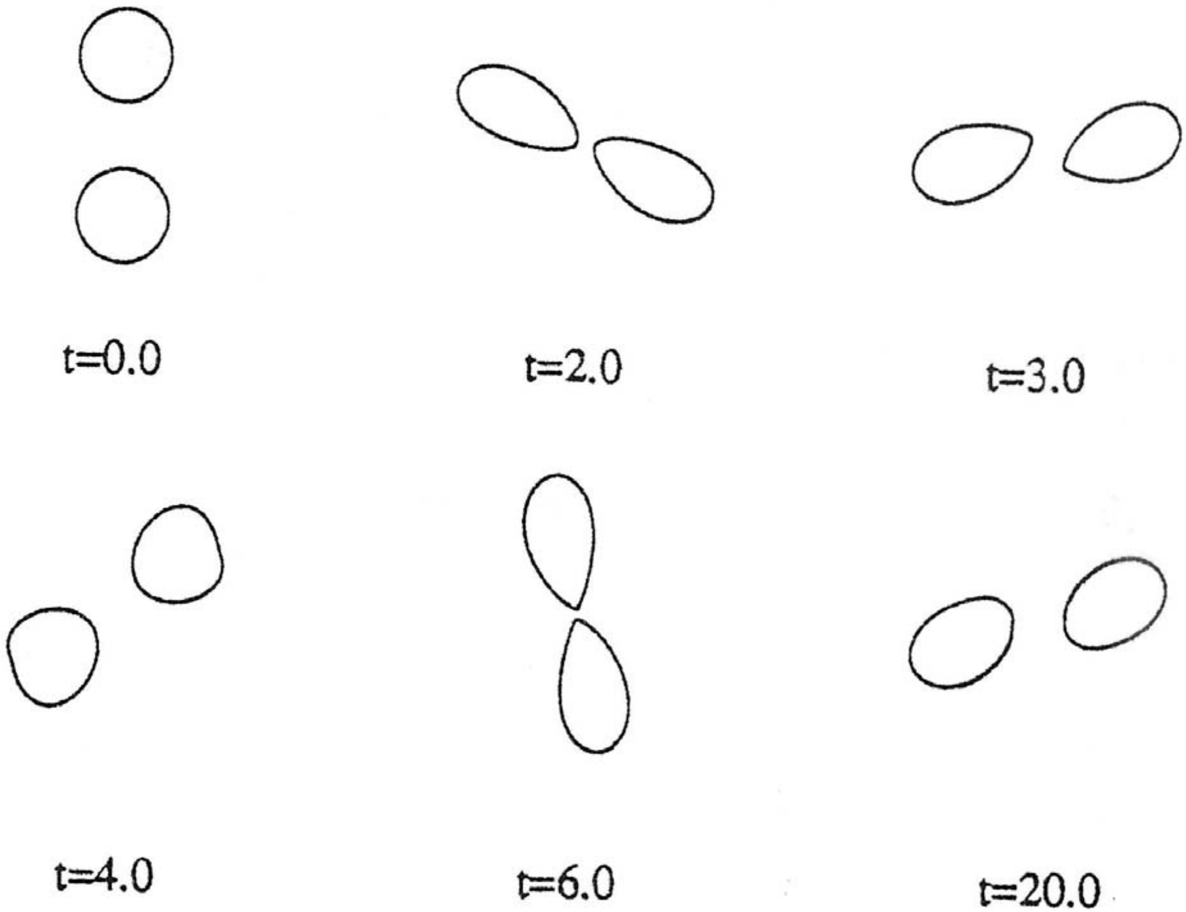

雙颱風的互繞 ----藤原效應

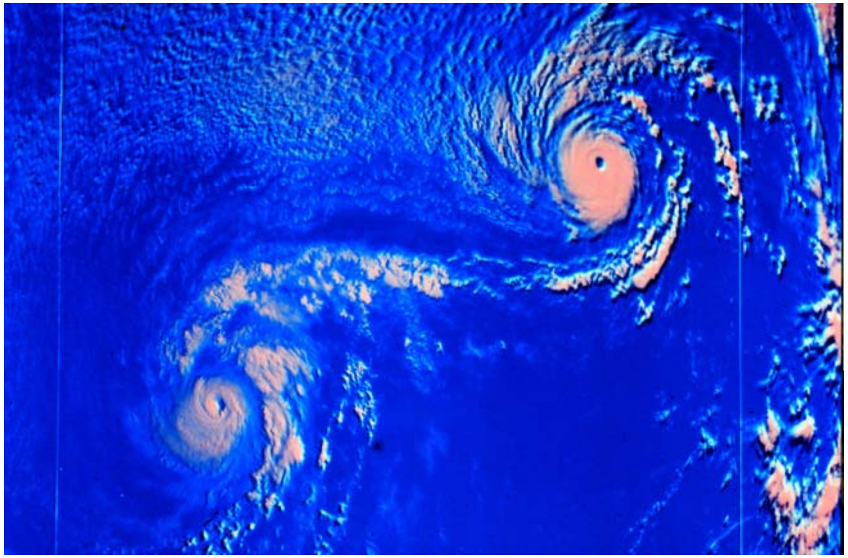

颱風 Ione 與 Kristen

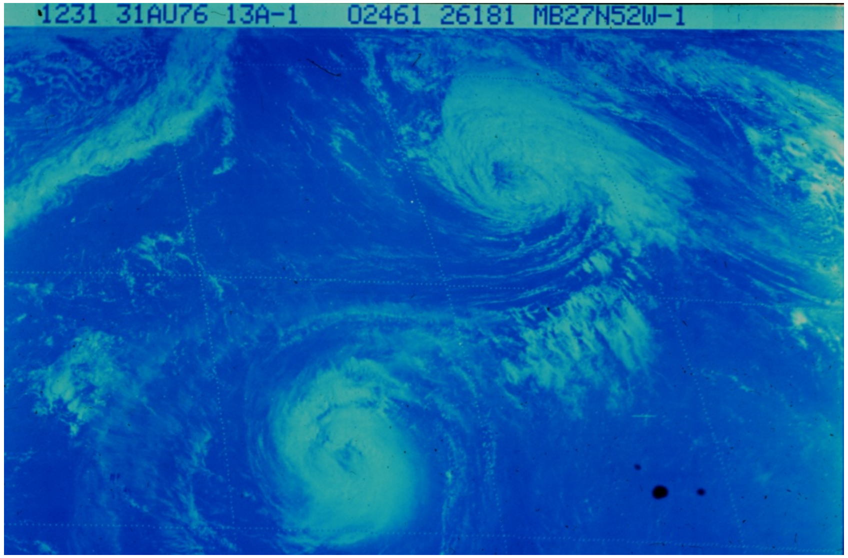

颱風 Emmy 與 Frances

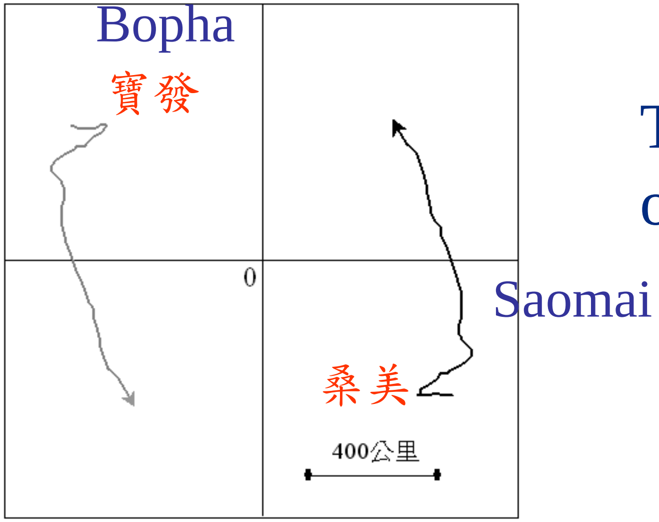

The unusual south movement of Typhoon Bopha

Merger regime

partial merger (PM)

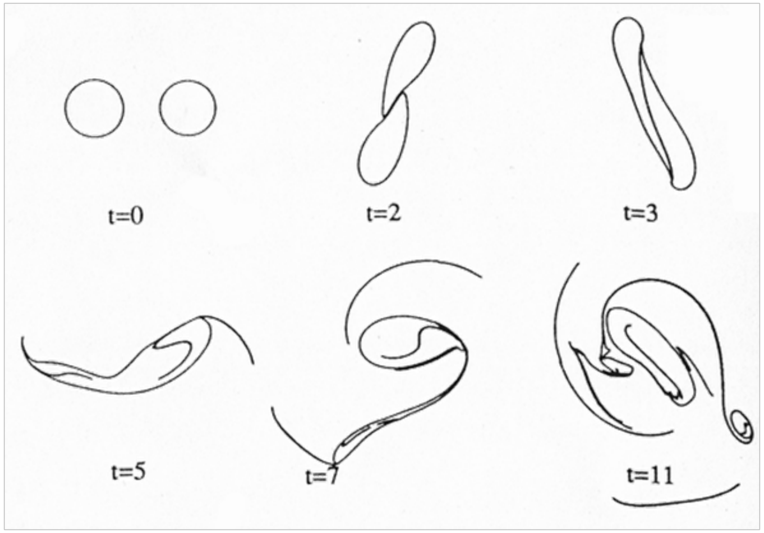

complete merger (CM)

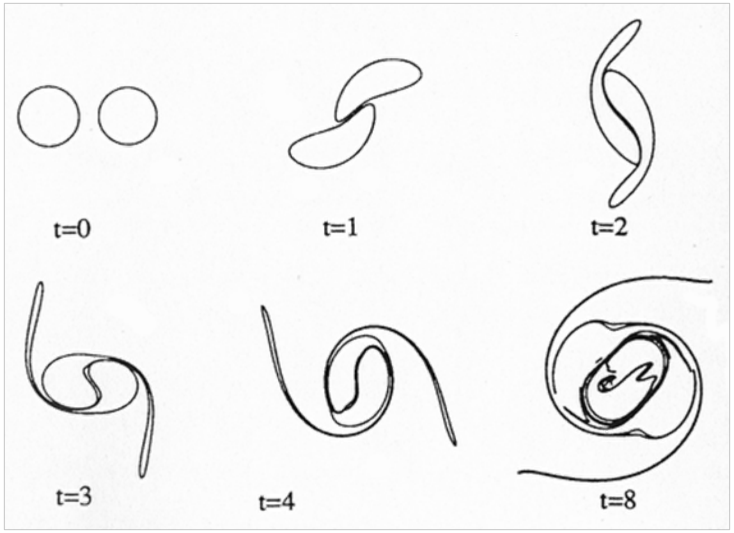

Why ‘merger’ ?

- Chang (1983) – diabatic heating
- DeMaria & Chan (1984) – vortex vorticity gradient
- Dritschel and Waugh (1992)
  – advection + selective decay of 2D turbulence

Merger ---- 颱風 PAT 與 RUTH (1994)

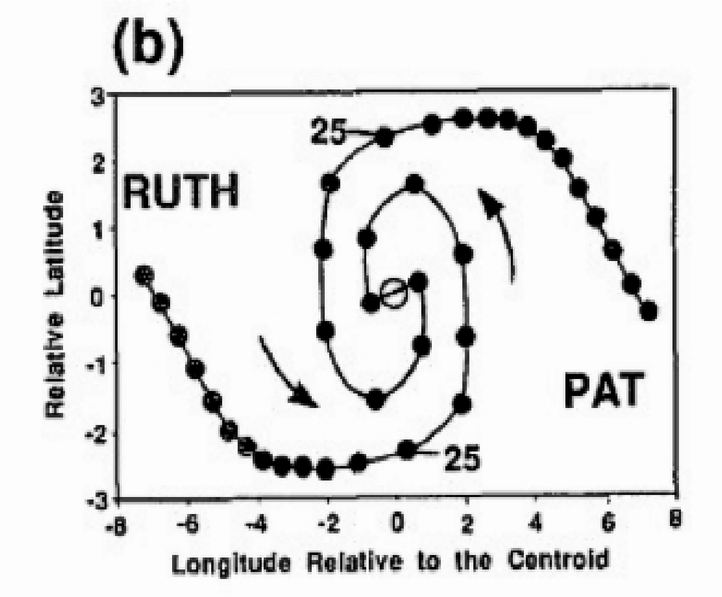

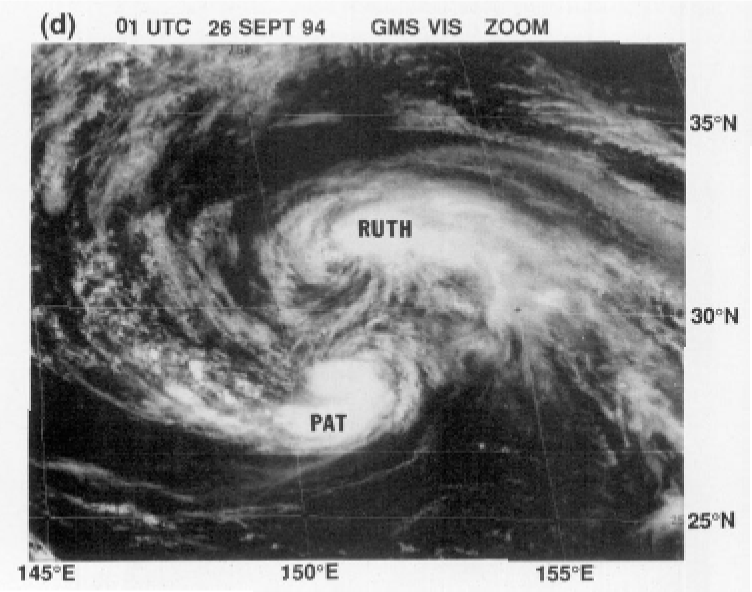

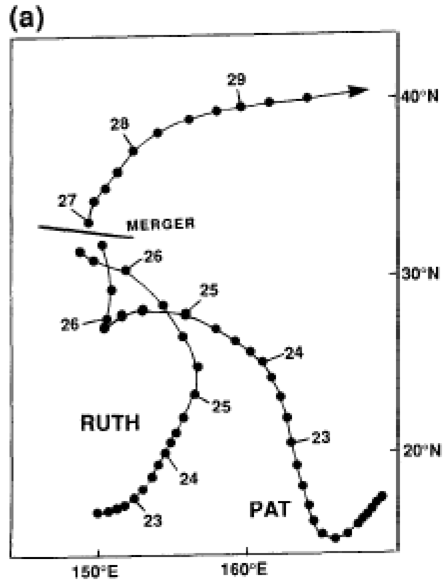

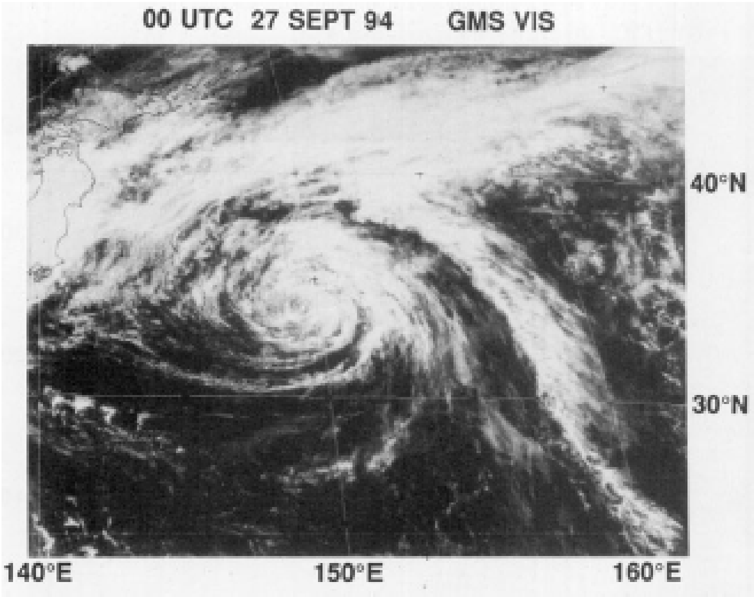

Lander 1995

Lander and Holland
(1993)

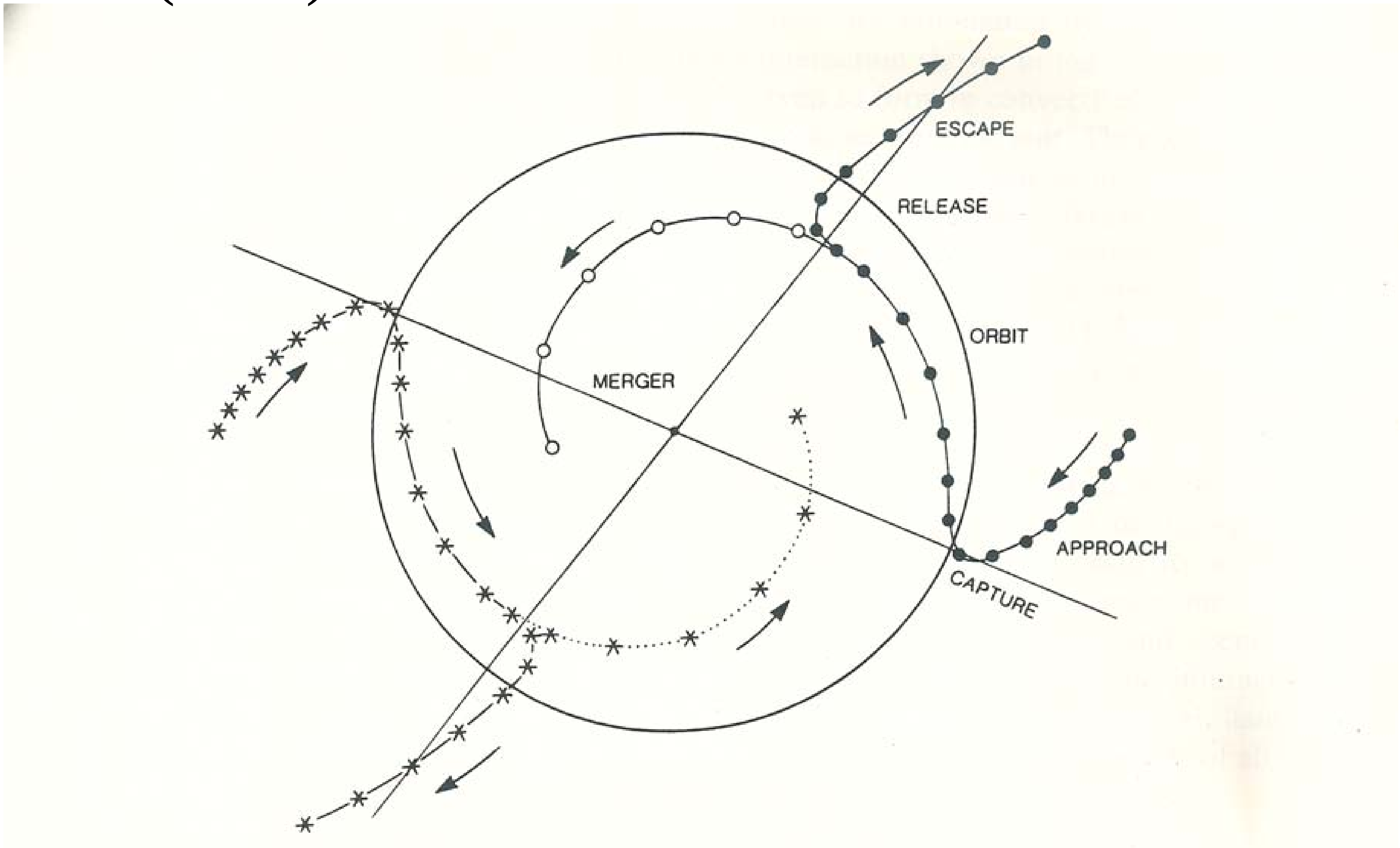

Merger and Elastic Interaction **Chaotic Behavior**

Lander and Holland (1993)

Tracks of mesoscale vortices

Centroid-relative motion of Alpha and Bravo

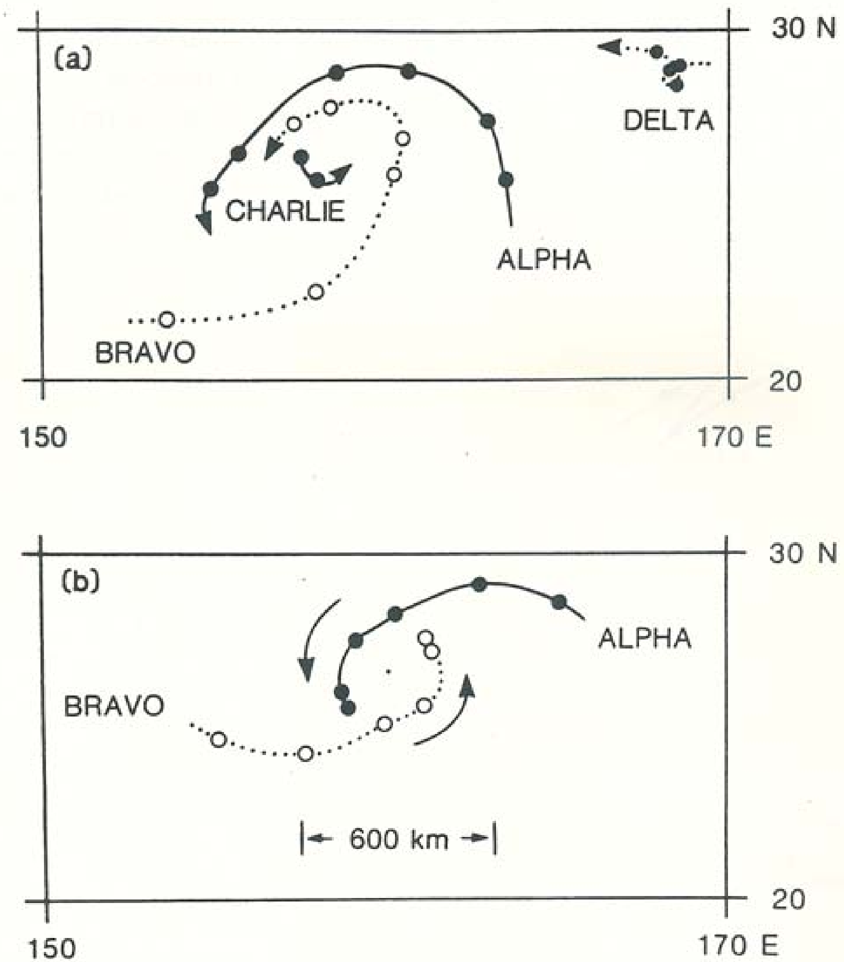

Figure 6. (a) Tracks of mesoscale vortices Alpha, Bravo, Charlie and Delta and (b) centroid-relative motion of Alpha and Bravo. Dots on the tracks are at irregular time intervals and show fixes obtained from visible satellite imagery.

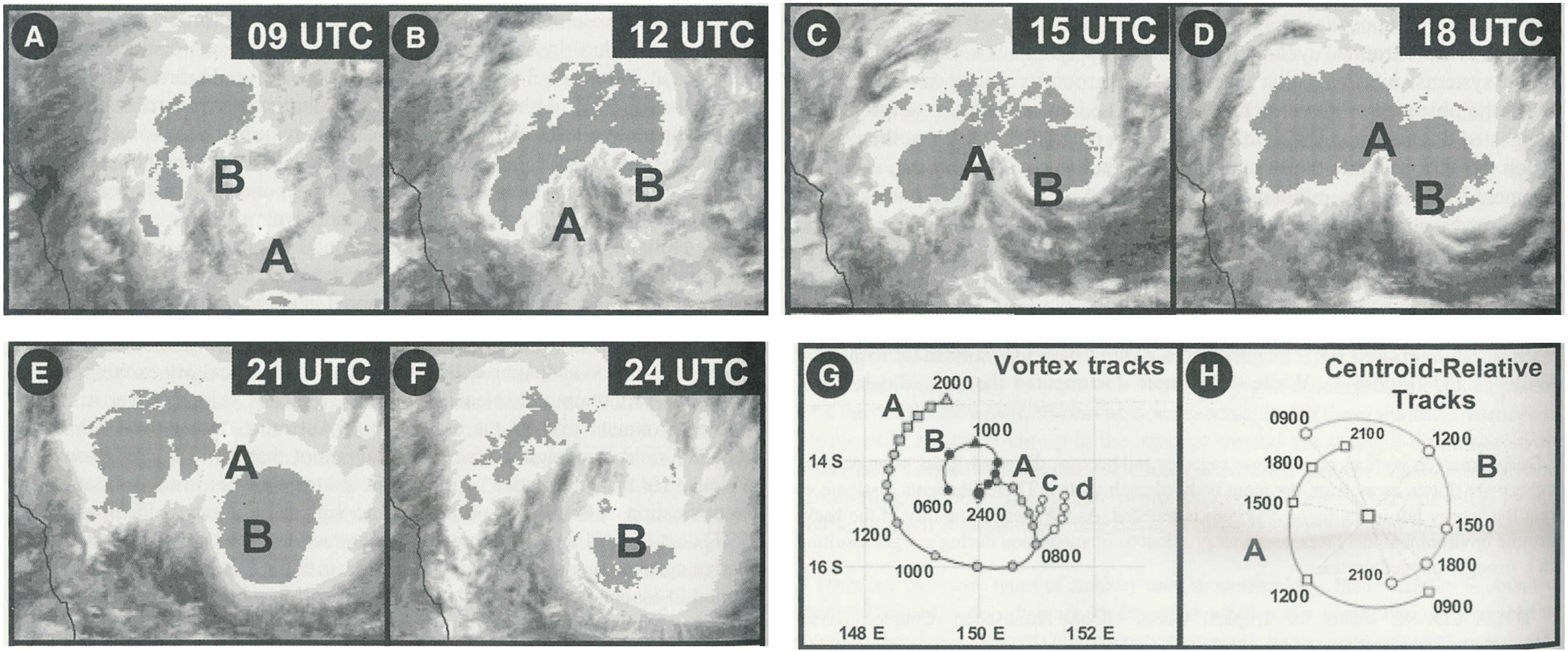

(A)-(F) The locations of the two mesovortices A and B during the development of Tropical Cyclone Oliver superposed on three-hourly satellite imagery for the period 0900 UTC February 4 to 0000 UTC February 5, 1993; (G) Tracks of four of the vortices obtained from radar data. The positions are not evenly spaced and so times (in UTC) of some of the vortex positions are marked; (H) three-hourly centroid-relative tracks of mesovortices A and B from 0900 UTC to 2100 UTC February 4[Simpson et al., 1997].

Hendricks et al. (2004)

"Vortical" Hot Towers

- The net effect of the hot towers is to produce strong small-scale (10km in diameter on average) lower-tropospheric (below z ≈ 5km) cyclonic PV towers.

- The strong updrafts in the hot towers converge and stretch existing low-level vertical vorticity into intense small-scale vortex tubes.

- Multiple mergers / axisymmetrization of these tubes in the lower troposphere.

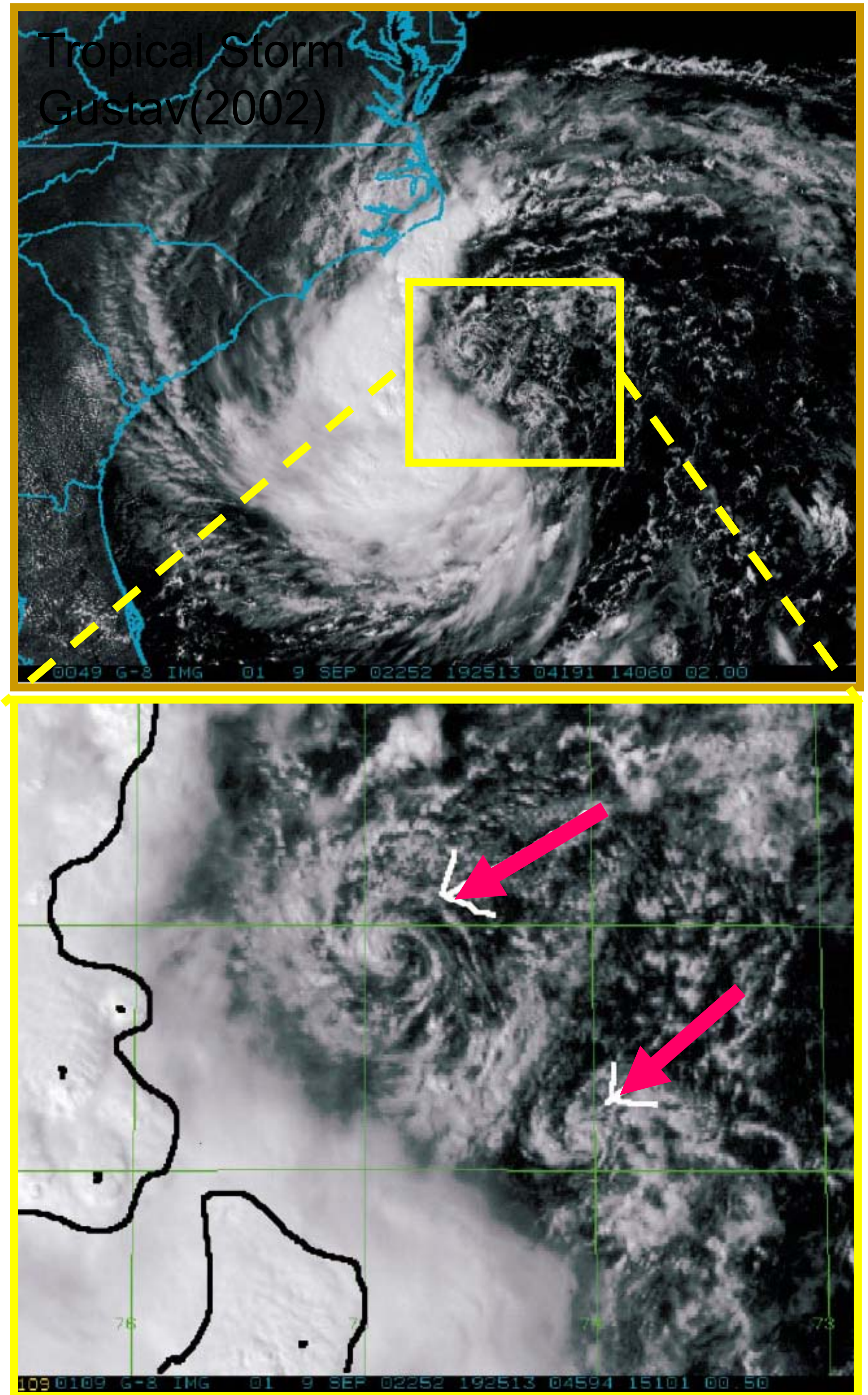

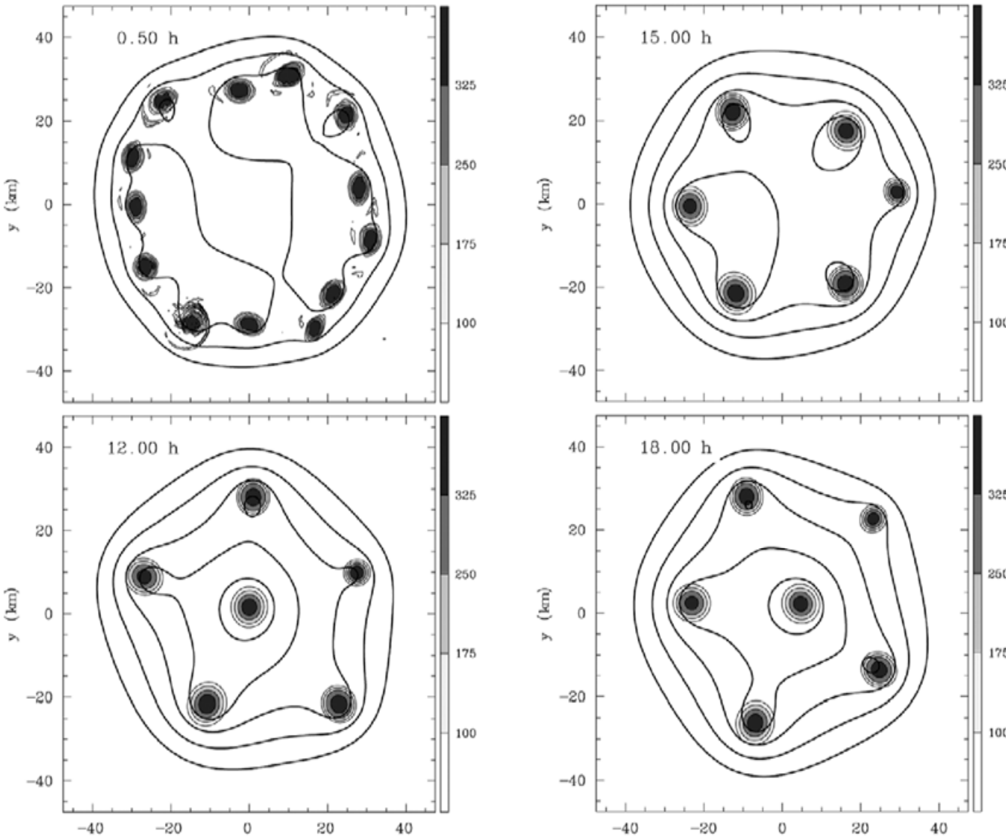

Fɪɢ. 2. Evolution of vorticity (shaded) and streamfunction contours (bold) for the numerical experiment of Kossin and Schubert (2001). Values along the label bar are in units of 10^{-4} s^{-1}. The shape of the streamlines transitions from a pentagon to a hexagon and back to a pentagon over 6 h.

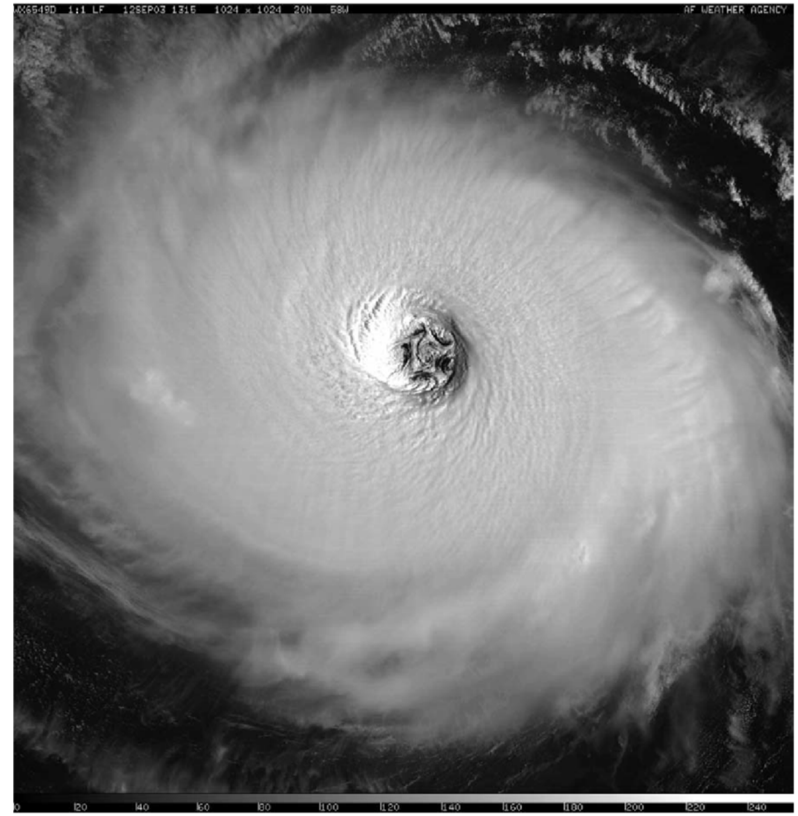

Fɪɢ. 1. Defense Meteorological Satellite Program (DMSP) image of Hurricane Isabel at 1315 UTC 12 Sep 2003. The starfish pattern is caused by the presence of six mesovortices in the eye—one at the eye center and five surrounding it.

MESOVORTICES IN HURRICANE ISABEL

BY JAMES P. KOSSIN AND WAYNE H. SCHUBERT

Importance of Asymmetric Vorticity Dynamics

納莉颱風眼附近的中尺度渦旋

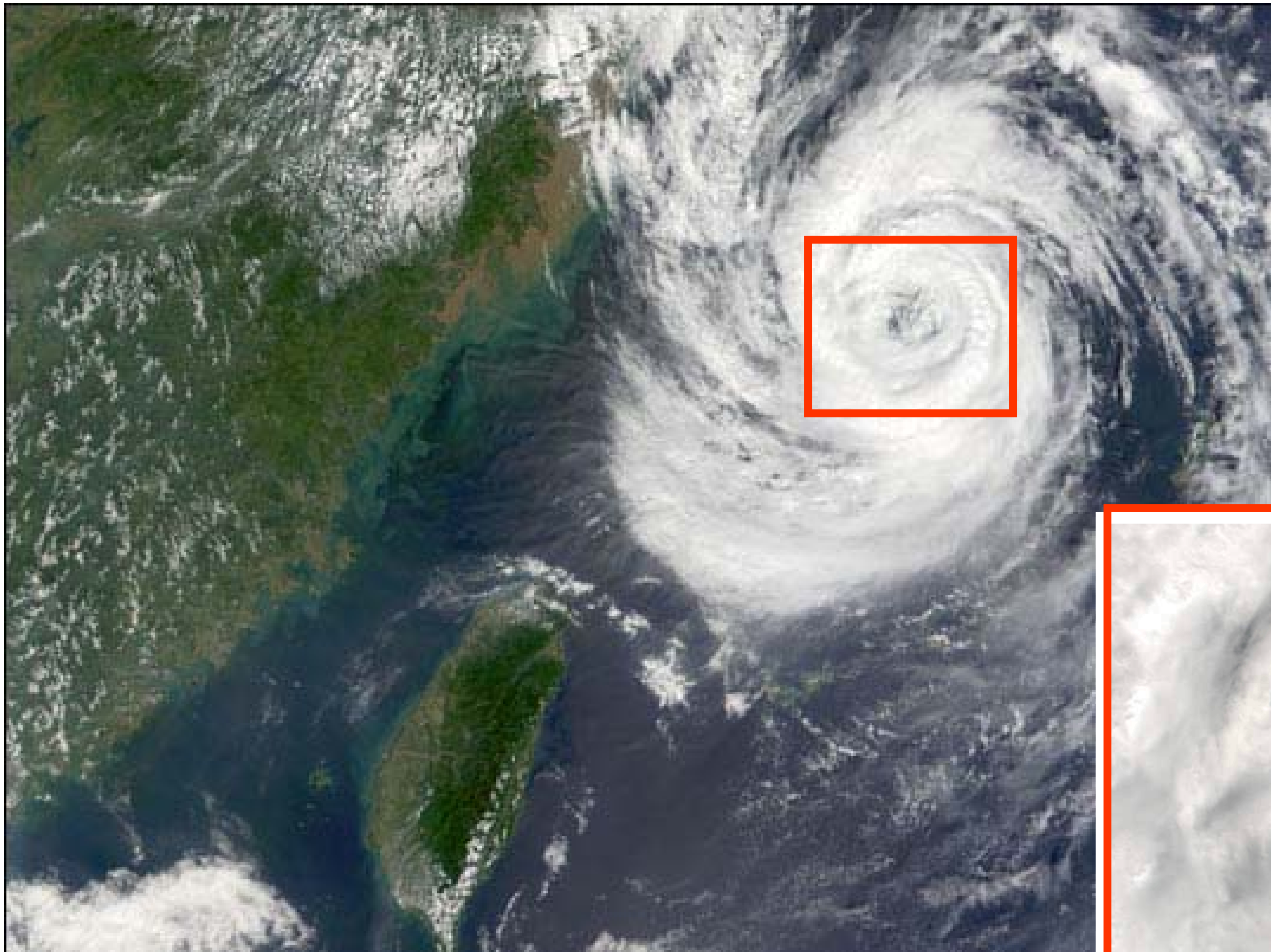

侵台納莉颱風登陸前颱風眼附近觀測到3 個中尺度渦旋

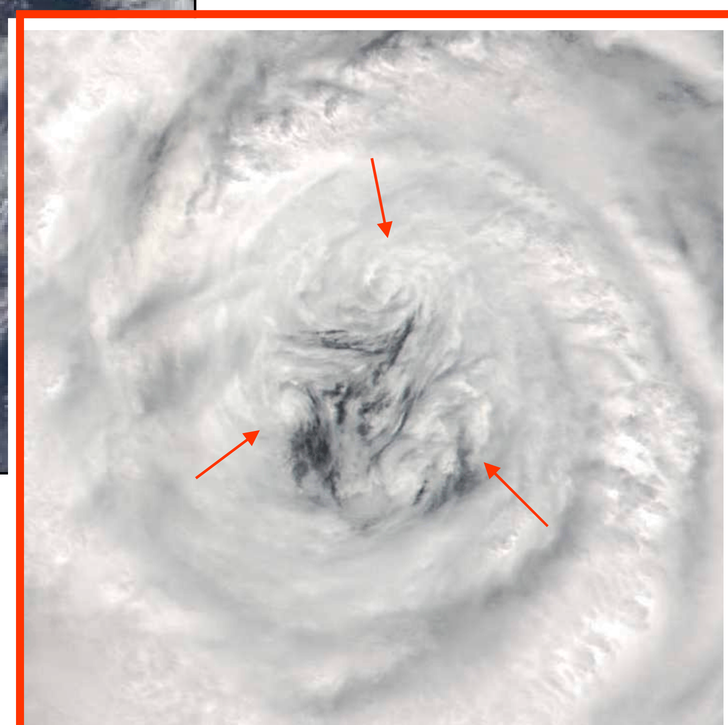

Kossin and Schubert (2002)
Mixing due to Barotropic Instability

20X20 km

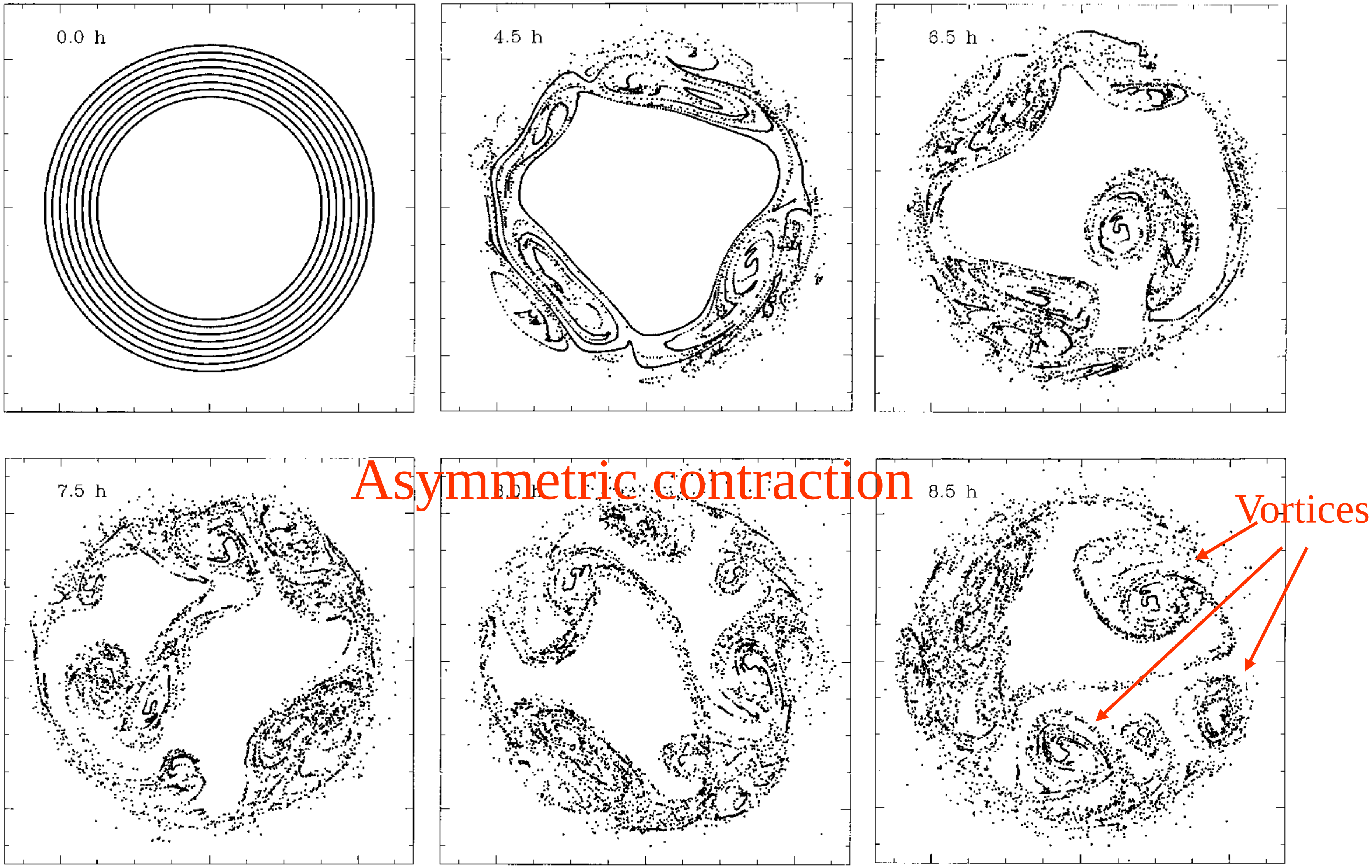

Advective rearrangement is different from the down-gradient diffusion

Straining out regime

partial straining - out (PSO)

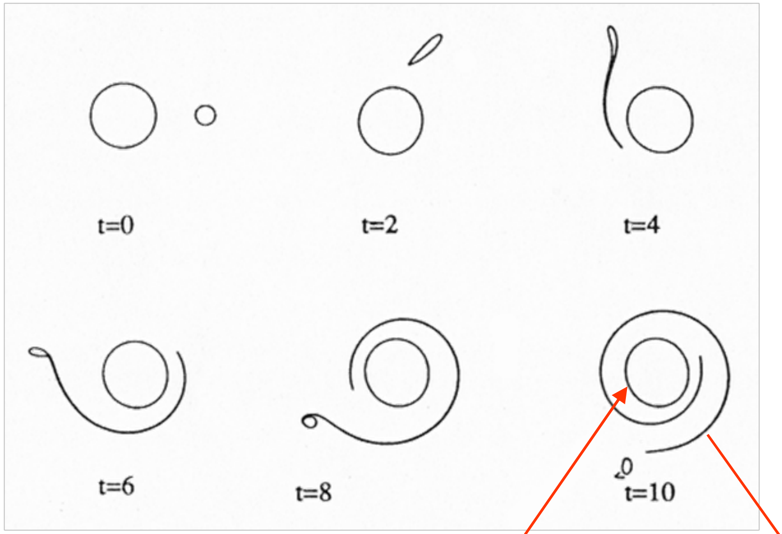

complete straining - out (CSO)

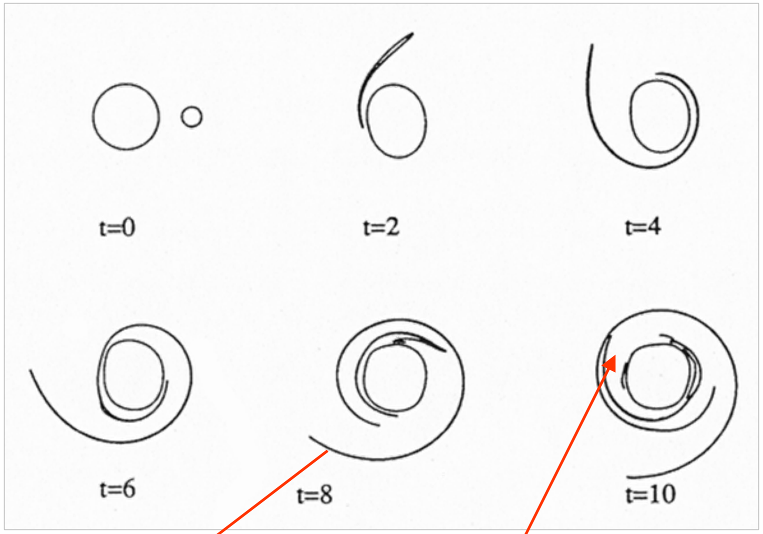

Clear gap

Clear gap

Adverse shear effect

The bands are too thin to be called concentric eyewalls.

Kuo et al. (2000) MWR

Typhoons Zeb and Alex ; straining – out regime

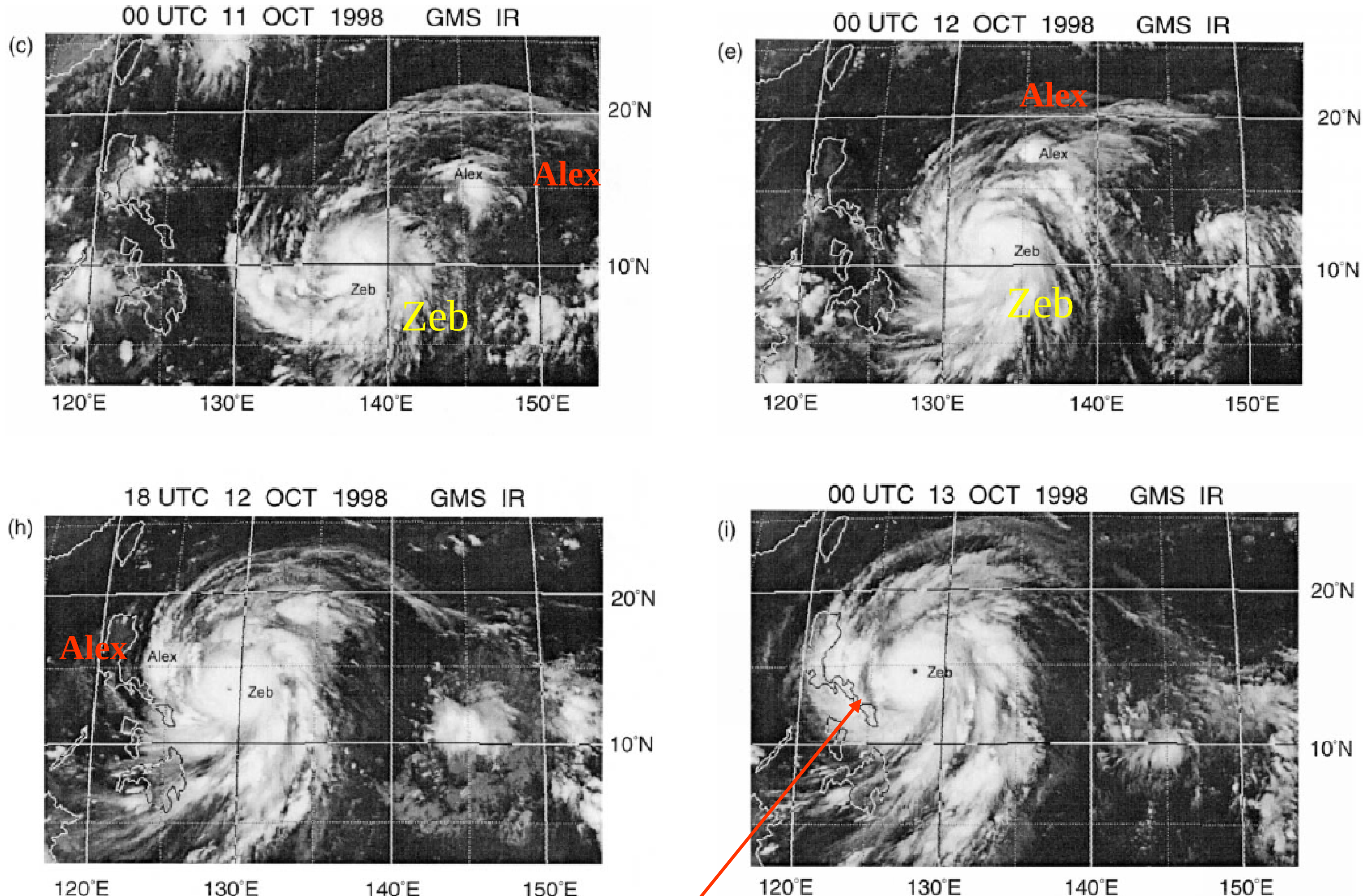

Clear gap between the Zeb and the remains of Alex

Binary vortex interaction

Kuo et al. (2004)

【Variables】

$$R_1, R_2;\ \Delta;\ \zeta_1, \zeta_2$$

【Parameters】

- Vortex radius ratio $(r) = \dfrac{R_1}{R_2}$
- Dimensionl ess gap $(\dfrac{\Delta}{R_1})$
- Vortex strength ratio $(\gamma) = \dfrac{\zeta_1}{\zeta_2}$

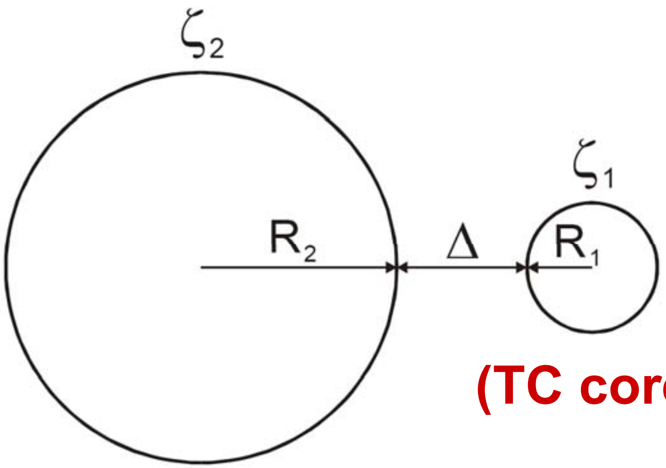

(TC core)

- **An extension of Dritschel and Waugh's (1992) work.**
- **In addition to the radii ratio and the normalized distance between the two vortices, the vorticity ratio is added as a third external parameters.**

$$\gamma = \frac{\zeta_1}{\zeta_2}$$

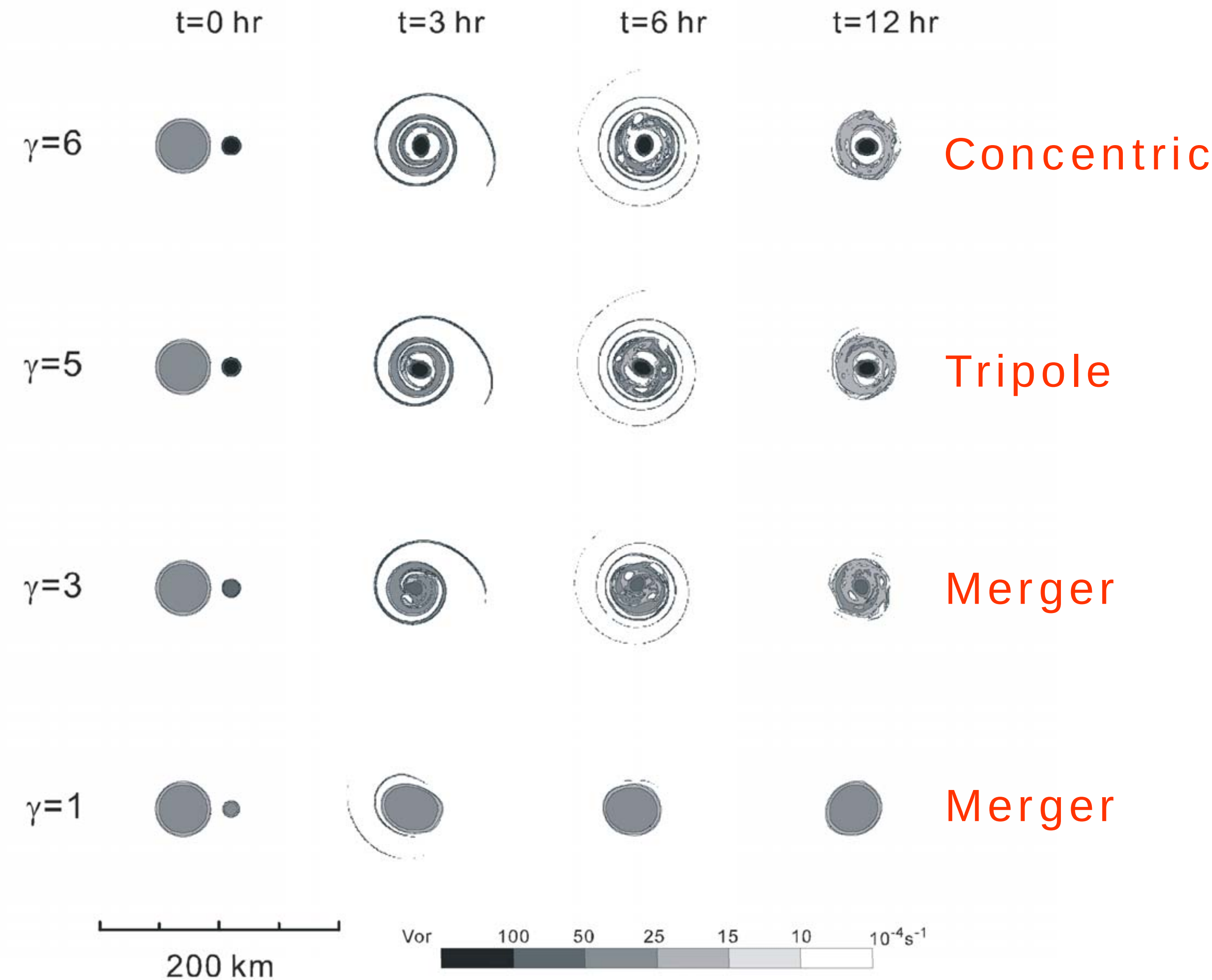

Figure 3: The sensitivity of the vorticity field in the binary vortex experiments with respect to the vorticity strength ratio (γ) at hour 0, 3, 6 and 12 with the dimensionless gap Δ/R_1=1, and the vortex radius ratio r=1/3.

Vortex radius ratio

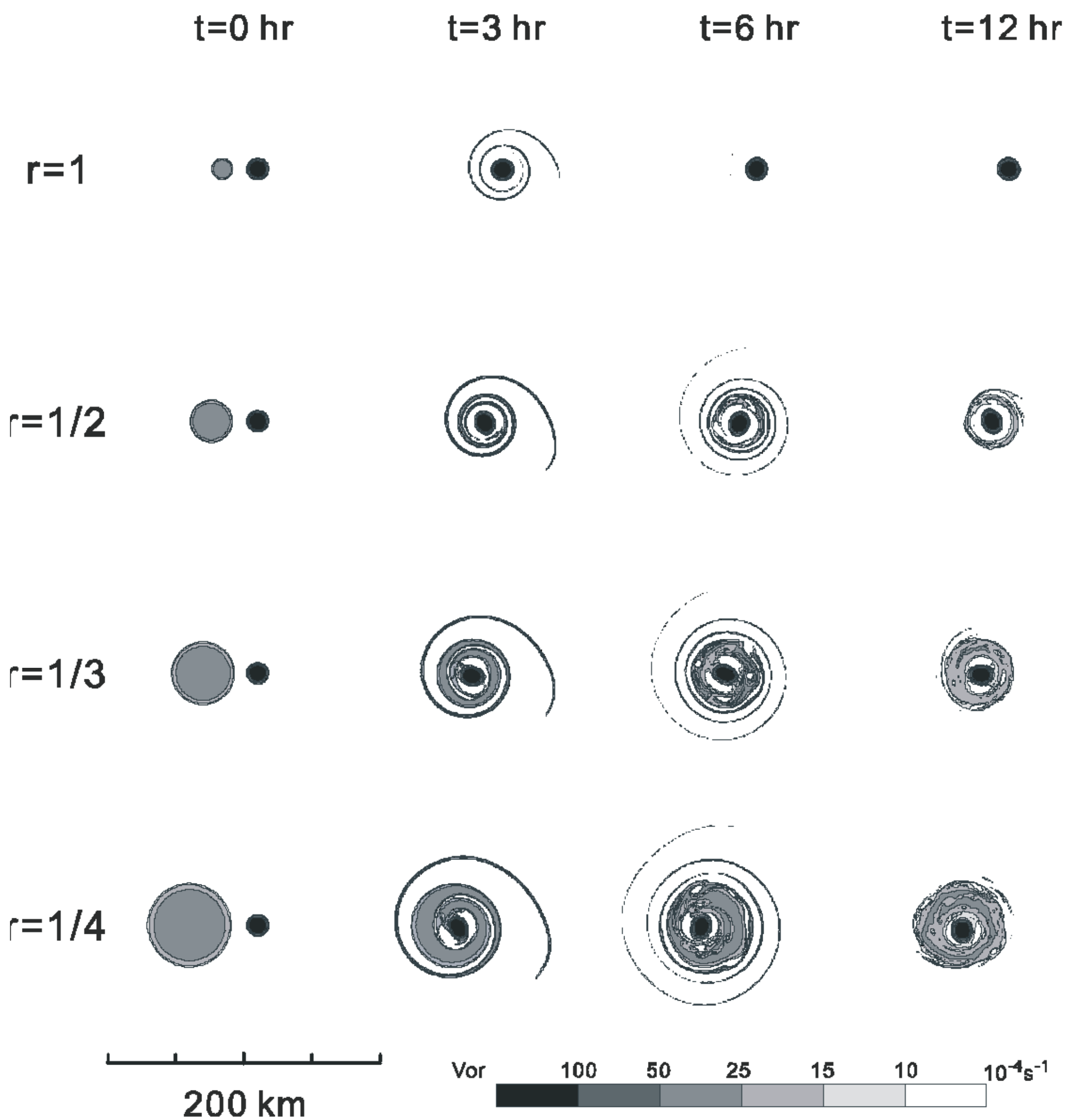

Figure 5: The sensitivity of the vorticity field in the binary vortex experiments with respect to the vortex radius ratio r at hour 0, 3, 6 and 12 with the vorticity strength ratio γ=5, and the dimensionless gap Δ/R_1=1.

$\gamma = 10$

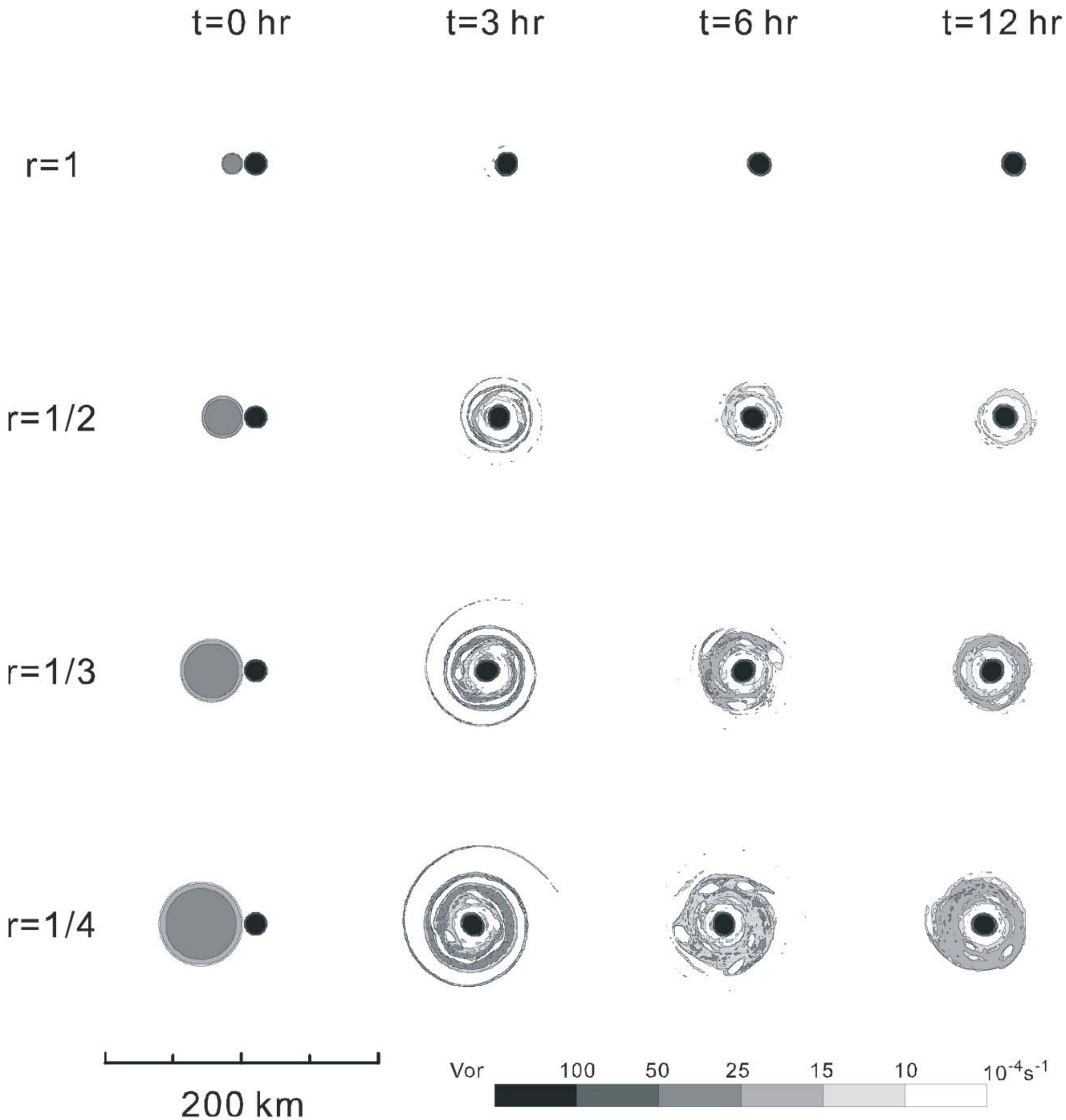

Figure 6: Similar to Figure 5 except that the dimensionless gap $\Delta/R_1=0$ and the vorticity strength ratio $\gamma=10$.

Same strain outside the RMW but different core vortex strength

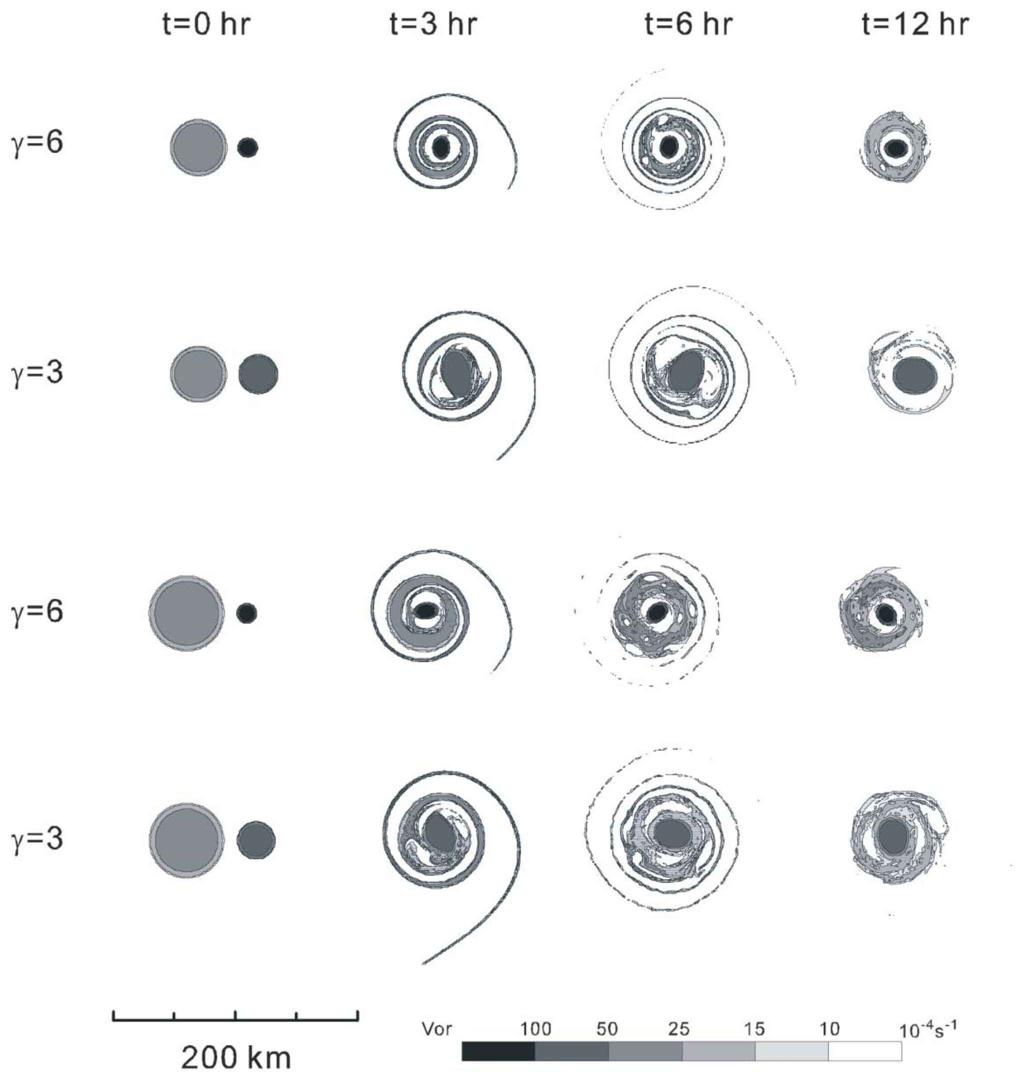

Figure 9: The sensitivity of the vorticity field in the binary vortex experiments with the core vortices process the same maximum wind but different radius of vorticity field. Two core vortices considered have the vorticity and radius of ($1.8 \times 10^{-2}s^{-1}$, 10 km) and ($0.9 \times 10^{-2}s^{-1}$, 20 km) respectively. The dimensionless gap is 1 in the experiments. The outer vortices considered have the radius of 30 km and 40 km respectively.

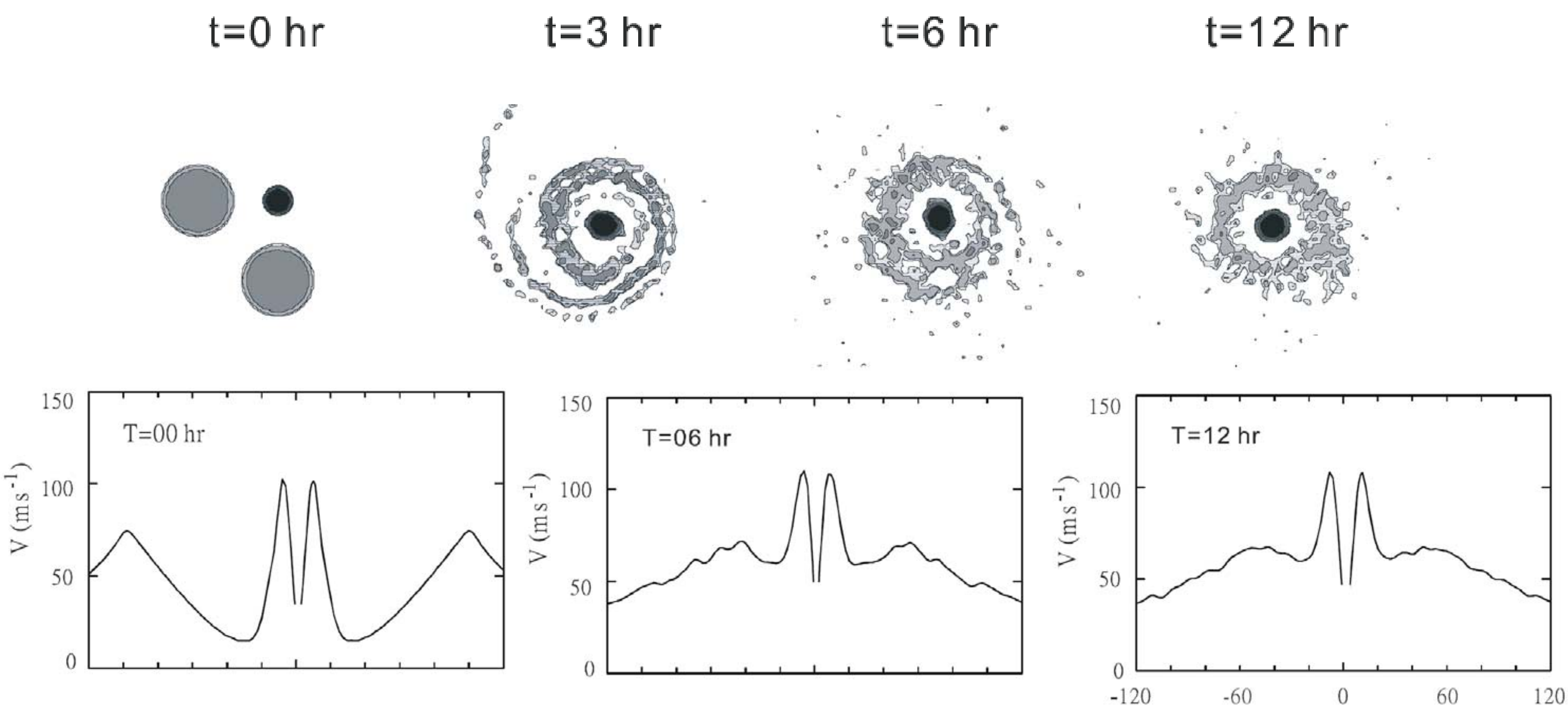

Figure 13: The tangential wind speed for radial arms toward the west (left portion) and the south (right portion) that emanate from the vortex center at various times for the experiment in the second row of Figure11.

The contraction of the secondary wind maximum by nonlinear advective dynamics.

Kuo et al. (2004)

- **A very strong core vortex at least six times stronger than the neighboring vorticity**
- **A relative larger neighboring vorticity area**
- **A separation distance within three to four times the core vortex radius**

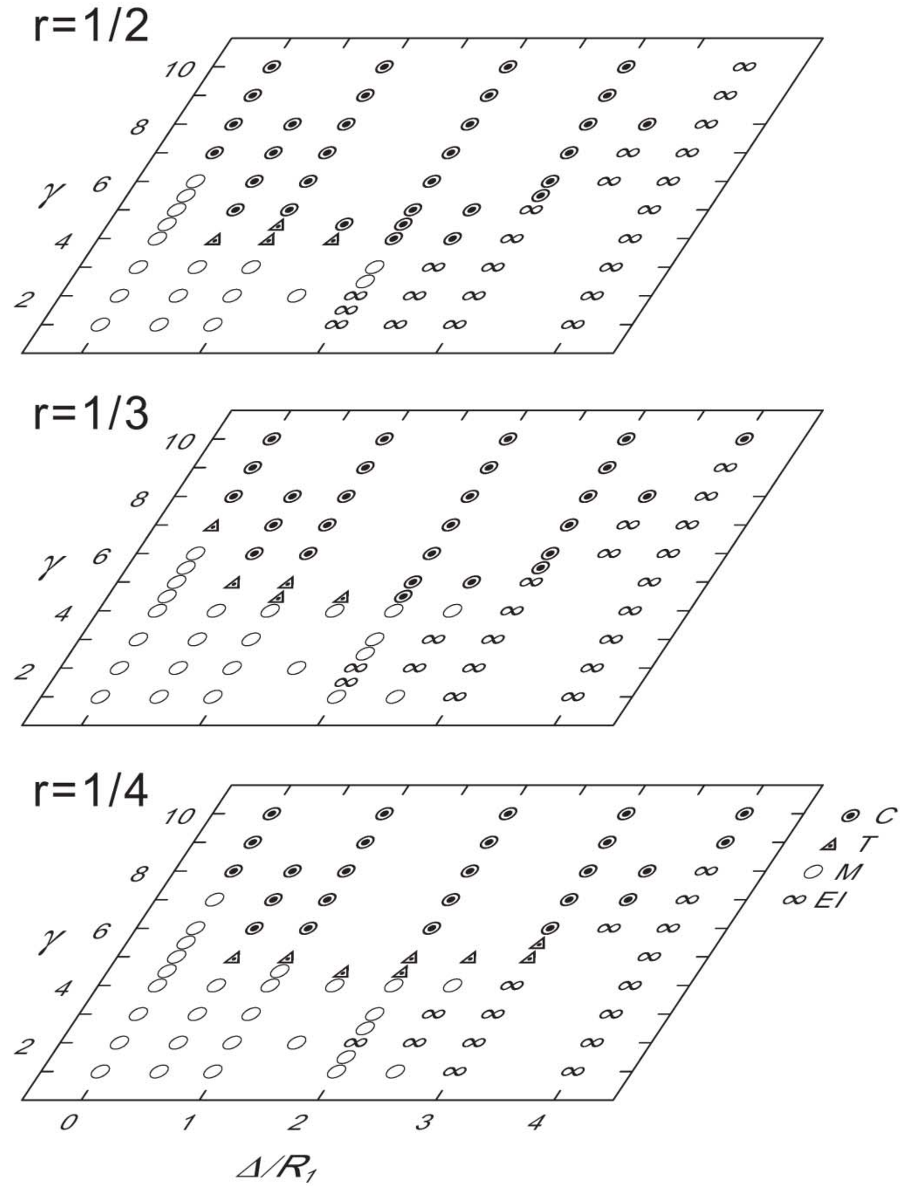

Fig 10. Summary of numerical experiments with the parameters of the vorticity strength ratio (γ), the dimensionless gap Δ/R_1, and the vortex radius ratio r. We have classified the resulting structures into the C (concentric), T (tripole), M (complete or partial merger), and EI (elastic interaction) regimes.

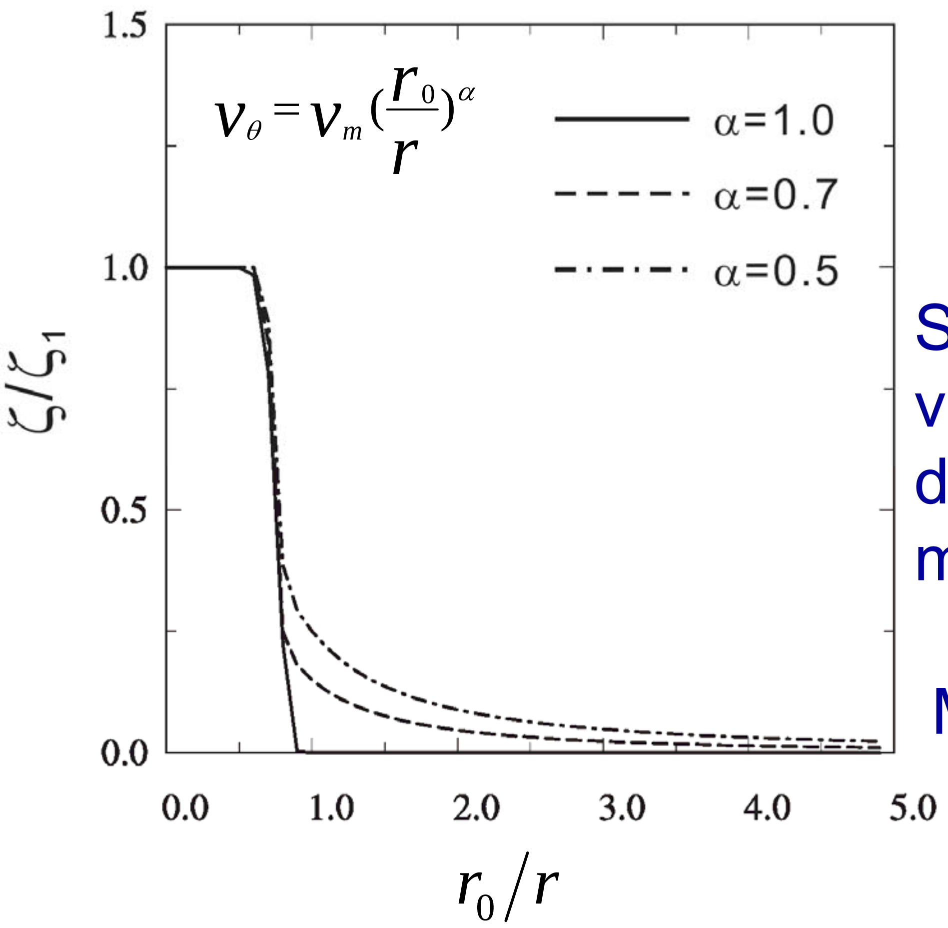

Skirt of significant cyclonic relative vorticity (slow tangential wind decrease outside the radius of maximum wind).

Mallen et al. 2005

Radial profile of the vorticity for the core vortex with the skirt parameter (α) 1.0, 0.7 and 0.5.

Dritschel and Waugh (1992) $\rightarrow$ $R_1,\ R_2,\ \Delta,\ \zeta$

$$r = \frac{R_1}{R_2},\ \Delta/R_1$$

Kuo et al. (2004) $\rightarrow$ $R_1,\ R_2,\ \Delta,\ \zeta_1,\ \zeta_2$

$$r = \frac{R_1}{R_2},\ \Delta/R_1,\ \gamma = \frac{\zeta_1}{\zeta_2}$$

Kuo et al. (2008) $\rightarrow$ $R_1,\ R_2,\ \Delta,\ \zeta_1,\ \zeta_2,\ \alpha$

$$r = \frac{R_1}{R_2},\ \Delta/R_1,\ \gamma = \frac{\zeta_1}{\zeta_2},\ \alpha$$

Examples of the vorticity field at hour 12, showing different classifications of binary vortex interactions involving a skirted core vortex.

Straining out

Concentric

Tripole

Merger

Elastic Interaction

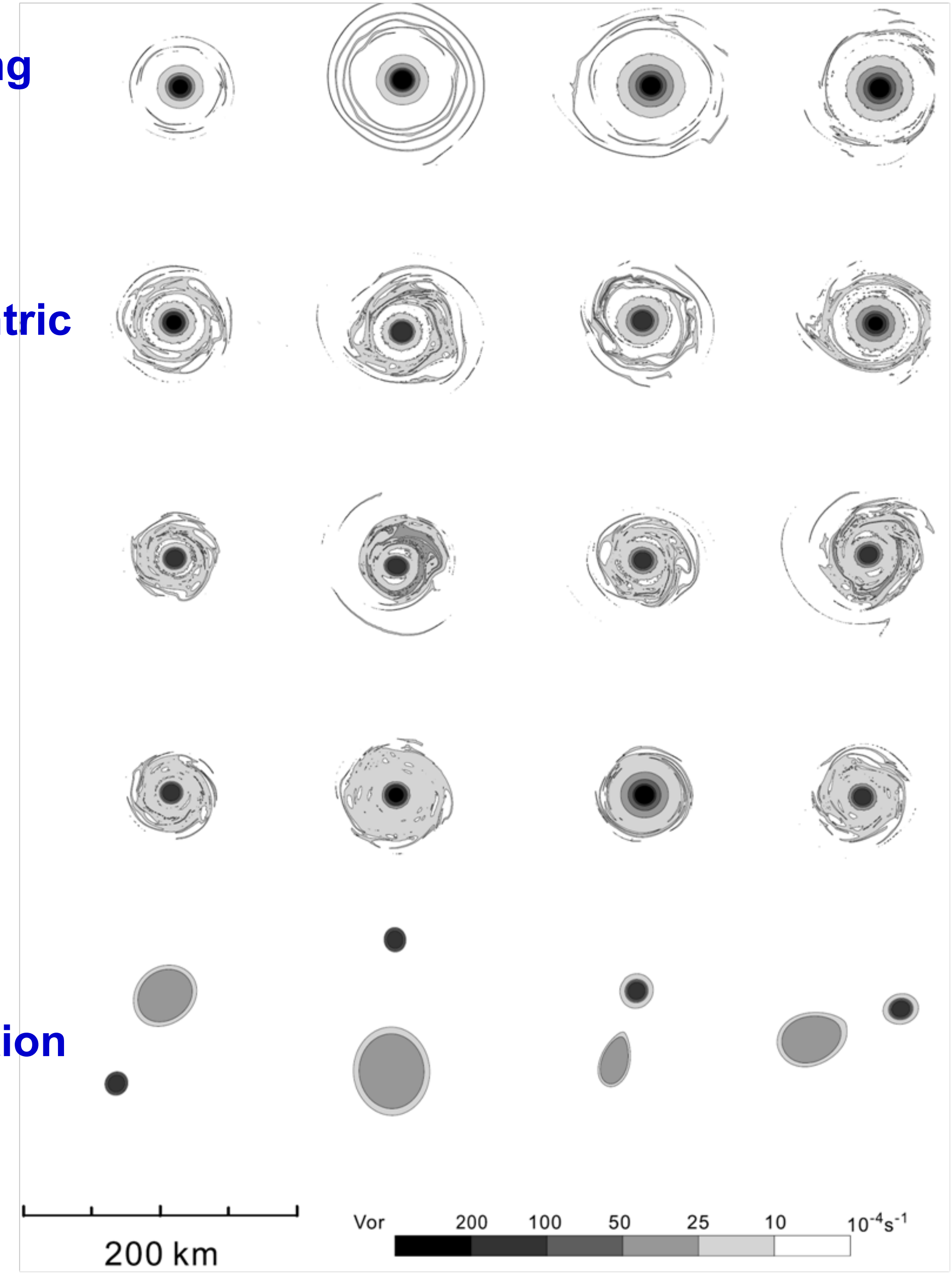

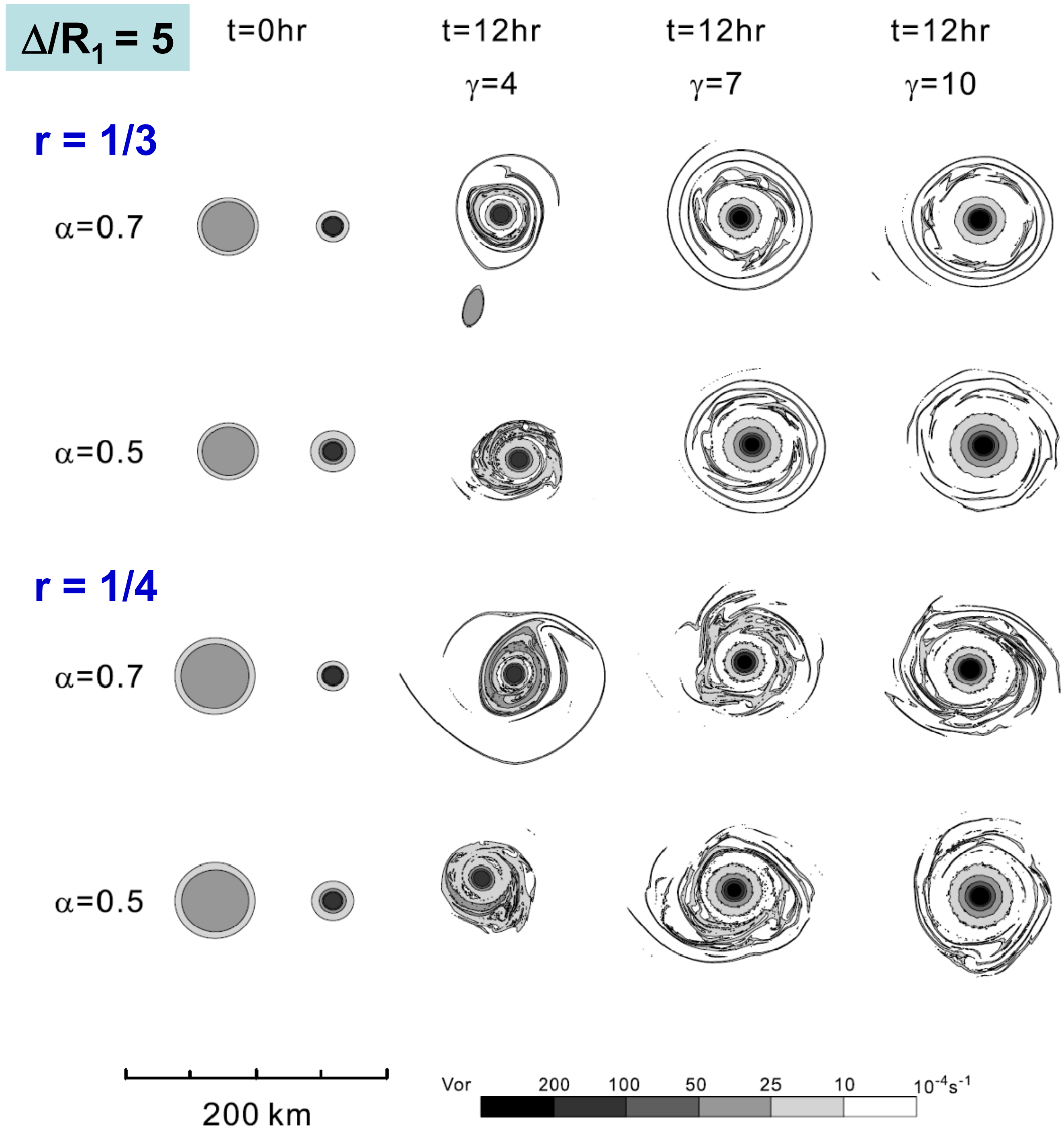

Δ/R1 = 5
t=0hr
t=12hr
γ=4
t=12hr
γ=7
t=12hr
γ=10
r = 1/3
α=0.7
α=0.5
r = 1/4
α=0.7
α=0.5
200 km
Vor
200
100
50
25
10
10-4s-1

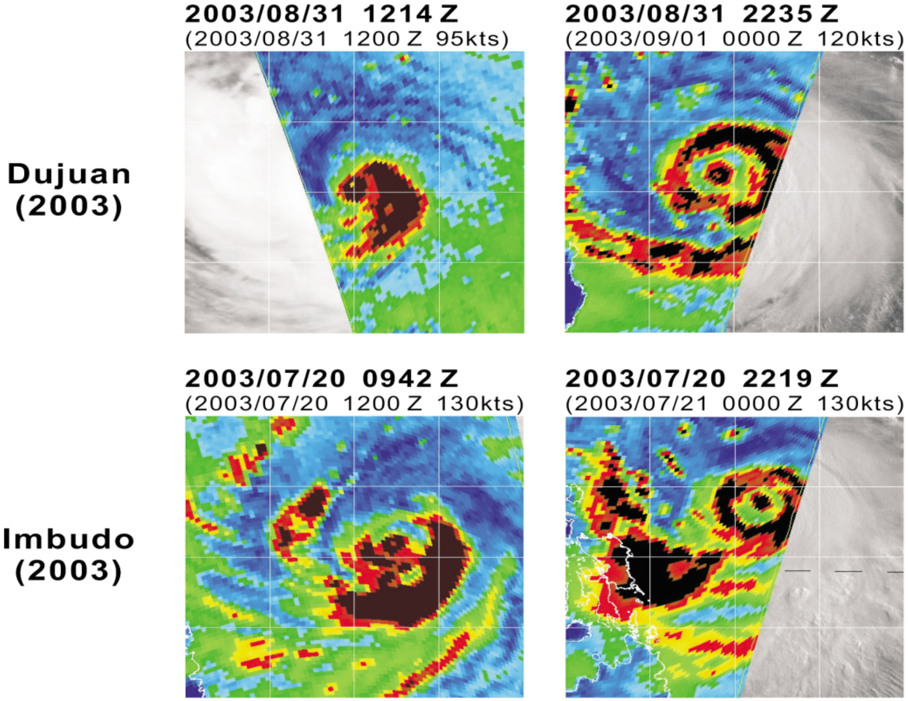

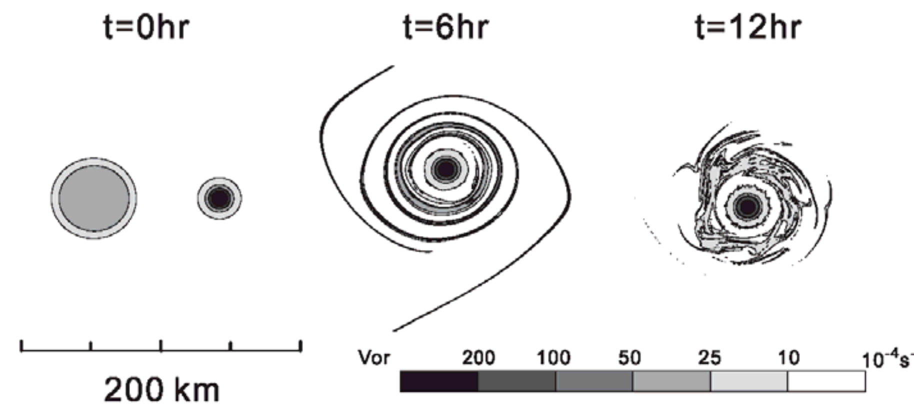

The contraction and the increase of the secondary wind maximum by nonlinear advection dynamics.

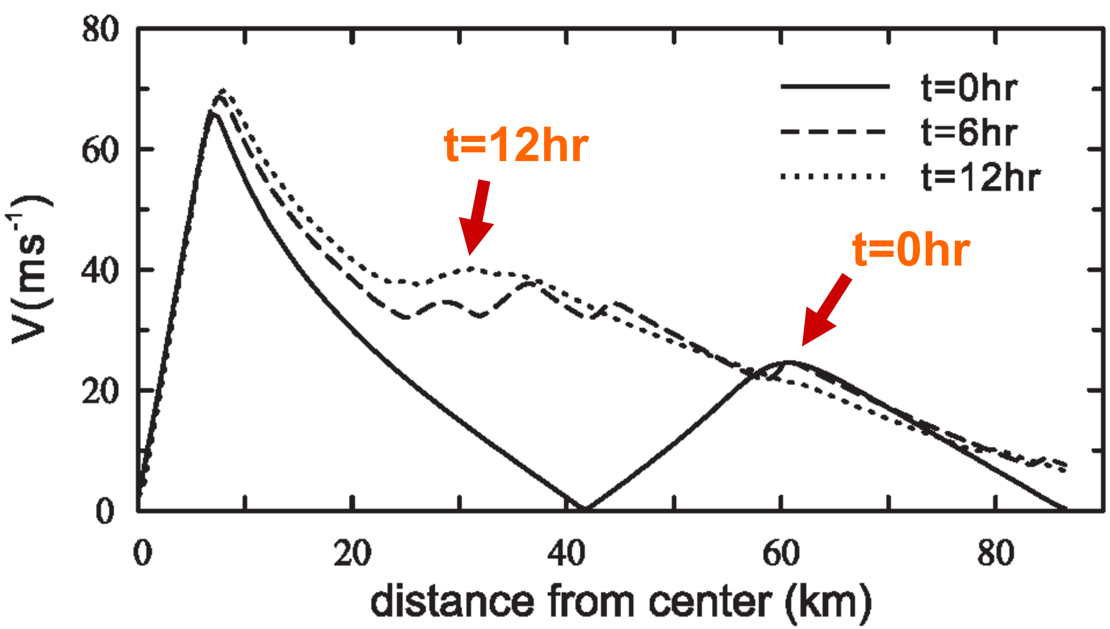

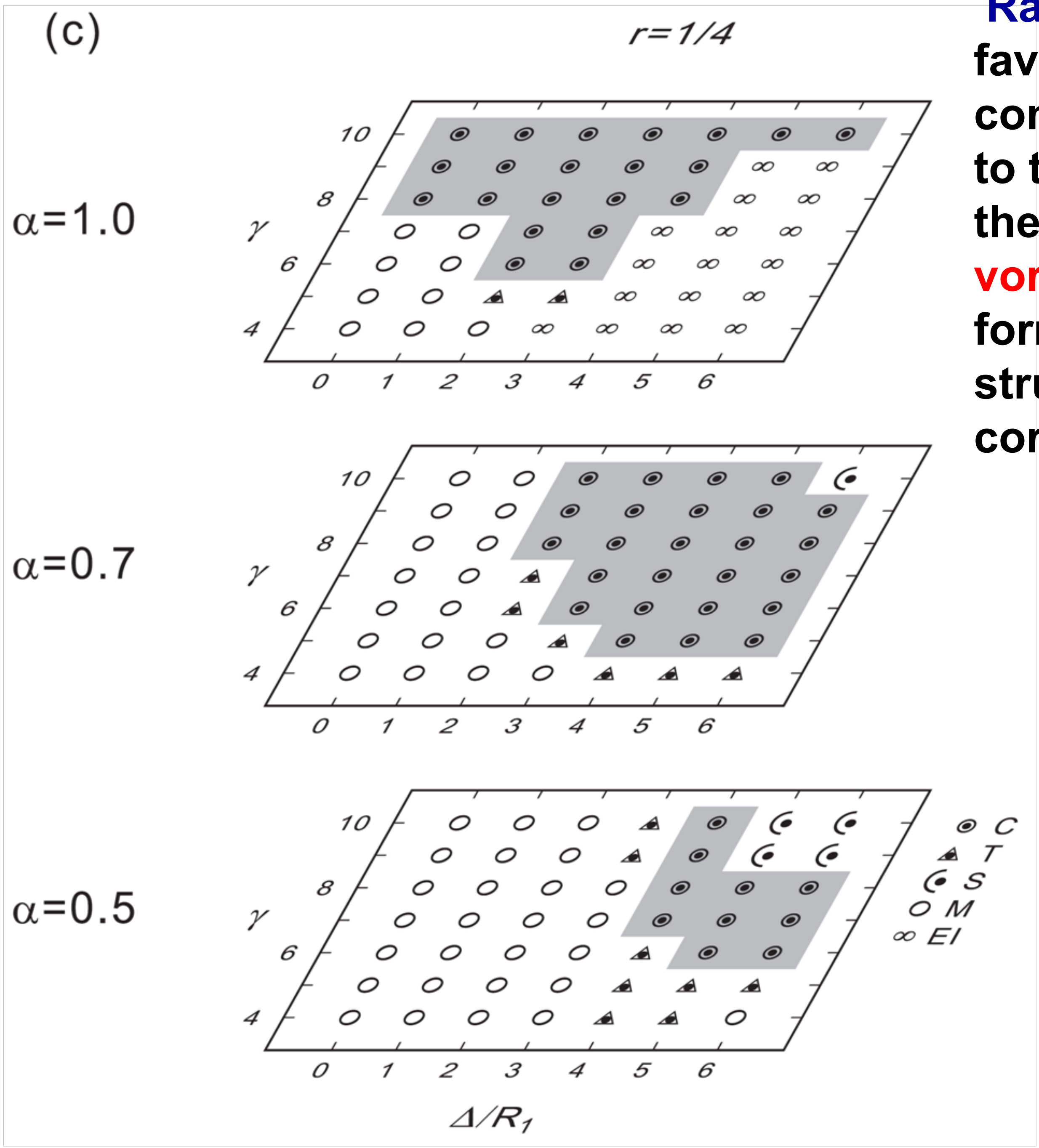

Rankine vortex (α = 1.0) favors the formation of a concentric structure closer to the core vortex, while the α = 0.7 and α = 0.5 vortices favor the formation of concentric structures farther from the core vortex.

Examples of asymmetric → symmetric concentric formations.

~ 12 hours.

Initial Δ (outer deep convection region - vortex core distance):

Typhoon Dujuan: nearly 0 km
Typhoon Imbudo nearly 50 km
Typhoon Maemi: nearly 100 km
Typhoon Winnie nearly 260km

A wide range of radii of concentric eyewalls

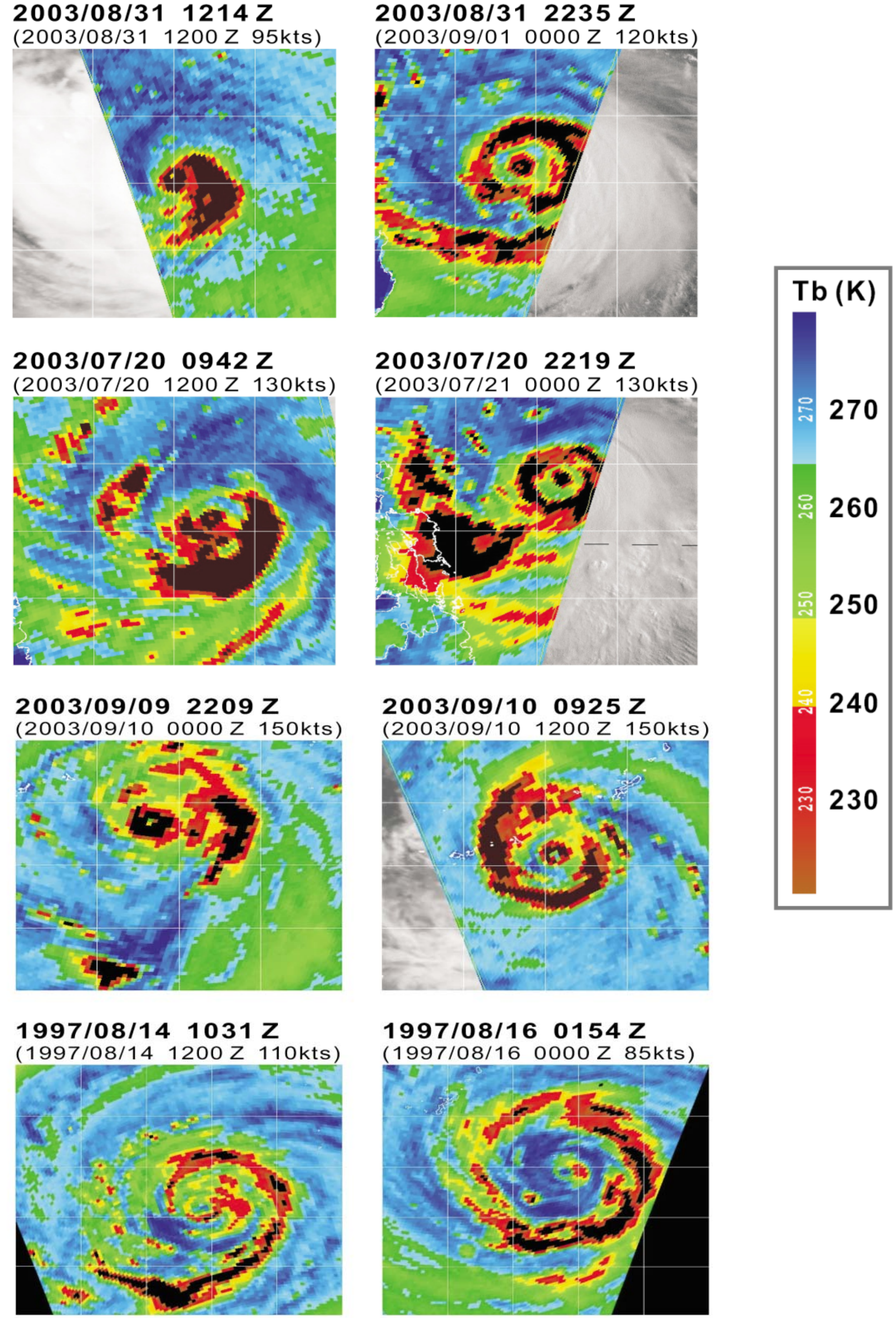

Summary

- Tropical cyclones of sufficient strength (e.g. sustained wind speed $\geq$ 120 kts) often form double eyewalls. Inner eyewall weakens and/or die.

- Area of asymmetric convection outside the core vortex that wraps around the inner eyewall to form the concentric eyewalls in about 12 hours.

- The contraction of the secondary wind maximum and the formation of the moat are features of the vorticity dynamics. The moat formation by subsidence, rapid filamentation, and advective dynamics.

- Double eyewall of different sizes maybe explained by the binary vortex interaction with skirted parameter.

- The pivotal role of the vorticity strength of the core vortex in maintaining itself, and in strectching, organizing and stabilizing the outer vorticity field, and the shielding effect of the moat to prevent further merger and enstrophy cascade processes in concentric eyewall dynamics.

- Formation of concentric eyewalls is important for the TC intensity problem. A self-limiting process for TC intensity. A natural “STORMFURY”.**!!**

- The organizational aspects of outer eyewall formation from an asymmetric vorticity field outside the cyclone core. The importance of core vortex structure, the moat, and the spatial characteristics of the vorticity field outside the core in the formation of double eyewalls.

- Need to understand the vorticity generating meso-scale processes in the TC environment.

June JGR 2008

Table 1. List of Secondary Eyewall Formation Hypotheses With Summary of Relevance to our Modeled Hurricanes[a]

Authors	Hypothesis Summary	Relevance to Current Model Results	Type
Willoughby et al. [1982] borrowing from the squall line research of *Zipser* [1977]	Downdrafts from the primary eyewall force a ring of convective updrafts.	Few downdraft-forced updrafts during this time in the simulations.	O
Willoughby [1979]	Internal resonance between local inertia period and asymmetric friction due to storm motion.	No systematic storm motion in the simulated storms.	A
Hawkins [1983]	Topographic effects	No topographic forcing in the simulations.	O
Willoughby et al. [1984]	Ice microphysics	"Warm-rain" (no-ice) sensitivity case also produces secondary eyewall.	A
Molinari and Skubis [1985] and *Molinari and Vallaro* [1989]	Synoptic-scale forcings (e.g., inflow surges, upper-level momentum fluxes)	No synoptic-scale forcings in the simulations	O
Montgomery and Kallenbach [1997], *Camp and Montgomery* [2001] and *Terwey and Montgomery* [2003]	Internal dynamics-axisymmetrization via sheared vortex Rossby wave processes; collection of wave energy near stagnation or critical radii	Possible explanation	N
Nong and Emanuel [2003]	Sustained eddy momentum fluxes and WISHE feedback	Possible explanation	A
Kuo et al. [2004, 2008]	Axisymmetrization of positive vorticity perturbations around a strong and tight core of vorticity.	Possible explanation	N

[a]The type column refers to the type of model or observations that were used to formulate the hypothesis. O stands for observationally-based; A stands for axisymmetric model; N stands for nonaxisymmetric model.

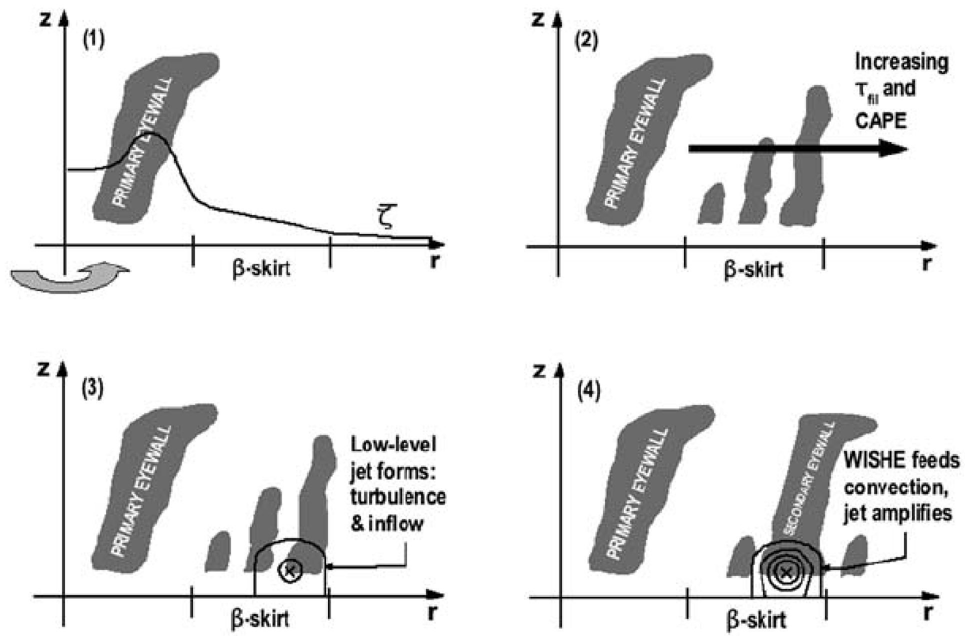

Figure 6. Proposed conceptual model of the β-skirt axisymmetrization (BSA) mechanism for the formation of a secondary eyewall.

My research curiosity:
Mesoscale convection development in a strong rotating environment??
[Under strong filamentation process]

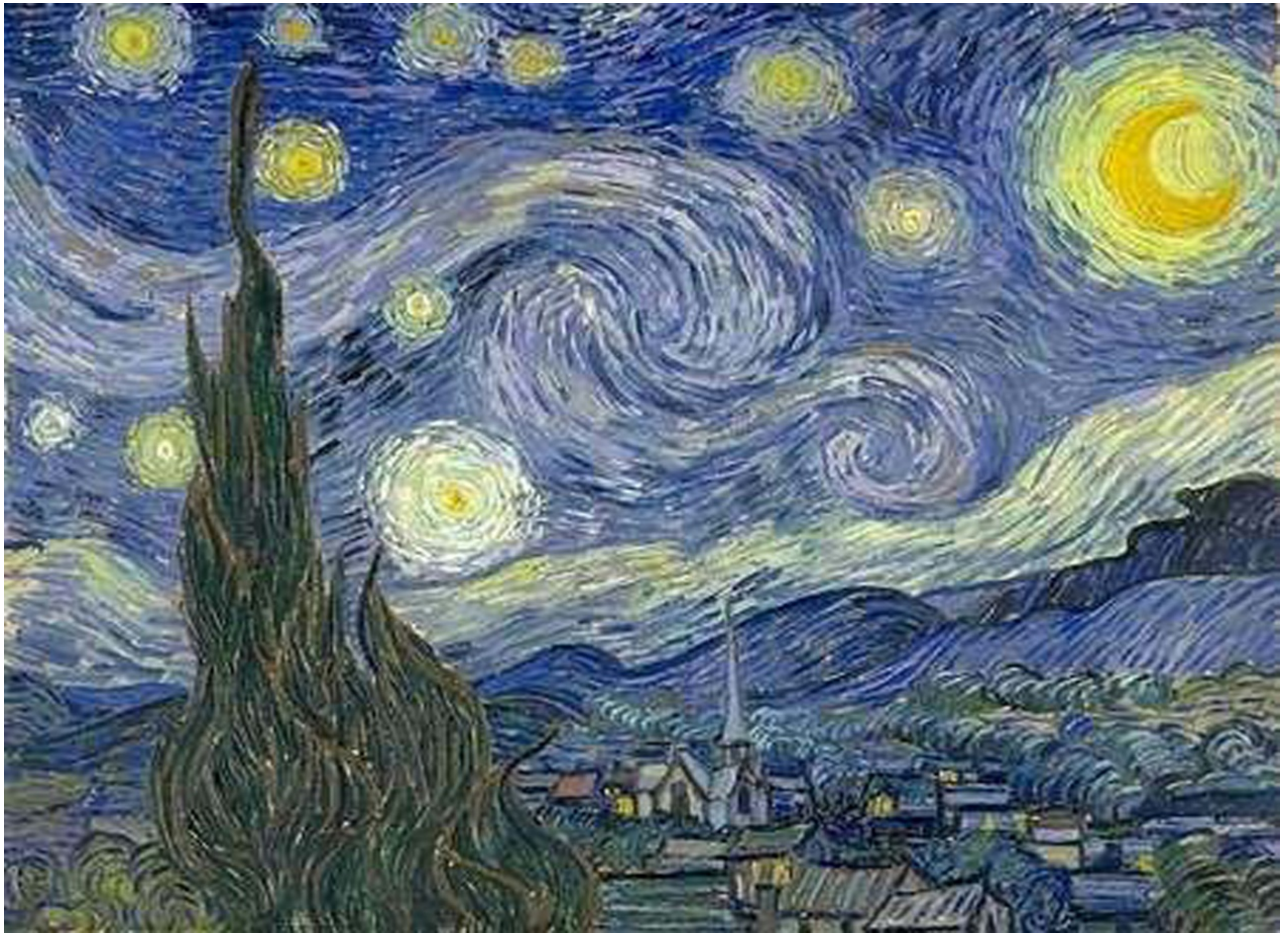

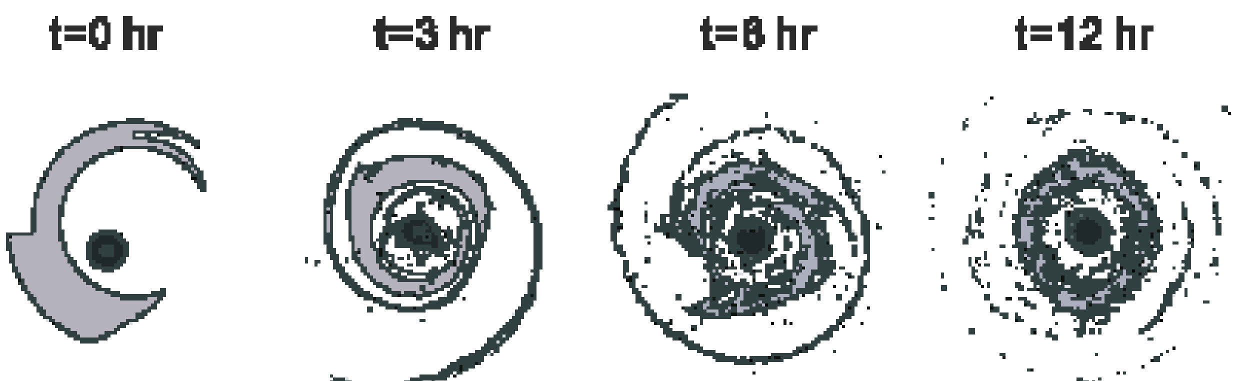

t=0 hr
t=3 hr
t=6 hr
t=12 hr

- A new dimension is added to the Dritschel-Waugh binary vortex interaction scheme that provides a proper concentric vorticity structure, the tripole vortex strucuture and the multiple eyewalls structure. Two important parameters are the vorticity strength ratio and the skirt parameters.

- The contraction of the secondary wind maximum and the formation of the moat are features of the vorticity dynamics. The moat formation by subsidence, rapid filamentation, and advective dynamics.

A Western North Pacific Climatology (1997-2005)

- **Microwave data**
  - NRL Monterey tropical cyclone Web page
    - SSM/I and TMI 85.5GHz W
  - Region
    - WNPAC, ATL
  - Space resolution
    - SSM/I：12.5 km TMI：6.7 km
  - Time resolution
    - 6 hrs~12 hrs
- **Best track data**
  - JTWC Annual Tropical Cyclone Reports and NHC Hurricane Season Tropical Cyclone Reports
  - Time resolution
    - 6 hrs

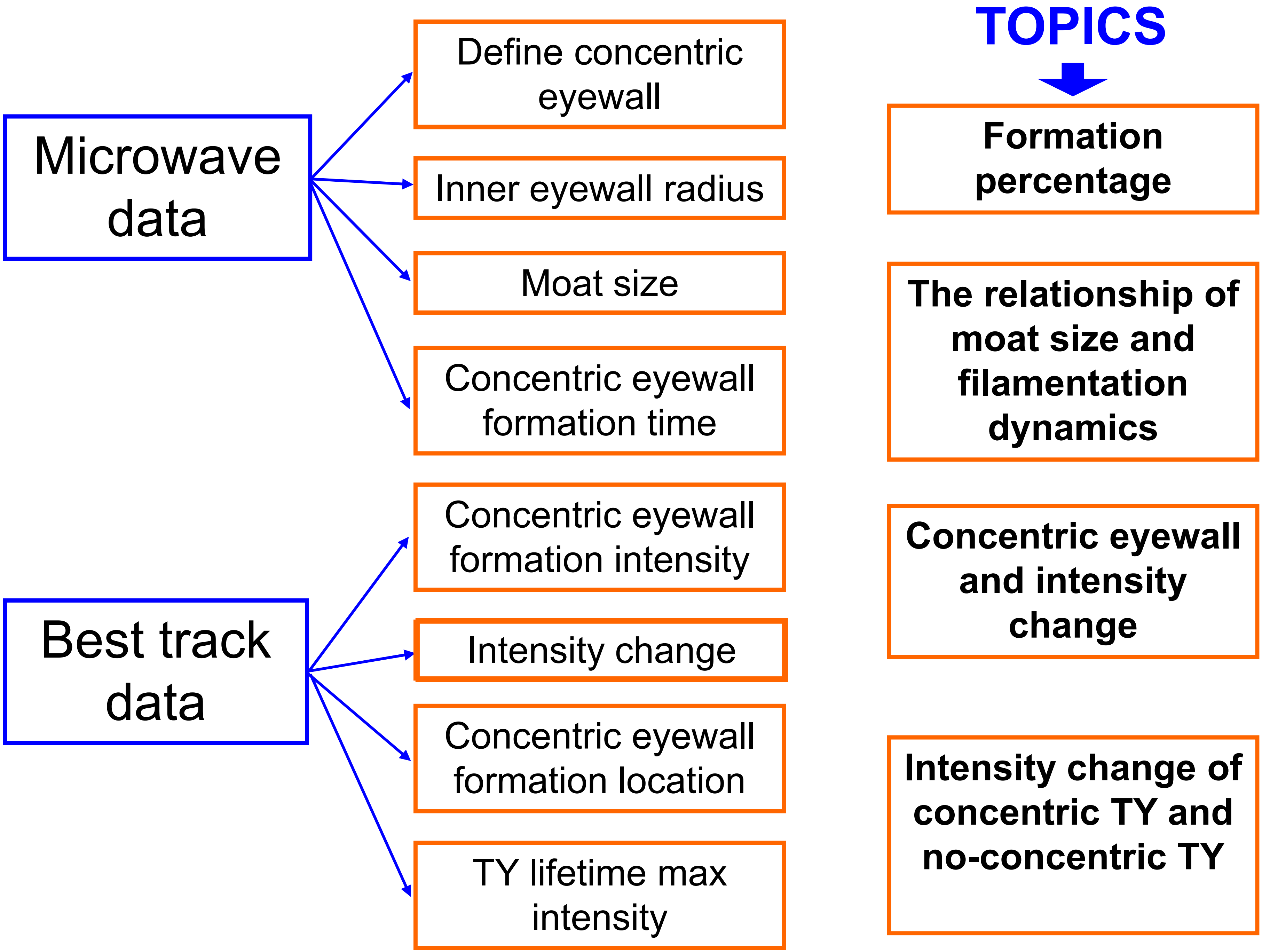
TOPICS
Microwave data
Best track data
Define concentric eyewall
Inner eyewall radius
Moat size
Concentric eyewall formation time
Concentric eyewall formation intensity
Intensity change
Concentric eyewall formation location
TY lifetime max intensity
Formation percentage
The relationship of moat size and filamentation dynamics
Concentric eyewall and intensity change
Intensity change of concentric TY and no-concentric TY

Moat size (r_0) estimated from filamentation time

$$\tau_{fil} = 2 \Big/ \sqrt{\left(\frac{\partial v_\theta}{\partial r} - \frac{v_\theta}{r}\right)^2 - \left(\frac{\partial v_\theta}{\partial r} + \frac{v_\theta}{r}\right)^2}$$

$$\tau_{fil} = \frac{r}{v_\theta \sqrt{\alpha}} = \boxed{\frac{2}{\zeta}\left(\frac{r}{r_m}\right)^{\alpha+1} \alpha^{-\frac{1}{2}} = \tau_0}$$

$$\frac{r}{r_m} = \left(\frac{\zeta}{2}\tau_0 \alpha^{\frac{1}{2}}\right)^{\frac{1}{\alpha+1}}$$

$$\boxed{r_0 = r - r_m = \left(\frac{\zeta}{2}\tau_0 \alpha^{\frac{1}{2}}\right)^{\frac{1}{\alpha+1}} r_m - r_m}$$

v_m : best track data

r_m : inner eyewall radius

$$v_\theta = v_m \left(\frac{r_m}{r}\right)^\alpha$$

$$\zeta = 2\frac{v_m}{r_m}$$

$$\tau_0 = 30\,\text{min}$$

Moat width
v.s.
Core size

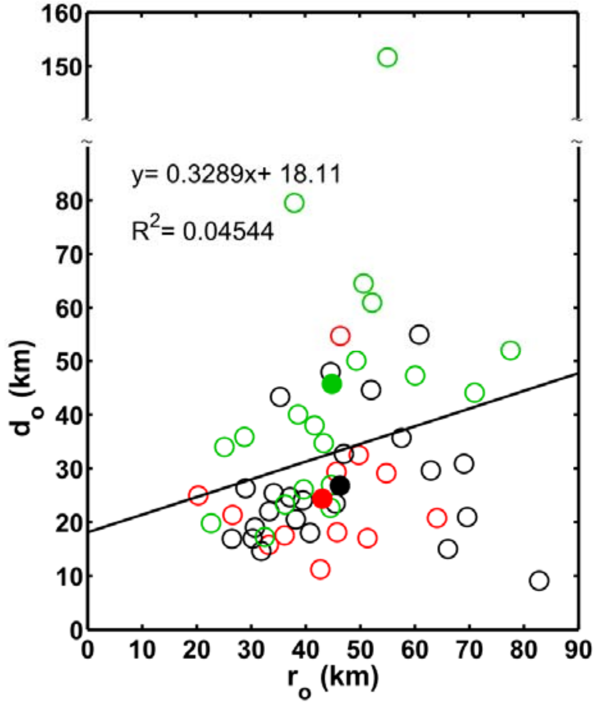

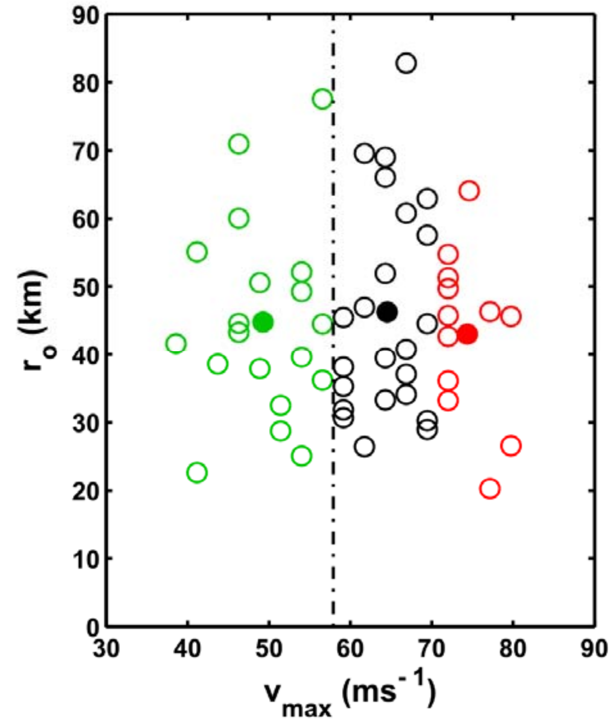

Core size
v.s.
Intensity

Moat width
v.s.
Core vorticity

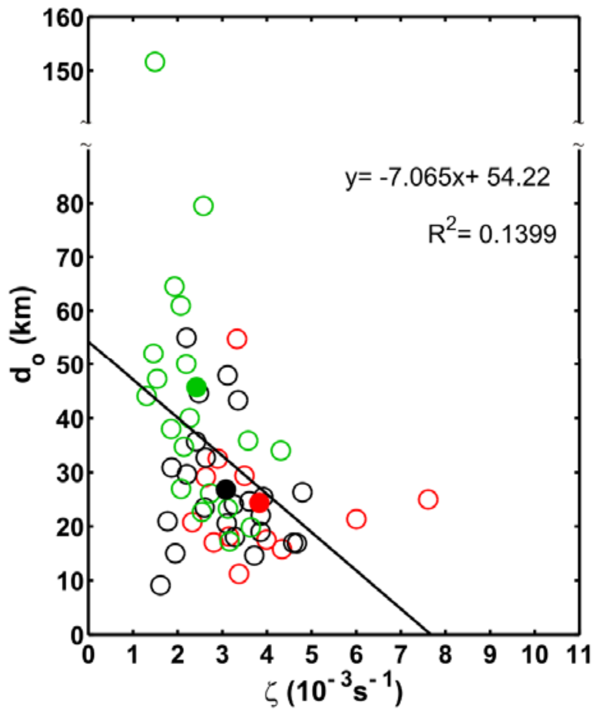

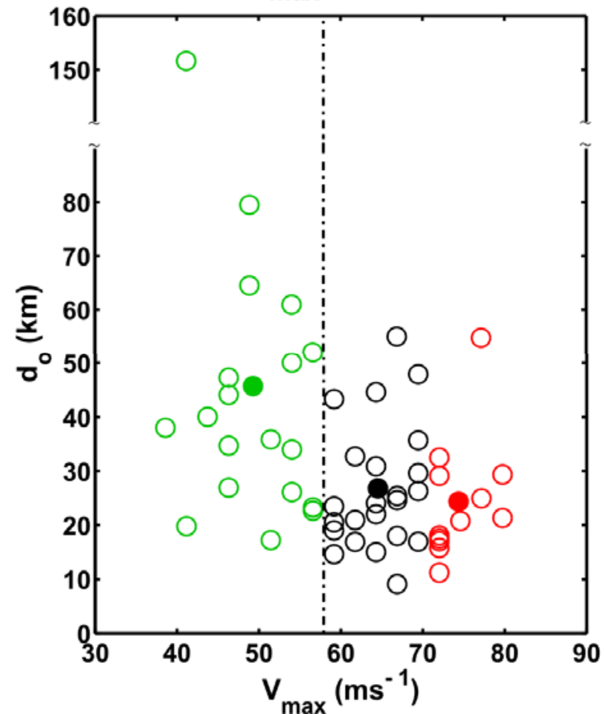

Moat width
v.s.
Intensity

Nondimensional moat width v.s. nondimensional filamentation moat width

All cases

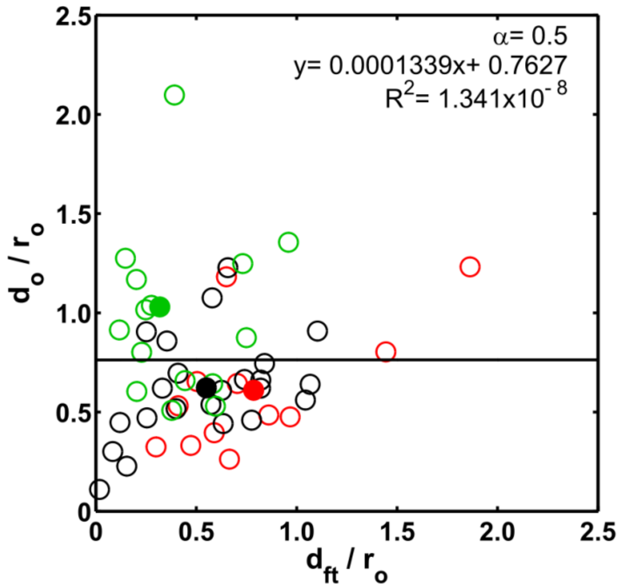

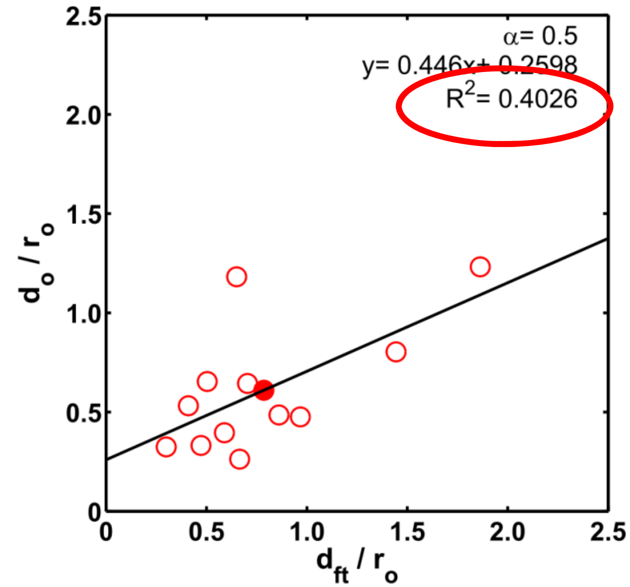

Cat 5

Cat 4

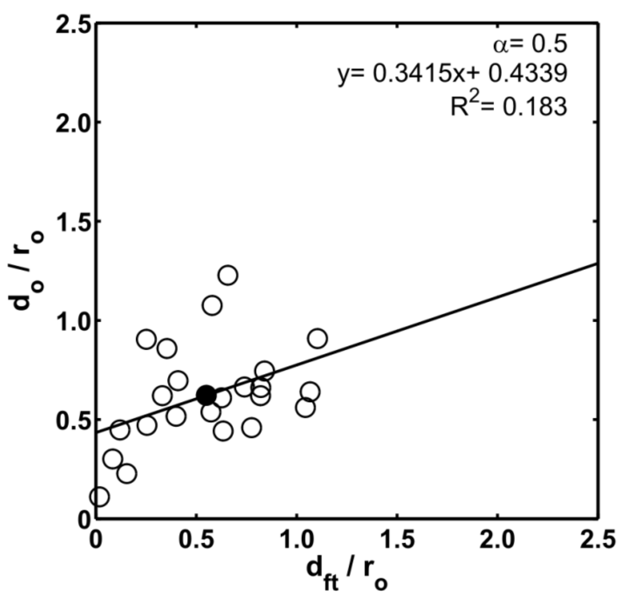

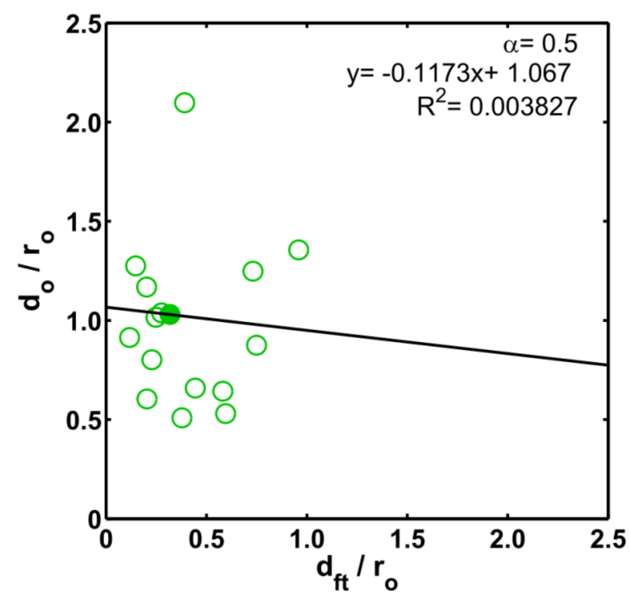

Cat 3

Nondimensional moat width v.s. nondimensional filamentation moat width

All cases

Cat 5

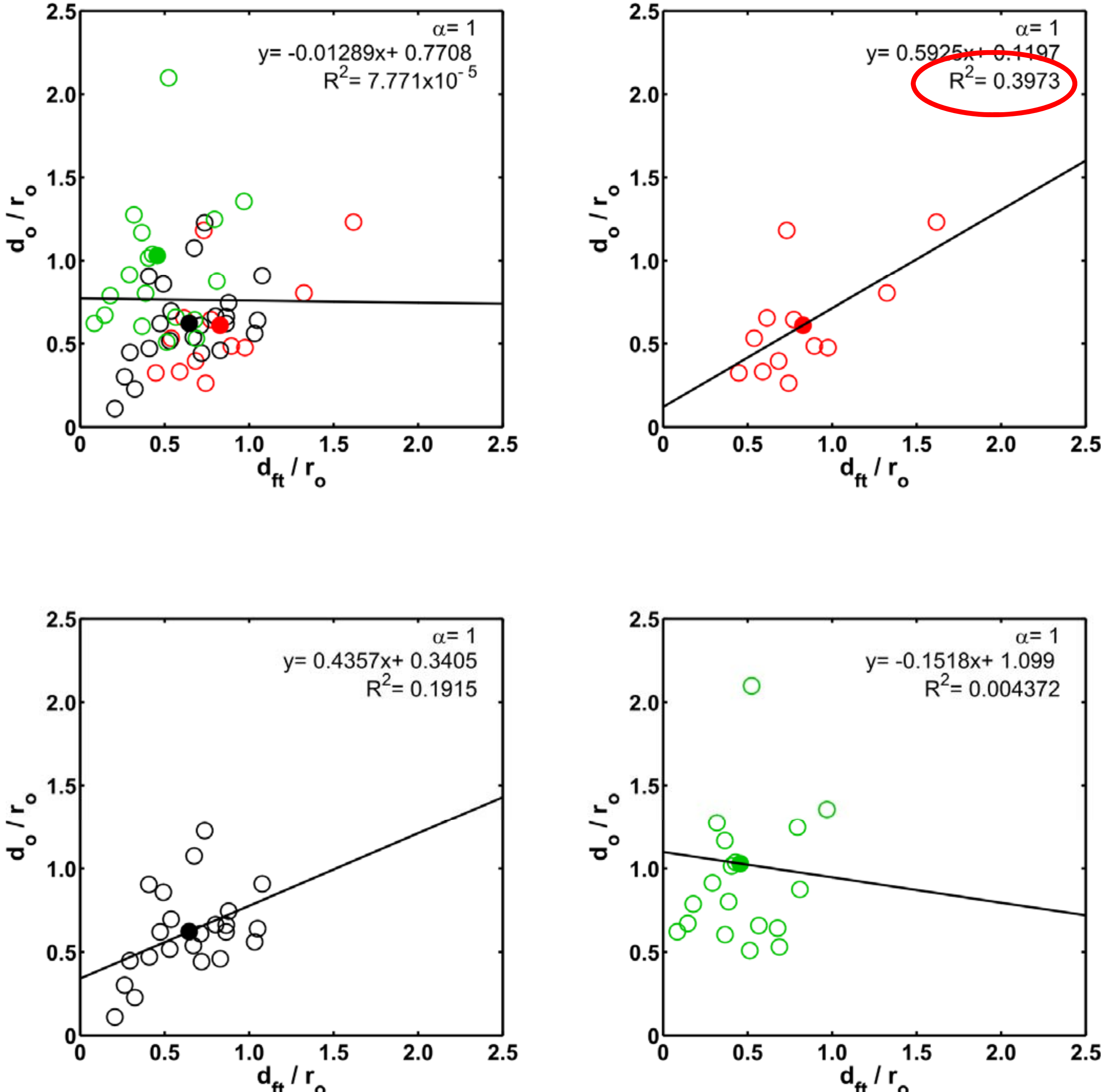

Cat 4

Cat 3

Intensity change 24h before and after the formation of concentric eyewalls

+:intensity increase (P)   - : intensity decrease (N)

+-

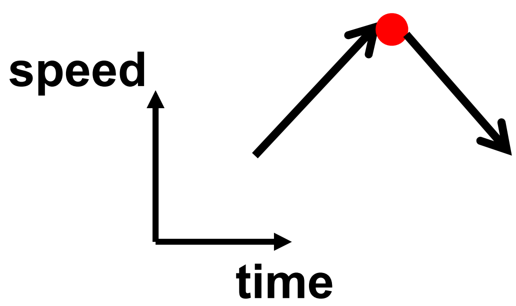

--

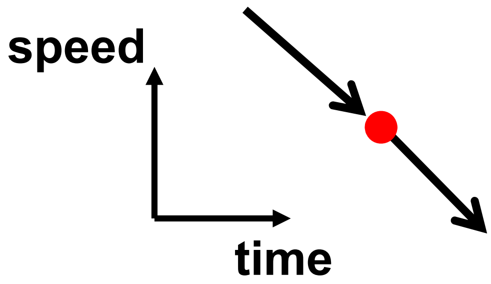

++

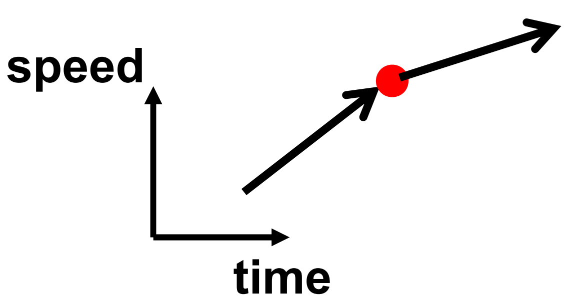

-+

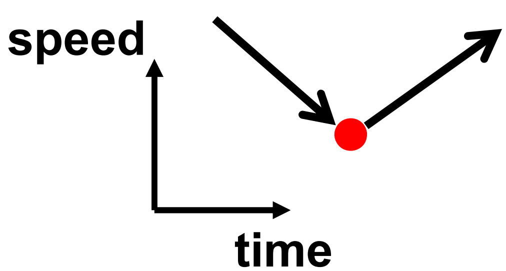

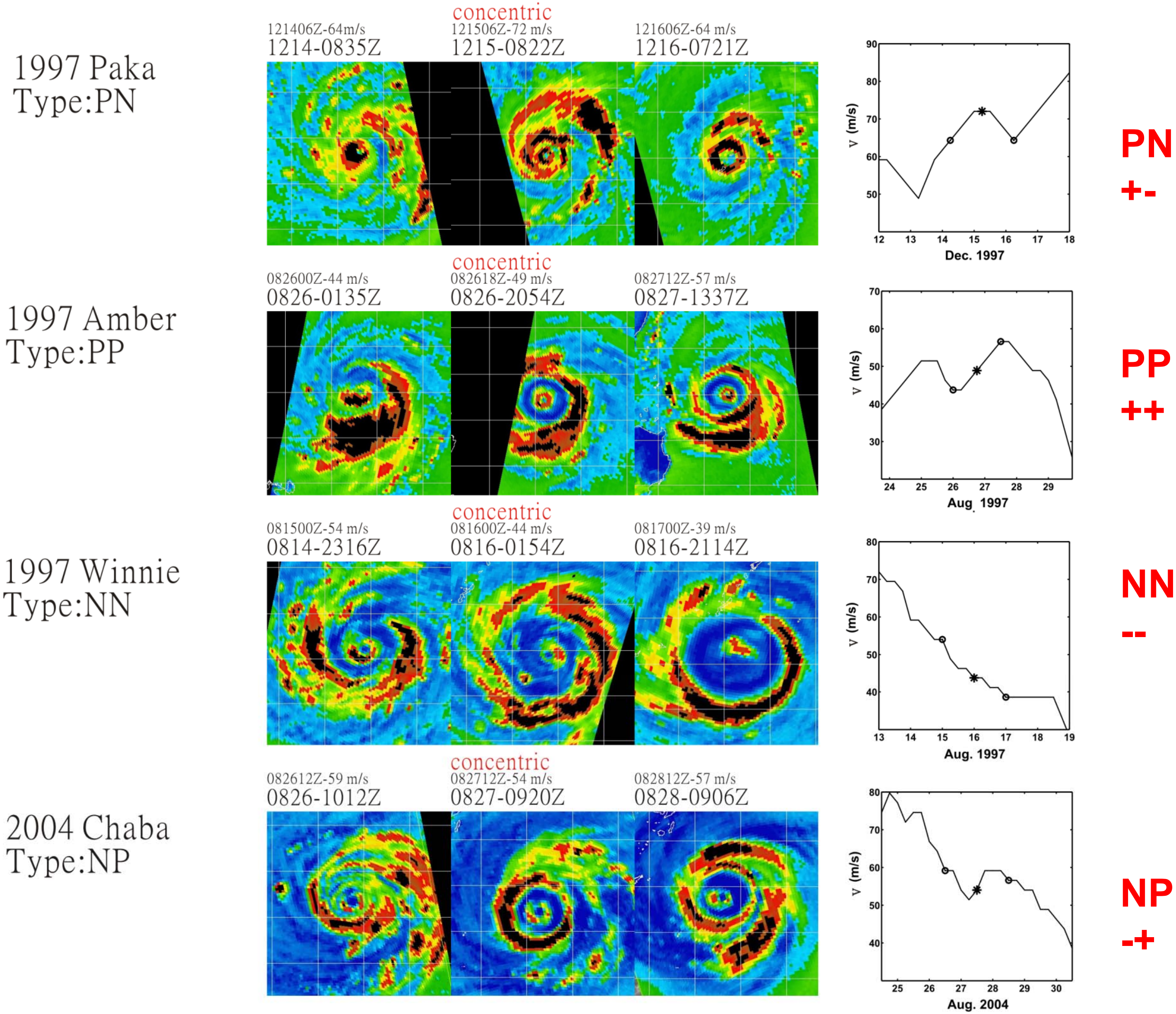
1997 Paka
Type:PN
concentric
121406Z-64m/s
1214-0835Z
121506Z-72 m/s
1215-0822Z
121606Z-64 m/s
1216-0721Z
V (m/s)
Dec. 1997
PN
+-
1997 Amber
Type:PP
concentric
082600Z-44 m/s
0826-0135Z
082618Z-49 m/s
0826-2054Z
082712Z-57 m/s
0827-1337Z
V (m/s)
Aug. 1997
PP
++
1997 Winnie
Type:NN
concentric
081500Z-54 m/s
0814-2316Z
081600Z-44 m/s
0816-0154Z
081700Z-39 m/s
0816-2114Z
V (m/s)
Aug. 1997
NN
--
2004 Chaba
Type:NP
concentric
082612Z-59 m/s
0826-1012Z
082712Z-54 m/s
0827-0920Z
082812Z-57 m/s
0828-0906Z
V (m/s)
Aug. 2004
NP
-+

Composite time series of the intensity for the NP, NN, PN, and PP cases

- **74%** (PN+PP) cases intensity increase 24h before concentric eyewalls formation

- **72%** (PN+NN) cases intensity decrease 24h after the concentric eyewalls formation

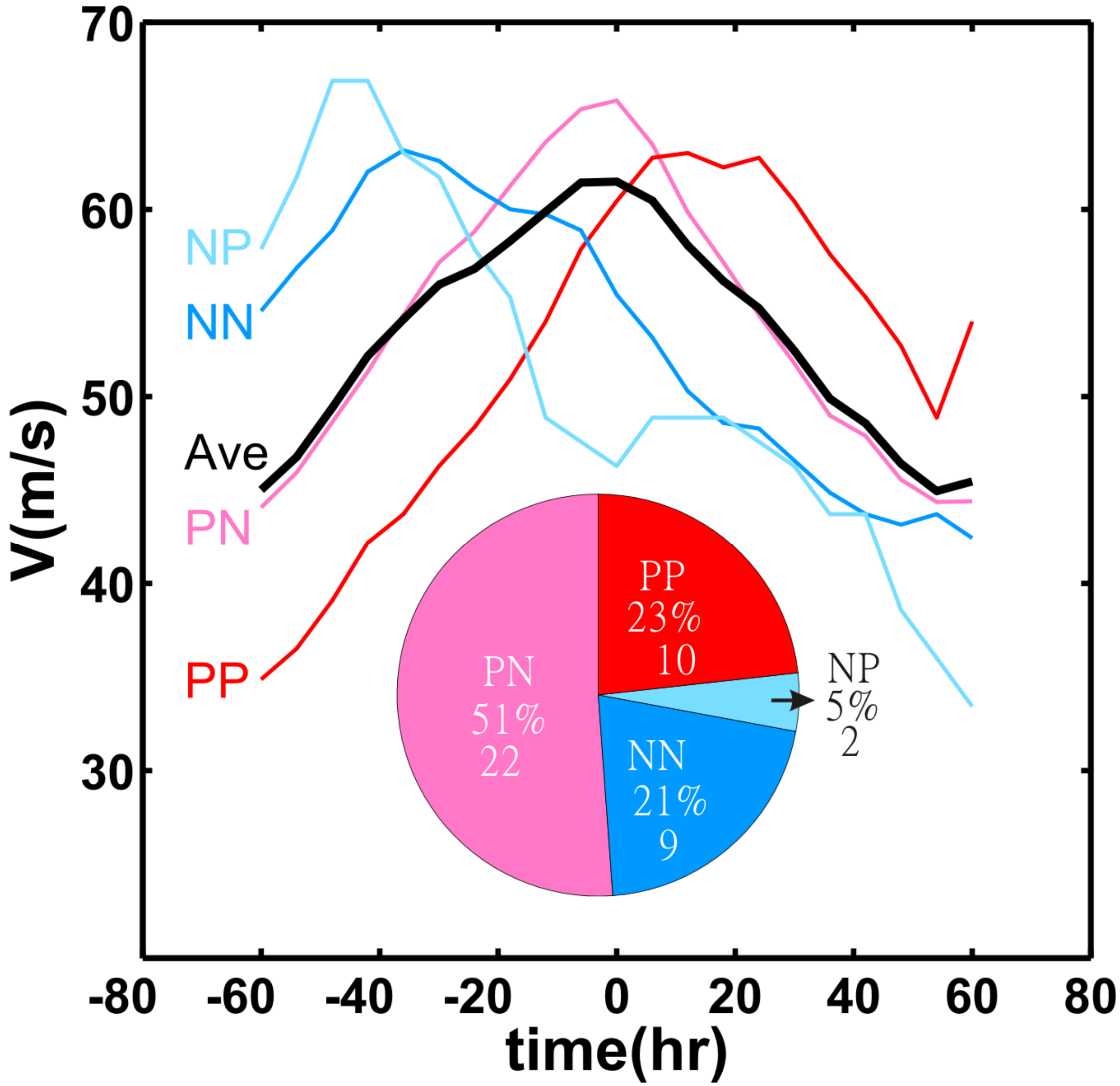

Summary

1. TCs with the concentric structure in the western North Pacific between 1997 and 2005 are studied.

2. Core size, intensity, core vorticity, and moat width are all little related.

3. Many strong TCs possess the concentric structure:
   - Formation occurred in 23% of WNPAC TCs
   - 64% of formation were categories 4 and 5
   - 51% of category 4 and 76% of category 5 possessed it.

4. The mechanism of moat formation through rapid filamentation dynamics, in addition to the subsidence effect, is important in strong typhoons.

- The “filamentation moat size” explains 40% of the variance of the satellite observed size for category 5 typhoons.

5. The intensity of the concentric eyewall typhoons tends to peak at the time of concentric eyewalls formation.

- Approximately 74% cases intensify 24h before concentric formation and approximately 72% cases weaken 24h after formation.

6. Compared to the no-concentric eyewall typhoons, the formation depends on the maintenance of a relatively high intensity for a longer duration, rather than a rapid intensification process that can reach a higher intensity. The intensity tendencies of both concentric and non-concentric typhoons are similar in the weakening phase.

Composite time series of intensity for concentric and non-concentric cases

Cat 4 and 5

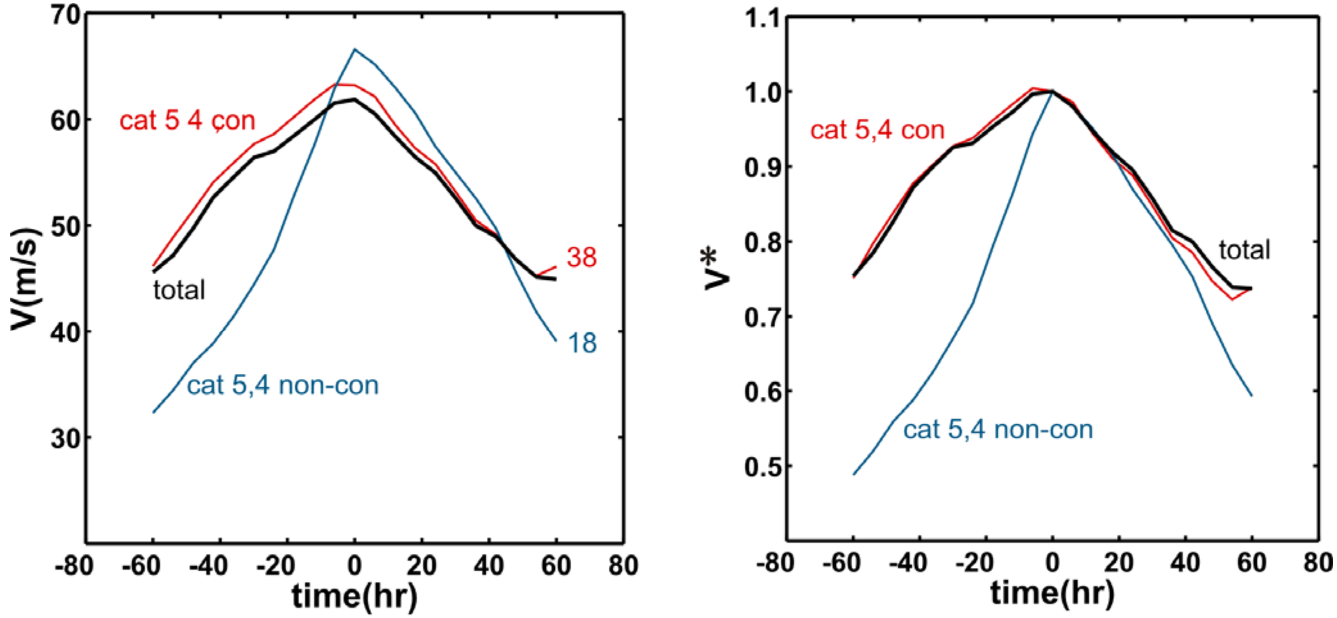

Cat 2 and 3

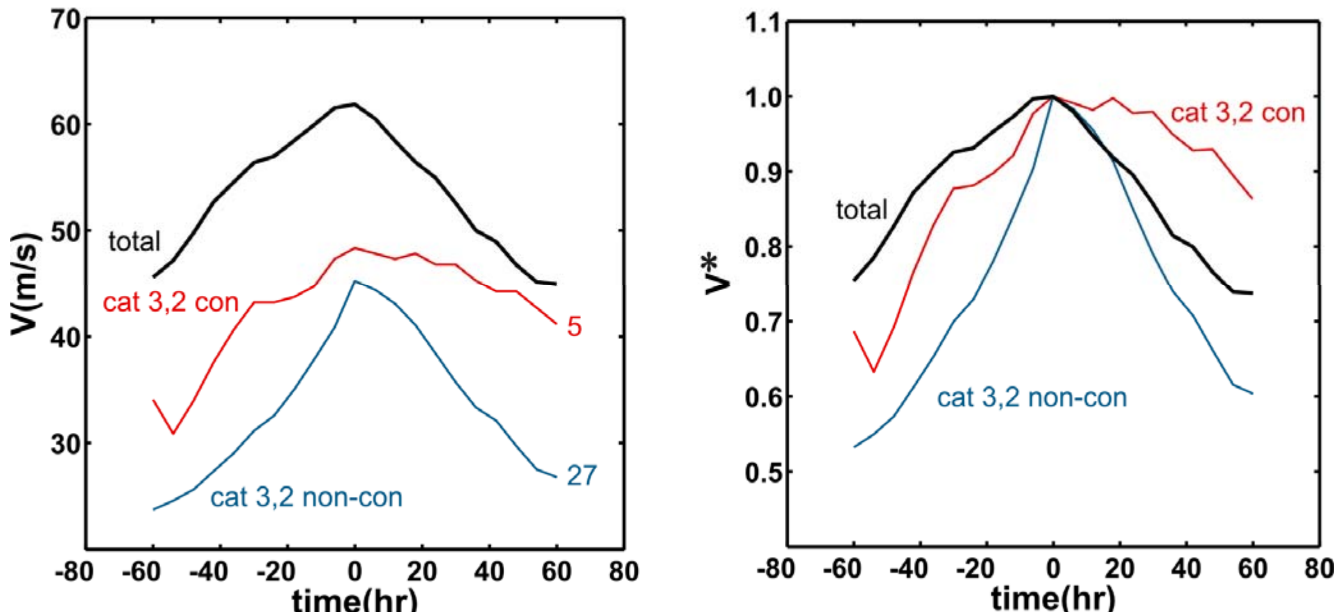

WNPAC Concentric eyewalls formation locations, intensity, and tracks

Kuo et al. (2006)

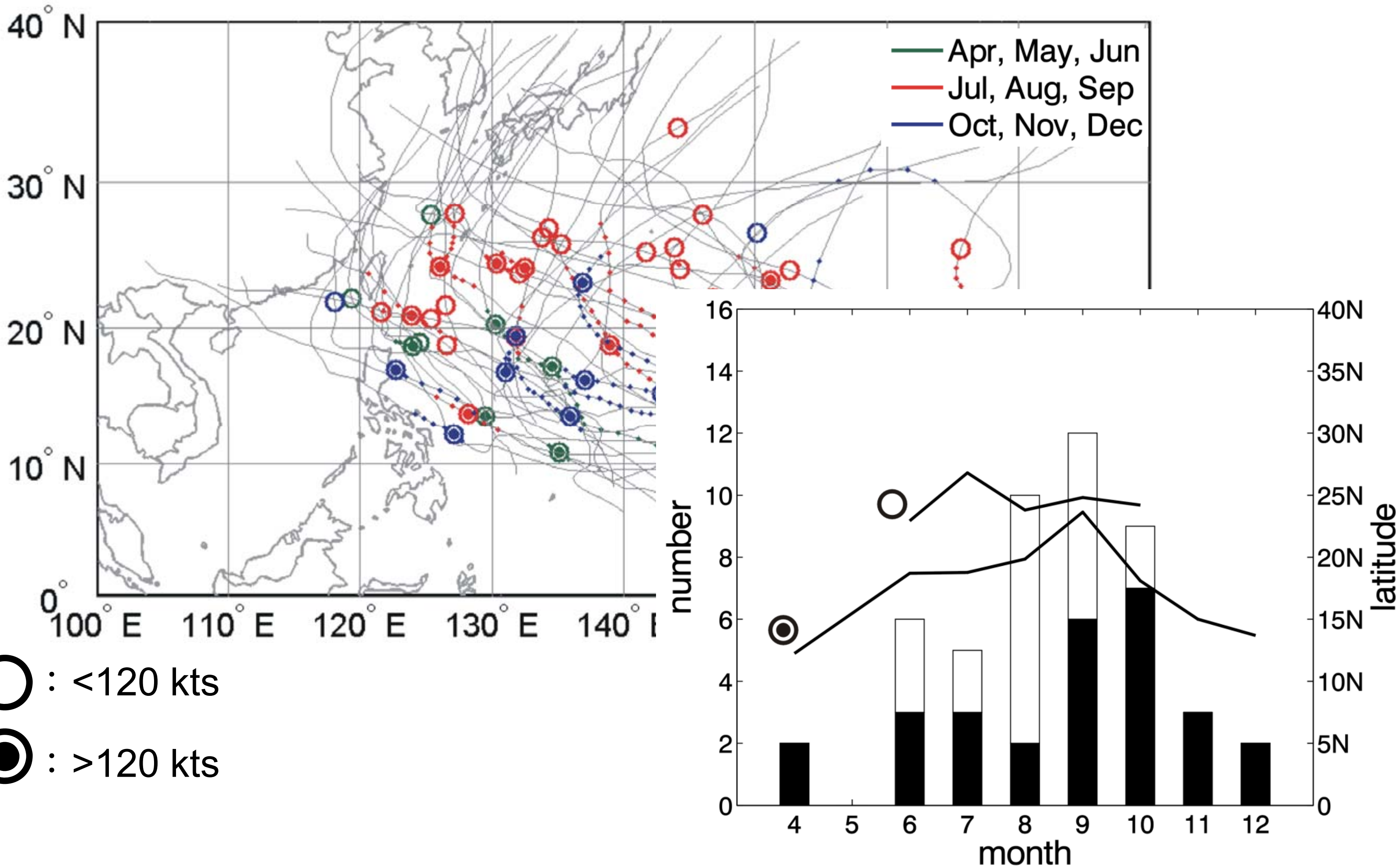

: <120 kts

: >120 kts

(3 km) **Hurricane Rita** **RAINEX (2005)**

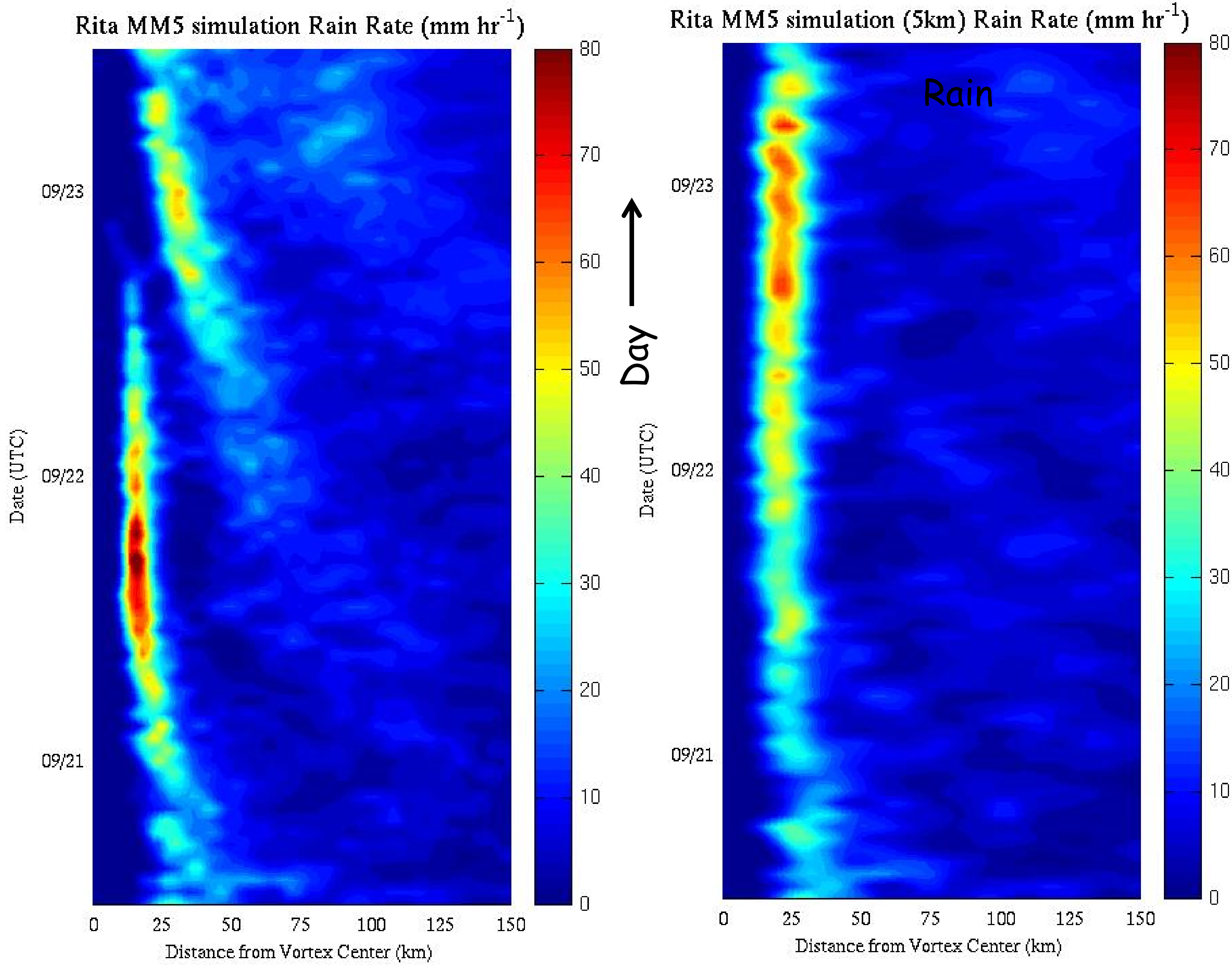

- Kirchhoff vortex (nonlinear) Lamb, 1932

$$\frac{x^2}{a^2}+\frac{y^2}{b^2}=1$$

a ~ 30 km b ~ 20 km

$$\zeta\frac{ab}{(a+b)^2}=\omega$$

P ~ (2π/ζ)*4 ζ ~ 3*10^{-3} s^{-1}

rotating period **P** = $\dfrac{2\pi}{\zeta}\dfrac{(a+b)^2}{ab}$

Vmax ~ 50 ms^{-1}

- Kelvin PV wave (linear)

$$c=V_{\max}(1-\frac{1}{m}) \qquad m=2$$

angular velocity = $c/r=\dfrac{V_{max}}{2r}$

rotating period **P**

$$\sim\frac{2\pi}{\omega}=\frac{2\pi}{2\frac{V_{\max}}{r}}*4=\frac{2\pi}{\zeta}*4$$

Same as Kirchhoff vortex !!

Chang (1983)

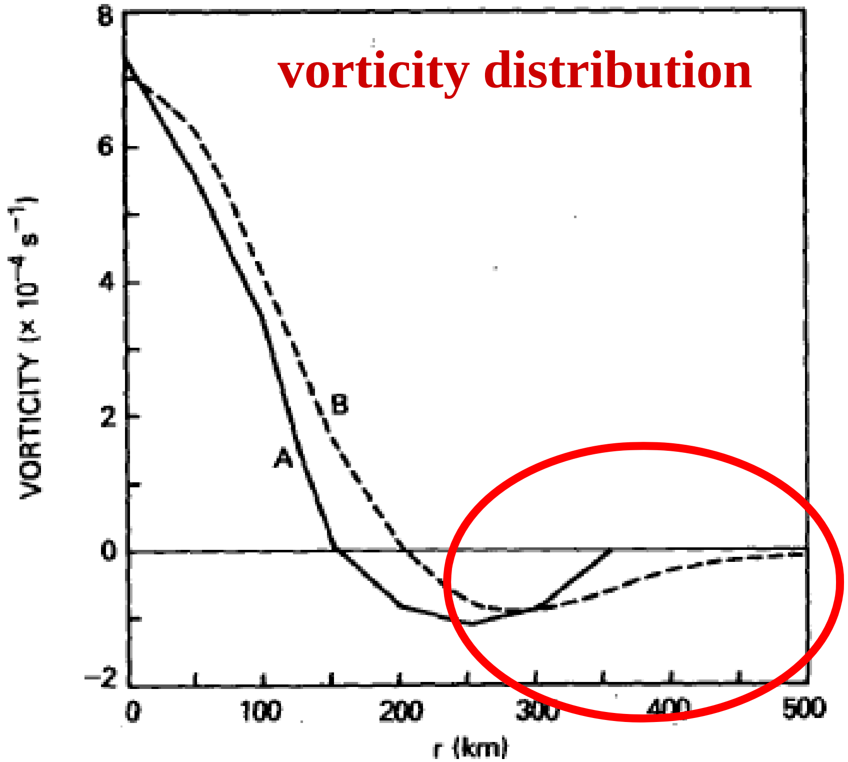

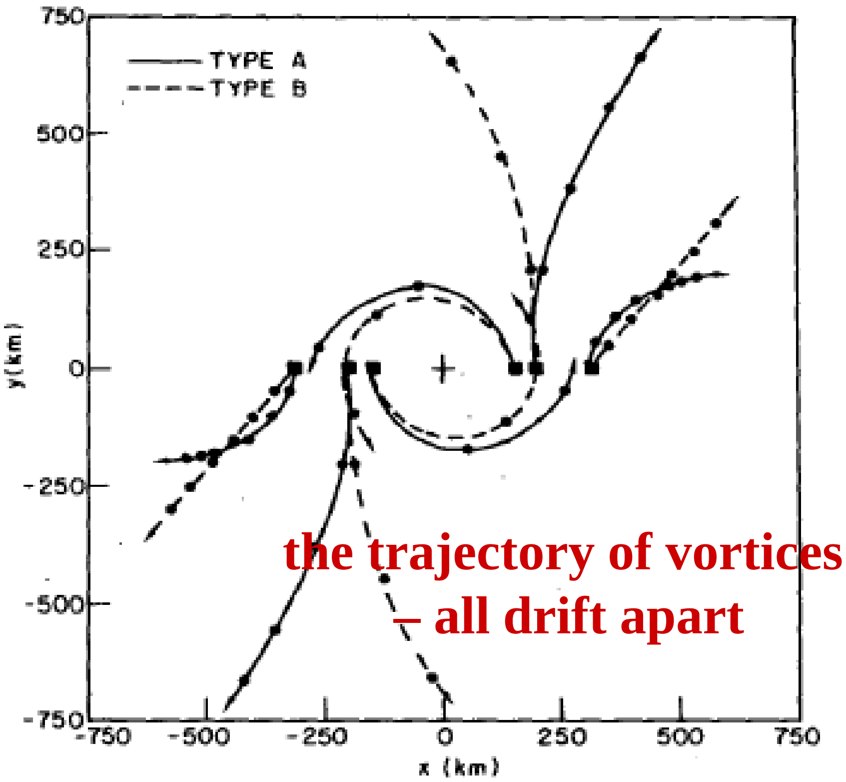

non-diabatic heating

Chang (1983)

diabatic heating

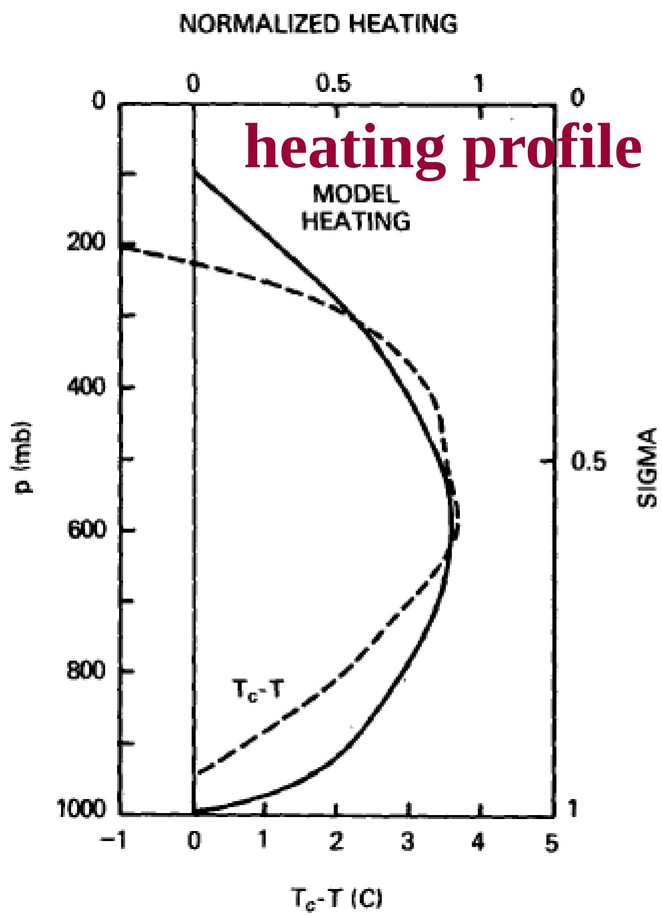

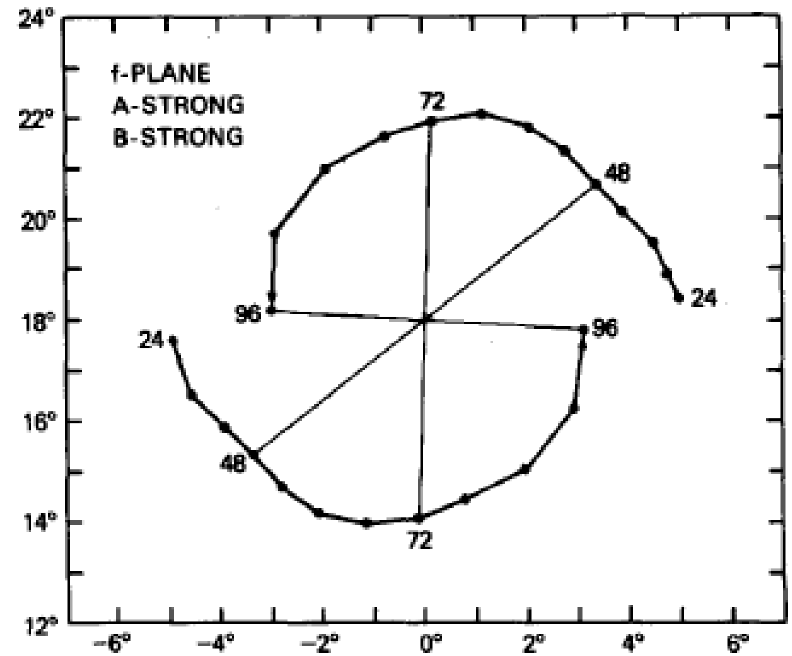

$$\frac{dQ}{dt} = 200\ (K\ day^{-1})$$

The distance between two vortices decreases with time

DeMaria & Chan (1984)

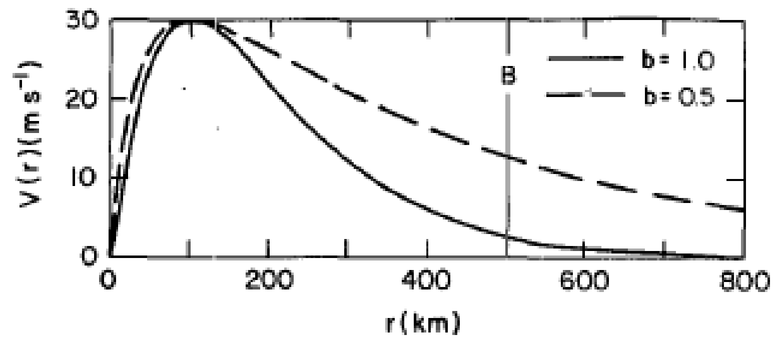

$$V(r) = V_m\left(\frac{r}{r_m}\right)\exp\left\{\frac{1}{b}\left[1-\left(\frac{r}{r_m}\right)^b\right]\right\},$$

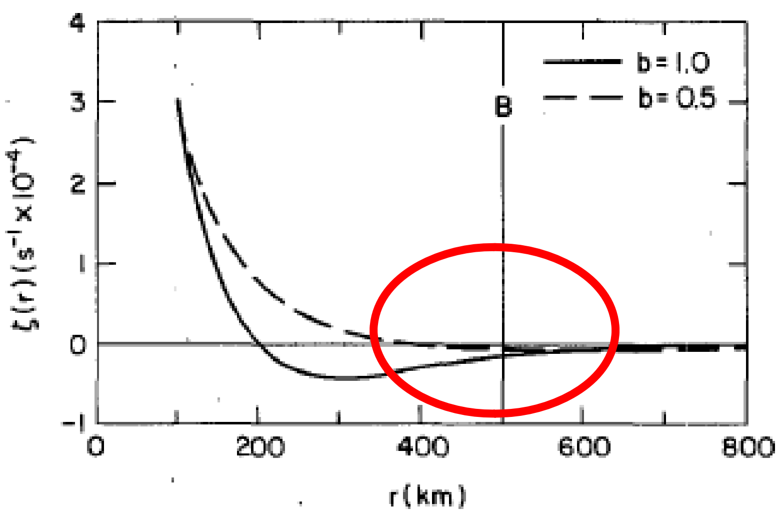

$$\zeta_{(r)} = \frac{2V_m}{r_m}\left[1-\frac{1}{2}\left(\frac{r}{r_m}\right)^b\right]\exp\left\{\frac{1}{b}\left[1-\left(\frac{r}{r_m}\right)^b\right]\right\}$$

b : the factor determines the rate of tangential wind decays

DeMaria & Chan (1984)

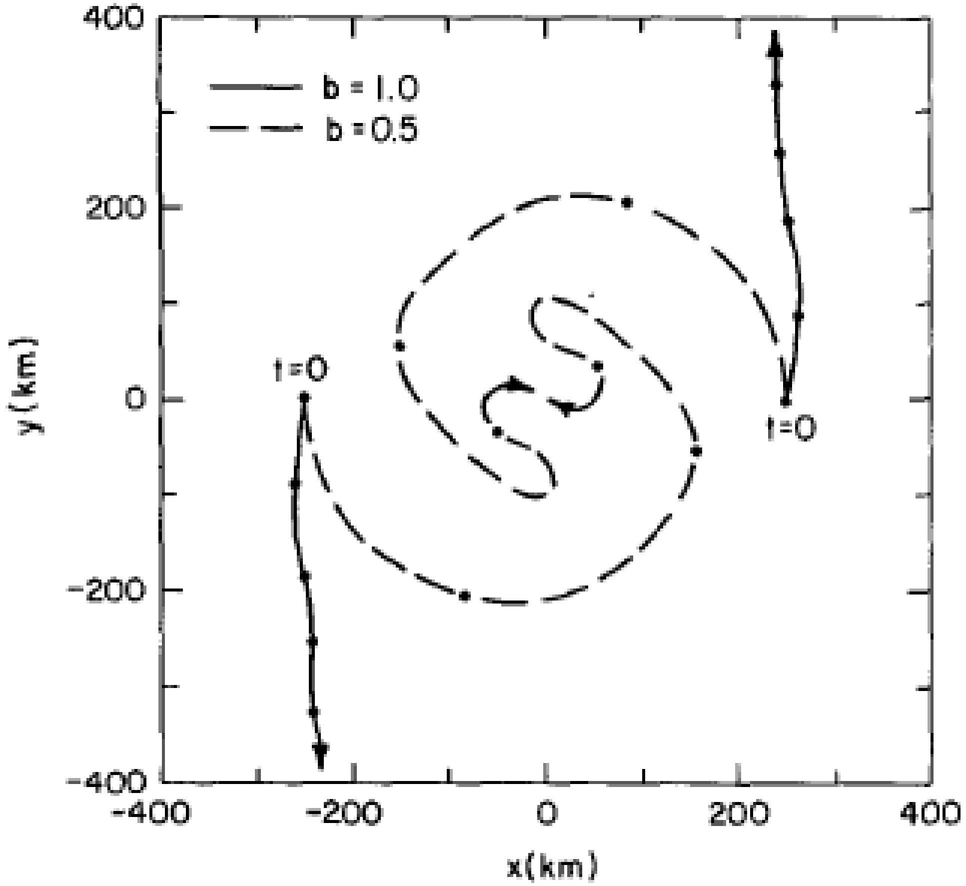

b = 1.0 drift apart

b = 0.5 merge

Kuo et al. (2008)

- 1997~2005
- 221 tropical cyclones
- 205 tropical cyclones examined
- 48 concentric tropical cyclones (23%)
- higher intensity, higher percentage of concentric eyewall

WNPAC

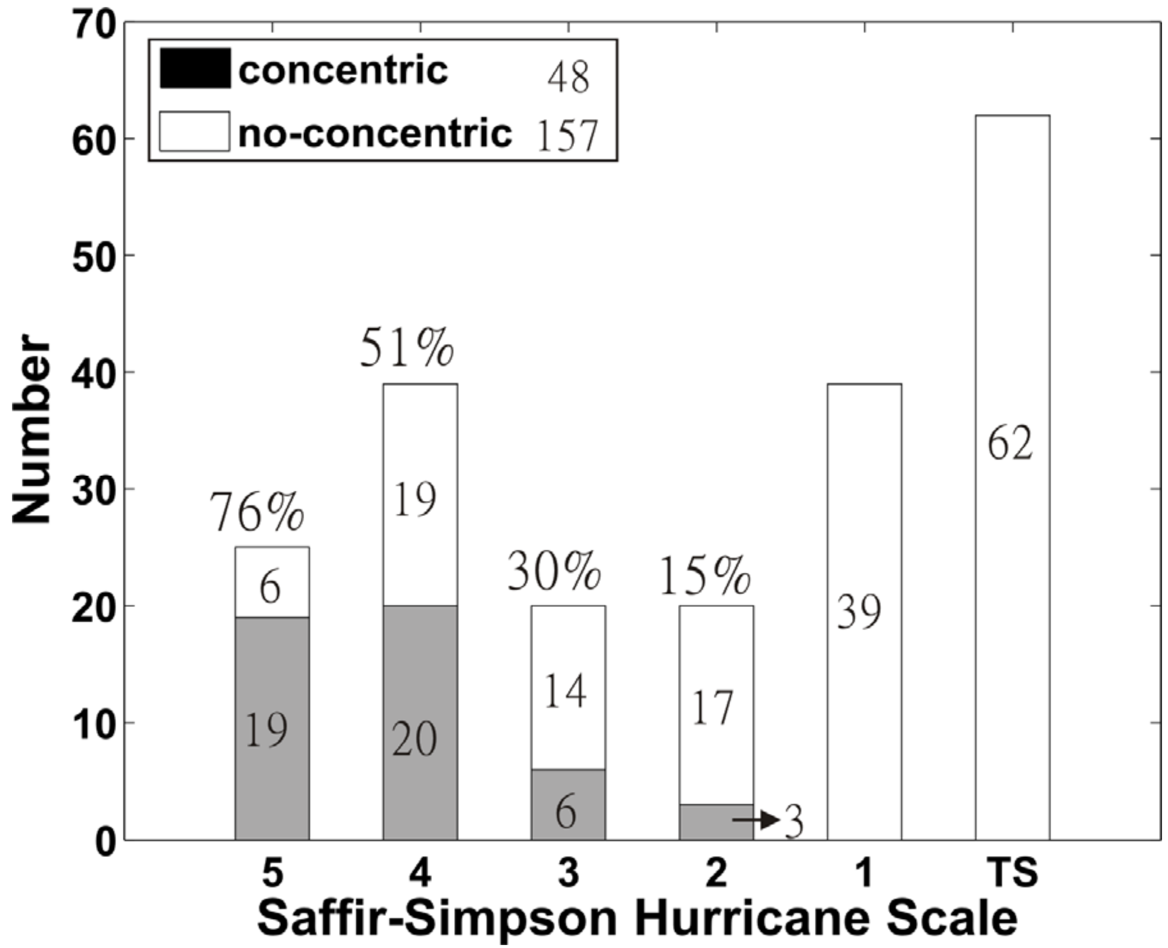

category 5 (135+ kts) category 4 (114-135 kts)

category 3 (96-113 kts) category 2 (83-95 kts)

category 1 (64-82 kts) TS(63- kts)

$$\frac{D\mathbf{V}}{Dt} + 2\boldsymbol{\Omega} \times \mathbf{V} = -\frac{1}{\rho}\nabla_{\mathbf{z}}\mathbf{p} + \nu\nabla^{2}\mathbf{V}.$$

$$\frac{D\mathbf{V}}{Dt} + f\mathbf{k} \times \mathbf{V} = -\nabla_{\mathbf{p}}\phi + \nu\nabla^{2}\mathbf{V}.$$

Geostrophy

Rotation Dynamics

$$\epsilon\frac{D\mathbf{V}^{*}}{Dt^{*}} + \boxed{\mathbf{k} \times \mathbf{V}^{*} = -\nabla^{*}_{\mathbf{p}}\phi^{*}} + \frac{\epsilon}{\mathbf{Re}}\nabla^{*2}\mathbf{V}^{*}.$$

Singular Perturbation Problems

Quasi-balanced Dynamics

Boundary Layer Dynamics

Nearly Invicid

$$\epsilon = \frac{1/f}{L/U}$$

Rotation time scale / Advective time scale

$$Re = \frac{L^{2}/\nu}{L/U}$$

Diffusion time scale / Advective time scale